



# University of HUDDERSFIELD

## University of Huddersfield Repository

Andrijanto, Eko

The study of heterogeneous catalysts for biodiesel synthesis

### Original Citation

Andrijanto, Eko (2012) The study of heterogeneous catalysts for biodiesel synthesis. Doctoral thesis, University of Huddersfield.

This version is available at <http://eprints.hud.ac.uk/id/eprint/17497/>

The University Repository is a digital collection of the research output of the University, available on Open Access. Copyright and Moral Rights for the items on this site are retained by the individual author and/or other copyright owners. Users may access full items free of charge; copies of full text items generally can be reproduced, displayed or performed and given to third parties in any format or medium for personal research or study, educational or not-for-profit purposes without prior permission or charge, provided:

- The authors, title and full bibliographic details is credited in any copy;
- A hyperlink and/or URL is included for the original metadata page; and
- The content is not changed in any way.

For more information, including our policy and submission procedure, please contact the Repository Team at: [E.mailbox@hud.ac.uk](mailto:E.mailbox@hud.ac.uk).

<http://eprints.hud.ac.uk/>

# **The study of heterogeneous catalysts for biodiesel synthesis**

**By EKO ANDRIJANTO**



*University of*  
**HUDDERSFIELD**

**A thesis submitted in partial fulfilment of the requirements for the degree of Doctor of Philosophy**

**Department of Chemical and Biological Sciences**

**The University of Huddersfield**

**October 2012**

## ABSTRACT

A study in search of new heterogeneous catalysts that can be used in place of homogeneous catalysts for biodiesel synthesis has been carried out. The objective of this study is to investigate and evaluate the use of solid catalysts for transesterification of triglycerides and esterification of free fatty acid for biodiesel synthesis. Two types of heterogeneous catalyst have been studied that are solid acid and solid base. Three different solid acids and two solid bases were explored. The solid acids investigated were sulfonated hypercrosslinked polystyrene resin, sulfonated polyvinyl alcohol and sulfated zirconia. The solid bases were lithium zirconate and composite calcium oxide-magnetite.

Sulfonated hypercrosslinked polystyrene resin has been studied in the esterification reaction of oleic acid with methanol and rearrangement of  $\alpha$ -pinene to camphene and limonenes. The activity of this catalyst was compared with conventional macroporous polystyrene sulfonic acids such as Amberlyst-15, Amberlyst-35 and Nafion SAC-13 which is a composite of Nafion and silica. The activity of this catalyst is superior to those of Amberlysts and SAC-13 in the esterification of oleic acid. This catalyst also has high reusability at elevated temperature.

Sulfonated polyvinyl alcohol catalyst has been studied in the same way the esterification of oleic acid and rearrangement of  $\alpha$ -pinene. The activity of the catalyst was compared with sulfonated macroreticular polystyrene resin Amberlyst-35 and Nafion SAC-13. In the esterification reaction, sulfonated polyvinyl alcohol shows a better activity than SAC-13 and the Amberlyst-35 resin catalyst. In the rearrangement/isomerisation reaction, the sulfonated polyvinyl alcohol is the least active.

The activity of sulfated zirconia as a solid acid catalyst has been studied in the esterification of oleic acid and in simultaneous esterification-

transesterification of a mixture oleic acid and triglycerides. In the simultaneous reaction, the activity of this catalyst was compared with sulfonated polystyrene catalysts (Amberlyst-15 Amberlyst-35 and Purolite D5081) and commercial sulfated zirconia XZO-1720. The result showed that in the transesterification reaction, the sulfated zirconias are more active but in the esterification reaction the sulfonated polystyrene catalysts are better than sulfated zirconia. The effect of calcination temperature on the catalytic activity of the catalyst was also studied. The study shows that 600 °C calcination gives the best catalytic activity.

The lithium zirconate is one of the solid base catalysts evaluated in this study. The catalyst was very active in the transesterification of tributyl glycerate with methanol. The effect of calcination temperature on its activity in the transesterification reaction of tributyl glycerate was studied. The study shows that 700 °C calcination yielded the highest catalytic activity which is associated with the formation of the tetragonal phase which gives the highest concentration of basic sites and basic strength.

A composite between calcium oxide and magnetite is the last catalyst reported in this study. The study of this catalyst is due to ease of separation by an external magnetic field. The catalytic performance in the transesterification of tributyl glycerate and methanol was studied. The catalytic activity of the catalyst was maximum at the calcination temperature of 700 °C. Loss of catalytic activity and magnetic properties were shown at higher calcination temperature.

Despite the relatively high activities found for the catalysts studied, further improvement is needed if the catalysts are to be applied for industrial use. However, sulfonated hypercrosslinked polystyrene resin catalysts showed promising activity for the pre-esterification reaction and it is one of the best catalysts for reducing free fatty acid in low grade vegetable oil.

## DEDICATION

“I would like to dedicate my dissertation to my beloved mother, **Surati** (RIP, 2010) and father, **Kaldini** for their pray, love, and support. The achievement that I had is a result of their their excellence parenting”.

and

“I would like also to dedicate my work to my loving wife, **Herlina**, my son **Noval**, my daughter **Nabilla and Alliza** whose love and support have accompanied me during my PhD.

## ACKNOWLEDGEMENTS

First and foremost, I wish to express my sincere appreciation and deepest gratitude to my supervisor, Prof. Robert Brown, my advisor, to whom I am indebted for his guidance, motivation and support throughout this study. I also convey my gratitude to Dr. Nick Powles who acted as my second supervisor during my PhD.

I would like to express my heartfelt thanks to all those individuals whose wisdom support and encouragement made my work possible, Prof. Mike Page, Prof. John Atherton (IPOS University of Huddersfield), Dr. Emiliana Dvinov and Dr. Hazel Stephenson of MEL Chemicals UK, Dr. Lisa Dawson at the University of Huddersfield for her assistance, friends in research office and in our research group. I would like to thanks to my examiners Dr. Duncan Mcquarrie (York University), Dr. Gareth Parkes (internal examiner).

And last, but not least I am also gratefully acknowledging to the DGHE (Directorate General for Higher Education) the government of Indonesia for the financial support for this work. The grateful acknowledgement is also made to MEL Chemicals UK and The University of Huddersfield for the great support.

# Table of Contents

ABSTRACT .....	i
DEDICATION.....	iii
ACKNOWLEDGEMENTS.....	iv
APPENDIXES.....	x
LIST OF FIGURES .....	xi
LIST OF TABLES .....	xvi
ABBREVIATIONS .....	xvii
<b>CHAPTER 1 .....</b>	<b>1</b>
<b>INTRODUCTION.....</b>	<b>1</b>
1.1. Background .....	2
1.2. Research objectives.....	4
1.2.1. General objectives.....	4
1.2.2. Specific objectives.....	4
1.3. Report structure .....	5
References.....	8
<b>CHAPTER 2 .....</b>	<b>9</b>
<b>LITERATURE REVIEW .....</b>	<b>9</b>
2.1. Introduction .....	10
2.1.1. Biodiesel Chemistry .....	10
2.1.2. Biodiesel feedstock.....	10
2.1.3. Biodiesel properties .....	11
2.1.4. Advantages and disadvantages of biodiesel .....	12
2.1.5. Biodiesel production process .....	13
2.2. Parameters affecting the yield of biodiesel.....	14
2.2.1. Reaction temperature.....	14
2.2.2. Reaction time .....	14

2.2.3. Alcohol to oil ratio.....	15
2.2.4. Catalyst concentration .....	15
2.2.5. The effect of free fatty acids .....	16
2.2.6. The effect of mixing .....	16
2.3. Transesterification reaction .....	17
2.3.1. Mechanism for acid catalysed transesterification.....	18
2.3.2. Mechanism of base-catalysed transesterification .....	19
2.4. Homogeneous acid and base catalysis.....	20
2.5. Heterogeneous acid and base catalysis .....	22
2.6. Heterogeneous acid catalyst studied in this work .....	24
2.6.1. Ion-exchange resin catalysts.....	24
2.6.2. Sulfonated polyvinyl alcohol .....	27
2.6.3. Sulfated zirconia catalysts .....	29
2.7. Solid base catalysts used in this work .....	33
2.7.1. Lithium zirconate.....	33
2.7.2. Calcium oxide magnetite composite.....	34
References.....	36
<b>CHAPTER 3 .....</b>	<b>48</b>
<b>SULFONATED HYPERCROSSLINKED RESIN AS SOLID ACID CATALYST ...</b>	<b>48</b>
3.1. Overview .....	49
3.2. Introduction .....	50
3.3. Experimental methods.....	54
3.3.1. Materials.....	54
3.3.2. Catalyst characterization .....	54
3.3.3. Catalyst testing.....	56
3.4. Results .....	58
3.4.1. Catalyst characterization.....	58
3.4.2. Catalyst testing.....	60
3.3.3. Catalyst reusability .....	64
3.3.4. Vapour sorption.....	65
3.3.5. Ammonia adsorption calorimetry .....	67

3.5. Discussion .....	69
3.6. Conclusions .....	75
References.....	76
<b>Chapter 4</b> .....	<b>80</b>
<b>SULFONATED POLYVINYL ALCOHOL AS SOLID ACID CATALYST</b> .....	<b>80</b>
4.1. Overview .....	81
4.2. Introduction .....	82
4.3. Experimental methods.....	85
4.3.1. Materials.....	85
4.3.2. Catalyst preparation.....	85
4.3.3. Catalyst characterization .....	86
4.3.4. Ion exchange capacity (IEC) measurement .....	87
4.3.5. Catalytic testing.....	87
4.4. Results and discussion.....	88
4.4.1. Catalyst characterization.....	88
4.4.3. Catalyst testing.....	91
4.4.4. Catalyst reusability.....	99
4.4.5. Kinetic study .....	101
4.5. Conclusions .....	102
References.....	103
<b>CHAPTER 5</b> .....	<b>106</b>
<b>SULFATED ZIRCONIA AS SOLID ACID CATALYST</b> .....	<b>106</b>
5.1. Overview .....	107
5.2. Introduction .....	108
5.3. Experimental methods.....	111
5.3.1. Materials.....	111
5.3.2. Catalysts preparation .....	111
5.3.3. Catalyst characterization.....	111
5.3.4. Catalyst testing.....	112
5.4. Results and discussions.....	113

5.4.1. Catalyst characterization.....	113
5.4.2. Catalytic activities.....	120
5.5. Conclusions .....	128
References.....	129
<b>CHAPTER 6 .....</b>	<b>132</b>
<b>LITHIUM ZIRCONATE AS SOLID BASE CATALYST.....</b>	<b>132</b>
6.1. Overview .....	133
6.2. Introduction .....	134
6.2. Experimental .....	136
6.2.1. Materials.....	136
6.2.2. Catalyst preparation .....	136
6.2.3. Catalyst characterization.....	137
6.2.4 . Catalytic activity .....	138
6.3. Results and discussion.....	139
6.3.1. Catalyst characterization.....	139
6.3.2. Catalytic activity .....	145
6.3.3. Reusability and leaching test.....	149
6.4. Conclusions .....	151
References.....	153
<b>CHAPTER 7 .....</b>	<b>156</b>
<b>CALCIUM OXIDE-MAGETITE AS SOLID BASE CATALYST .....</b>	<b>156</b>
7.1. Overview .....	157
7.2. Introduction .....	157
7.3. Experimental and methods.....	160
7.3.1. Materials.....	160
7.3.2. Magnetite (Fe <sub>3</sub> O <sub>4</sub> ) preparation .....	161
7.3.3. CaO-magnetite (CaFe) catalyst preparation .....	161
7.3.4. Catalytic testing.....	162
7.3.5. Catalyst characterization.....	162
7.4. Results and discussion.....	163

7.4.1. Catalyst characterization.....	163
7.4.2. Catalytic activities.....	168
7.4.3. Magnetic susceptibility.....	169
7.4.4. Catalyst Reusability.....	170
7.5. Conclusions.....	172
References.....	172
<b>CHAPTER 8 .....</b>	<b>175</b>
<b>CONCLUSIONS AND RECOMMENDATIONS.....</b>	<b>175</b>
8.1. Conclusion .....	176
8.1.1. Use of sulfonated hypercrosslinked polystyrene resin as a solid acid catalyst.....	176
8.1.2. Sulfonated polyvinyl alcohol as a solid acid catalyst.....	177
8.1.3. Sulfated zirconia as a solid acid catalyst.....	179
8.1.4. Lithium zirconate as a solid base catalyst.....	180
8.1.5. Calcium oxide-magnetite composite as a recoverable solid base catalyst.....	181
8.2. Recommendations for future work.....	181
8.2.1. Sulfonated hypercrosslinked polystyrene resin catalyst.....	181
8.2.2. Sulfonated polyvinyl alcohol catalyst.....	182
8.2.3. Sulfated zirconia catalyst.....	182
8.2.4. Lithium zirconate catalyst.....	183
8.2.5. Calcium oxide – magnetite composite catalysts.....	183

# APPENDIXES

<b>APPENDIX – A :</b>	Biodiesel feedstock, targets and production in selected countries.....	185
<b>APPENDIX – B :</b>	Nitrogen Adsorption : Micromeritics ASAP 2020.....	186
<b>APPENDIX – C :</b>	Microcalorimetry Measurement.....	188
<b>APPENDIX – D :</b>	Dynamic Vapour Sorption (Advantage™).....	189
<b>APPENDIX – E :</b>	Glass reactor (50 ml).....	190
<b>APPENDIX – F :</b>	Gas Chromatography Clarus 500 Perkin Elmer.....	191
<b>APPENDIX –G :</b>	Pressurised Reactor (Autoclave Engineer™).....	193
<b>APPENDIX – H :</b>	CALCULATION OF TOF for CATALYSTS.....	194
<b>APPENDIX – I :</b>	FTIR (Fourier transform infra red – Nicolet 380).....	195
<b>APPENDIX – J :</b>	Powder X-ray Diffraction Bruker D8.....	196
<b>APPENDIX – K :</b>	Programmable furnace : VULCAN 3-120™.....	197
<b>APPENDIX – L :</b>	Publications and Presentations.....	198

## LIST OF FIGURES

2.1.	Transesterification reaction of triglycerides with alcohol .....	10
2.2.	Transesterification reaction of triglycerides with alcohol in three steps.....	17
2.3.	Acid-catalyzed reaction mechanism transesterification.....	18
2.4.	Base-catalyzed reaction mechanism transesterification.....	19
2.5.	Sulfonated crosslinked polystyrene resin structure.....	25
2.6.	Structure model of a hypercrosslinked polystyrene resin.....	27
2.7.	Molecular structure of (a) PVA, (b) sulphosalicylic acid, (c) sulfosuccinic acid.....	28
2.8.	Esterification reaction of PVA with sulfosuccinic acid.....	28
2.9.	Structure model of sulfated zirconia proposed by Babou.....	32
3.1.	Esterification of oleic acid (a) and isomerisation of $\alpha$ -pinene (b)...	53
3.2.	Scanning electron microscope images of: (a) D5082 (hypercrosslinked resin) and (b) Amberlyst-35 (macroporous resin).....	59
3.3.	Esterification of oleic acid using solid acids catalyst at 65 °C.....	61
3.4.	Isomerisation of $\alpha$ -pinene using solid acid catalyst s.....	61
3.5.	The effect of reducing the particle size of the resin catalysts on their activities in the transesterification reaction for hypercrosslinked resin D5081 at 65 °C.....	63
3.6.	The effect of reducing the particle size of the resin catalysts on their activities in the transesterification reaction for macroreticular resin Amberlyst-15 at 65 °C.....	63
3.7.	Reusability tests carried out on D5081 in the oleic acid esterification reaction at 65 °C with different conditions.....	64
3.8.	Reusability tests carried out on D5081 catalyst in the oleic acid esterification reaction at 85 °C.....	65

3.9.	The adsorption isotherms for cyclohexane vapours for the resin catalyst.....	66
3.10.	The adsorption isotherms for water vapours for the resins catalyst.....	66
3.11.	The molar enthalpy of ammonia adsorption plotted against the amount of adsorbed ammonia for all the resins catalysts.....	69
4.1.	Reaction of polyvinyl alcohol and sulfosuccinic acid to form PVA-SSA.....	83
4.2.	Crosslinking reaction of PVA-SSA with glutaraldehyde to form PVA-SSA-GA.....	84
4.3.	FTIR spectra of the catalysts: Pure PVA (99%) and PVA-SSA-GA catalysts.....	89
4.4.	Relation between the IEC and the SSA content of the PVA-SSA-GA catalyst.....	91
4.5.	Effect of SSA content on the conversion of oleic acid at 60 °C.....	92
4.6.	First order plots for the conversion of oleic acid using PVA-SSA-GA catalysts.....	92
4.7.	Correlation between the rate constant and the amount of SSA in the catalysts.....	93
4.8.	The effect of temperature on the conversion of oleic acid using PVA-SSA-GA29 catalyst.....	94
4.9.	The effect of catalyst loading on the conversion of oleic acid at 60 °C using PVA-SSA-GA29 .....	95
4.10.	Esterification reaction of different free fatty acids (FFAs) using PVA-SSA-GA29.....	96
4.11.	Esterification of oleic acid and methanol using different solid acid catalysts.....	97

4.12.	Isomerisation of $\alpha$ -pinene using different solid acid catalysts.....	98
4.13.	Reusability tests of PVA-SSA29 and PVA-SSA-GA29 in the esterification of oleic acid after 4 h.....	100
4.14.	FTIR spectra of PVA-SSA-GA29 before and after being re-used.....	100
4.15.	First order plots for the conversion of oleic acid using PVA-SSA-GA29 at different temperature.....	101
4.16.	Arrhenius plot $\ln(k)$ vs $1/T$ of PVA-SSA-GA29.....	102
5.1.	Effect of calcination temperature on acidities of sulfated zirconia catalysts.....	115
5.2a.	Powder XRD patterns of sulfated zirconia (SZ-01) calcined at 400-900 °C and zirconia $ZrO_2$ at 600 °C. T = Tertagonal and M=Monoclinic....	117
5.2b.	Powder XRD patterns of sulfated zirconia XZO-1720 calcined at 400-900 °C, and zirconia $ZrO_2$ at 600 °C T=tetragonal, M=monoclinic.....	118
5.3.	FTIR spectra of sulfated zirconia (a) XZO-1720 (b) SZ-01 as function of calcinations temperature.....	119
5.4.	Catalytic activity of SZ-01 and XZO-1720 itransesterification of tributyrin at 120 °C.....	120
5.5.	Rate constant measurement of SZ-01 and XZO-1720 catalyst in the transesterification reaction of tributyrin.....	121
5.6.	The effect of calcination temperature on acidity and catalyst activity of sulfated zirconia SZ-01.....	122
5.7.	The effect of calcination temperature on acidity and catalyst activity of sulfated zirconia XZO-1720.....	123
5.8.	Catalytic activities of solid acid catalysts in simultaneous esterification and transesterification reactions at 120 °C after 2 h.....	125

5.9.	Reusability test of SZ-01 in transesterification of tributyrin esterification and transesterification reactions at 120 °C after 2 h.....	126
5.10.	Possible sulfate leaching mechanism in sulfated zirconia	128
6.1.	Transesterification reaction of tributyrin with methanol.....	136
6.2.	XRD patterns of synthesized $\text{Li}_2\text{ZrO}_3$ after calcination at 500-900 °C and $\text{ZrO}_2$ calcined at 600 °C. Notations: Z = zirconia, T = $\text{Li}_2\text{ZrO}_3$ tetragonal, M= $\text{Li}_2\text{ZrO}_3$ monoclinic, .....	141
6.3.	Scanning electron micrographs of (a) mixtures zirconium hydroxide and lithium acetate before calcinations (b) LIZA-500 (500 °C), (c) LIZA-700 (700°C) and (d) LIZA-900 (900 °C).....	143
6.4.	$\text{CO}_2$ adsorption microcalorimetry data for lithium zirconate catalysts.....	144
6.5.	Conversion vs time for tributyrin transesterification using lithium zirconate calcined at 500, 700 and 900 °C.....	145
6.6.	Conversion vs time for tributyrin transesterification using lithium catalyst on transesterification of tributyrin with methanol at 50°C.....	147
6.7.	Effect of tributyrin alcohol molar ratio on transesterification on the conversion/time plot for transesterification of tributyrin with methanol at 63 °C.....	148
6.8.	The effect of the catalyst amount on the tributyrin conversion at 63 °C.....	149
6.9.	Re-usability test of LIZA-700 on transesterification of tributyrin at 63 °C after 30 min.....	150
6.10.	Leaching test of LIZA-700 on transesterification of tributyrin.....	151
7.1.	Reaction mechanism of transesterification of triglycerides with with methanol using CaO as catalyst.....	159
7.2.	XRD patterns of CaO and CaO-Magnetite (CaFe) calcined at difference temperatures.....	164

7.3.	CO <sub>2</sub> adsorption calorimetric data for CaFe-500, CaFe-700 and CaFe900.....	165
7.4.	FTIR analysis of CaO and CaFe catalysts calcined at different temperature.....	167
7.5.	Catalytic activities of CaO-magnetite calcined at different temperature in the transesterification reaction of tributyrin with methanol at 63 °C.....	168
7.6.	Magnetic susceptibility of CaFe catalyst calcined at different temperatures.....	170
7.7.	Catalyst reusability of CaFe-700 in transesterification reaction of tributyrin at 63 °C (conversion after 30 minutes reaction).....	172

## LIST OF TABLES

2.1.	Comparison of typical properties of biodiesel and petrodiesel according ASTM standards of maximum allowed quantities in diesel and biodiesel.....	11
2.2.	Recommended FFA contents in biodiesel feedstocks.....	20
2.3.	Homogeneous acid catalyzed transesterification of vegetable oil using mineral acids and sulfonic acids.....	21
2.4.	Heterogeneous basic catalysts classification.....	22
2.5.	Heterogeneous base catalysts for biodiesel synthesis.....	23
2.6.	Solid acid catalysts for transesterification.....	24
2.7.	The acid strength of solid acids.....	30
3.1.	Characteristic supported resin sulfonic acid catalysts.....	58
3.2.	TOF for the catalysts in isomerisation and esterification reactions.....	60
4.1.	Properties of PVA and resin base catalysts.....	90
4.2.	Turnover frequencies of three different catalysts for esterification and isomerisation.....	98
5.1.	Properties of sulfated catalysts following calcination at 400-900 °C.....	114
5.2.	Properties of sulfated zirconia and resin catalysts.....	115
5.3.	Catalytic activities in simultaneous transesterification and esterification reactions.....	124
6.1.	Characteristics and properties of $\text{Li}_2\text{ZrO}_3$ catalysts.....	140
6.2.	Basic strength and basic sites concentration data for $\text{Li}_2\text{ZrO}_3$ .....	143
7.1.	Surface area and porosity data of CaO and CaFe.....	163
7.2.	Basic strength and basic sites concentration data for CaFe.....	166

## ABBREVIATIONS

ATR	-	Attenuated Total Reflectance
BJH	-	Barret Joyner Halenda
BET	-	Brunauer Emmett Teller
DG	-	Diglycerides
DVB	-	DiVinylBenzene
DVS	-	Dynamic Vapour Sorption
FAME	-	Fatty Acid Methyl Esters
FFA	-	Free Fatty Acids
FTIR	-	Fourier Transform Infra Red
GC	-	Gas Chromatography
GA	-	Glutaraldehydes
IEC	-	Ion Exchange Capacity
IPA	-	IsoPropylAlcohol
JCPDS	-	Joint Committee on Powder Diffraction Standards
MG	-	Monoglycerides
MW	-	Molecular Weight
PS	-	Polystyrene
PVA	-	Poly Vinyl Alcohol
SEM	-	Scanning Electron Microscopy
STO	-	Sulfated Tin Oxide
SZ	-	Sulfated Zirconia
SSA	-	Sulfo Succinic Acid
TCP	-	Tricaprylin

TG	-	Triglycerides
TMG	-	TriMethylGuanidine
TOF	-	Turn Over Frequency
WCO	-	Waste Cooking Oils
XRD	-	X-ray Diffraction

# **CHAPTER 1**

## **INTRODUCTION**

---

“In this chapter, the background and the objectives of this research are described. The structure of this thesis and a brief overview of individual chapter are also summarised”.

## 1.1. Background

The increasing demand for energy and depleting petroleum resources has led to the search for alternative renewable and sustainable fuel. An alternative renewable fuel must be technically feasible, economically competitive, environmentally acceptable, and readily available [1]. Biodiesel is one of the best candidates to substitute for petrodiesel and also most advantageous due to its being environmentally benign. This fuel is biodegradable, non-toxic and has low emission profiles as compared to petroleum diesel [2].

By definition biodiesel is an alternative fuel that is synthesized by reacting triglycerides (TG's) obtained from vegetable oils or fats with alcohols such as methanol to form fatty acid methyl ester (FAME) through a transesterification reaction which is catalyzed by base, acid or enzyme. The first two have been paid more attention due to short reaction times and low cost compared with the last [3].

The most frequently used method for making biodiesel today is using the base catalyzed reaction (NaOH, KOH). This is due to the fact that base catalyzed reaction gives a high yield of methyl ester and the reaction can be accomplished in very short time with minimum side reactions [4].

In alkali catalyzed transesterification, the triglycerides used must be low in free fatty acids (high quality oil) because free fatty acids will react with the catalyst producing soap and therefore difficult product and glycerine separation [5]. However to minimise the cost, it is very often low grade oil

that is used such as waste cooking oil (WCO). The problems arise because low grade oil usually contains high free fatty acids (FFAs). A pre-esterification step with methanol using acid catalyst is needed to convert the free fatty acids into methyl ester. Sulphuric acid is commonly used as catalyst for this step, but its use requires excessive washing to remove the catalyst [6]. Heterogeneous catalysts could replace homogeneous catalysts which potentially could lead to benefit because it removes the need for the washing process and, in addition the catalyst can be reused. The use of heterogeneous catalyst has potential to simplify the downstream operations, allowing the more economical process and also yielding higher quality biodiesel and glycerol.

This report describes the synthesis, characterization and the use of heterogeneous acid and base catalysts for biodiesel production. The activity of heterogeneous acid and base catalysts has been studied using model compounds. Oleic acid was chosen as model compound for the esterification reaction and tributyl glycerate (tributylin) for the transesterification reaction. The factors that contribute to the activity of the catalysts are also discussed.

In this research, three types of heterogeneous acid catalysts were studied: sulfonated hypercrosslinked polystyrene resin, sulfonated polyvinyl alcohol and sulfated zirconia. Moreover, two types heterogeneous basic catalysts were also reported: lithium zirconate and calcium oxide-magnetite composite.

## **1.2. Research objectives**

### **1.2.1. General objectives**

- (i) Develop and characterize solid base catalysts for the transesterification reaction of triglycerides in biodiesel synthesis.
- (ii) Develop and characterize solid acid catalysts for the pre-esterification reaction of free fatty acid in biodiesel synthesis.
- (iii) Develop and characterize solid acid catalyst for both transesterification and esterification process in biodiesel synthesis.

### **1.2.2. Specific objectives**

- (i) To evaluate and characterize the use of sulfonated hypercrosslinked resins in the esterification of free fatty acids for biodiesel production.
- (ii) To synthesize and characterize solid acid based on sulfonated polyvinyl alcohol for the esterification of free fatty acid in biodiesel production.
- (iii) To synthesize, characterize and compare of modified zirconia (sulfated zirconia) catalyst for simultaneous esterification and transesterification reactions in biodiesel production.
- (iv) To synthesize and characterize solid base lithium zirconate catalyst for the transesterification reaction of tributyrin to form its methyl ester.

- (v) To synthesize and characterize solid base CaO-magnetite composite (CaO-Fe<sub>3</sub>O<sub>4</sub>) catalyst for the transesterification reaction of tributyrin.

### **1.3. Report structure**

This report is divided into eight chapters: the introduction, literature review, the study of solid acid and solid base catalysts and conclusion. The introduction explains the research objective and the literature review explains the background and theory of the studied research. The rest of the chapters explain the synthesis, characterization and testing of individual catalysts studied. The last chapter discusses the conclusion of the work and recommendations for further work. The content of subsequent chapters are as follow.

#### ***Chapter 2***

Chapter 2 is literature review for the thesis. Homogeneous and heterogeneous catalysis, biodiesel properties, chemistry and biodiesel feedstock are discussed. The biodiesel process and the parameters affecting the process are explained based on the latest developments. The details of the catalytic transesterification and esterification are also reviewed. Background theory and literature of the solid acid and base catalysts studied are also explained in brief individually.

### ***Chapter 3***

This chapter describes the study of sulfonated hypercrosslinked resins Purolite D5081 and D5082 as heterogeneous acid catalysts for the esterification of free fatty acids in the production of biodiesel. In this chapter, superiority of this new type of sulfonated hypercrosslinked resins catalyst compared to existing sulfonated polystyrene resin is described. This chapter has been published in the Journal of Applied Catalysis B: Environmental [7], APPENDIX - L.

### ***Chapter 4***

Chapter 4 discusses the synthesis, characterization and testing of sulfonated polyvinyl alcohol (PVA) crosslinked with glutaraldehyde (PVA-SSA-GA) as solid acid catalyst for the esterification of free fatty acids. This chapter explains the effects of different parameters such as sulfosuccinic acid contents, temperature, reactant molar ratio and catalyst amount on the activity of PVA-SSA-GA in the esterification of oleic acid. Comparison of this catalyst with other solid acid resins in esterification and isomerisation are also discussed. The reusability of the catalyst is also reported.

### ***Chapter 5***

Chapter 5 describes the synthesis, characterization and testing of heterogeneous acid catalysts based on modified zirconia (sulfated zirconia) for both esterification and transesterification reactions in biodiesel

production. The parameters affecting the catalytic activity of the catalysts such as calcination temperature and acidity are also discussed.

### ***Chapter 6***

Chapter 6 explains the synthesis, characterization and testing of a new solid base catalyst  $\text{Li}_2\text{ZrO}_3$  for the transesterification reaction of triglycerides. The parameters affecting the activity such as calcination temperature, reactant molar ratio, catalyst amount and the reaction temperature are also discussed in details.

### ***Chapter 7***

Chapter 7 describes a new recoverable magnetic calcium oxide catalyst composite with magnetite ( $\text{Fe}_3\text{O}_4$ ) which includes the characterization and testing in a transesterification reaction. The activity towards the transesterification of tributyrin with methanol is discussed. The characterization of the catalyst as it is calcined shows phase transformation which are responsible for the developed catalytic activity of the CaO.

### ***Chapter 8***

Chapter 8 summarises the overall results and offers recommendations for future work.

## References

1. Meher, L. C.; Vidya Sagar, D.; Naik, S. N., Technical aspects of biodiesel production by transesterification: a review. *Renewable and Sustainable Energy Reviews* 2006, 10, (3), 248-268.
2. Atadashi, I. M.; Aroua, M. K.; Aziz, A. A., High quality biodiesel and its diesel engine application: A review. *Renewable and Sustainable Energy Reviews* 2010, 14, (7), 1999-2008.
3. Atadashi, I. M.; Aroua, M. K.; Aziz, A. A., Biodiesel separation and purification: A review. *Renewable Energy* 2011, 36, (2), 437-443.
4. Lotero, E.; Liu, Y.; Lopez, D. E.; Suwannakarn, K.; Bruce, D. A.; Goodwin, J. G., Synthesis of Biodiesel via Acid Catalysis. *Industrial & Engineering Chemistry Research* 2005, 44, (14), 5353-5363.
5. Wang, Y.; Ou, P. L. S.; Zhang, Z., Preparation of biodiesel from waste cooking oil via two-step catalyzed process. *Energy Conversion and Management* 2007, 48, (1), 184-188.
6. Zhang, Y.; Dube, M. A.; McLean, D. D.; Kates, M., Biodiesel production from waste cooking oil: 1. Process design and technological assessment. *Bioresource Technology* 2003, 89, (1), 1-16.
7. Andrijanto, E.; Dawson, E. A.; Brown, D. R., Hypercrosslinked polystyrene sulfonic acid catalysts for the esterification of free fatty acids in biodiesel synthesis. *Applied Catalysis B: Environmental* 2012, 115-116, (0), 261-268.

# **CHAPTER 2**

## **LITERATURE REVIEW**

---

“In this chapter discusses the biodiesel in general including the chemistry, properties, biodiesel production processes and parameter affecting the yield. Moreover, homogeneous and heterogeneous catalyst and catalysis in the biodiesel synthesis also described in brief. The background theory of heterogeneous catalysts studied in this work is also summarised”.

## 2.1. Introduction

### 2.1.1. Biodiesel Chemistry

Biodiesel is a fuel produced from the transesterification of fats and oils with alcohol to form fatty acid methyl ester in the presence of catalyst [1-4]. The major components in the vegetable oils or fats are triglycerides, as esters of fatty acids with glycerol (1,2,2-propane triol). Triglycerides of vegetable oils or fat normally contain several different fatty acids (FA). The free fatty acid content in different oils and fats result in different chemical and physical properties. Vegetable oils and fats are normally subjected to transesterification to form biodiesel as illustrated in Figure 2.1.

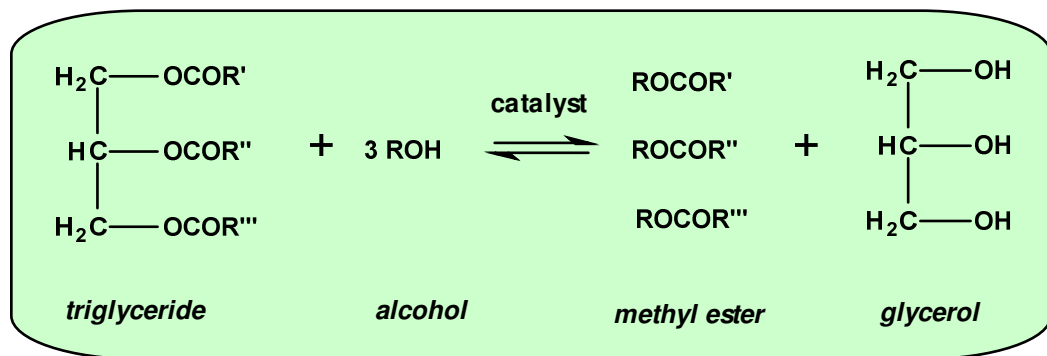


Figure 2.1. Transesterification reaction of triglycerides with alcohol.

### 2.1.2. Biodiesel feedstock

The feedstocks used in the production of biodiesel are varied. The most common feedstocks include vegetable oils (soybean, palm, peanut, rapeseed, sunflower, coconut) and animal fats (tallow) as well as waste cooking oil (WCO). Vegetable oils include edible and non-edible oils source [5]. The use of animal fats, waste greases and waste vegetable oils give more attractive prices, but edible vegetable oils still dominate the production of

biodiesel. Appendix-A shows feedstock used in biodiesel, target and production in selected countries reported by Oak Ridge National Laboratory [117].

### 2.1.3. Biodiesel properties

Biodiesel is miscible with petrodiesel in all proportions. Hence, very often biodiesel is blended with petrodiesel. The blend is normally denoted B5, B20 or B50. The B5 indicates a blend of 5 % of biodiesel and 95 % petrodiesel. Biodiesel demonstrates similarity to the petrodiesel in terms of cetane number. This property represents the ignition quality of a fuel. Other properties that are exhibited by biodiesel that are broadly similar to petrodiesel are its heat of combustion, pour point, cloud point, viscosity, and oxidative stability. The chemical and physical properties of biodiesel can be compared to petrodiesel as shown in Table 2.1 [6].

Table 2.1. Comparison of typical properties of biodiesel and petrodiesel according ASTM standards [6].

Property	Diesel (petro diesel)	Biodiesel
Standard	ASTM D975	ASTM D6751
Composition	HC(C10-C21)	FAME (C12-C22)
Kinetic viscosity (mm <sup>2</sup> /s) at 40°C	1.9-4.1	1.9-6.0
Specific gravity (g/ml)	0.85	0.88
Flash point (°C)	60-80	100-170
Cloud point (°C)	-15 to 5	-3 to 12
Pour point (°C)	-35 to -15	-15 to 16
Cetane Number	40-55	48-60

Cetane number (CN), is conceptually similar to the octane number used for gasoline. It is used for describing the ignition quality of petrodiesel or its components. Generally, a compound that has a high octane number tends to have a low CN and vice versa. As it is shown in Table 2.1., the cetane number of petrodiesel is between 40-55 and for biodiesel it is 48-60.

#### **2.1.4. Advantages and disadvantages of biodiesel**

The advantages of biodiesel compared to petrodiesel are as follows [7]:

- i. Biodiesel is a renewable energy source.
- ii. Biodiesel is degradable and can decompose under natural conditions.
- iii. Biodiesel has much less sulphur so is environmentally friendly.

Although biodiesel is greener than petrodiesel, biodiesel also has disadvantages:

- i. High viscosity which causes problems to fuel injection systems.
- ii. Biodiesel derived from vegetable oils contains more unsaturated compounds than petro diesel, which is easily subjected to oxidation.
- iii. Biodiesel is more expensive at the moment.
- iv. Biodiesel is often derived from edible oil and therefore its production is in competition with foods.

### 2.1.5. Biodiesel production process

Transesterification has been described above as the major method for biodiesel production. In fact there are several methods available to convert natural oils and fats into biodiesel [8].

- i. Transesterification reaction catalysed by base catalysts [9].
- ii. Acid catalysed transesterification [10].
- iii. Two steps processes ; acid catalysed pre-esterification of free fatty acids and followed by base catalyzed transesterification reaction [11].
- iv. Enzyme catalyzed transesterification [12,13].
- v. Supercritical alcohol transesterification [14].

The purpose of the transesterification reaction is to lower the viscosity of the oils and fats. Transesterification reaction is basically a sequential reaction of triglycerides into fatty acid methyl esters (biodiesel), and glycerol as by product. Biodiesel synthesis nowadays is mostly catalyzed by homogeneous base catalyst for several reasons [8] :

- i. Low temperature needed and atmospheric pressure.
- ii. The reaction time is short, giving high conversion and minimal side reactions.
- iii. No special construction materials are needed when a base catalyst is used, unlike when acid catalysts are used.

## **2.2. Parameters affecting the yield of biodiesel**

Several parameters have influence on the course of the transesterification such as: reaction temperature, reaction time, molar ratio alcohol to oil, catalyst type and concentration, free fatty acid content in feedstock.

### **2.2.1. Reaction temperature**

The temperature of reaction strongly influences the rate and the yield of biodiesel. Leung found that by operating above the optimum temperature, the saponification of triglyceride occurs [15]. In most studies, the temperature is kept close to the boiling point of the alcohol. If methanol is used, the temperature applied is normally 50-65 °C. This should be sufficient to produce high yield when the methanol to oil molar ratio is 6:1.

### **2.2.2. Reaction time**

Freedman transesterified peanut oils under conditions of methanol to oil molar ratio 6:1, 0.5% sodium methoxide catalyst and 60 °C [3]. He found that the conversion of the oil to ester was almost 98% after 1 h reaction.

Ma at al. explained that the transesterification reaction is normally very slow at the beginning due to the immiscibility of the alcohol and oil. When the reaction is underway and conversion reach the point where all components are miscible, and the reaction proceeds very fast and typically takes 1-2 h to complete [9].

### **2.2.3. Alcohol to oil ratio**

One of the most important parameters affecting the yield of biodiesel is the ratio of alcohol to oil [9, 16-18]. The alcohol-oil molar ratio to produce biodiesel stoichiometrically is 3 to 1. However, since the transesterification is a reversible reaction, an excess of alcohol is normally used to ensure that the oil is completely converted into ester. The most common alcohol:oil ratio used is 6:1, i.e. alcohol is in 100 % excess. Most studies revealed that the 6:1 molar ratio of alcohol to triglyceride produced essentially complete conversion [3, 18]. Further increase in alcohol content does not increase the yield of biodiesel significantly but does increase the cost of production [15]. However, the ratio of alcohol to oil can be much higher, up to 15:1, when the free fatty acid content in the oil is high and an acid catalyzed pre-esterification reaction is applied [15, 19]. Also some researchers reported the use of relatively high alcohol to oil ratios to obtain high yield of biodiesel using acid catalysts [18, 20].

### **2.2.4. Catalyst concentration**

The most common catalyst used in the production of biodiesel is NaOH or KOH (homogeneous catalysts). Freedman reported that the alkali-catalysed transesterification is faster than the acid-catalysed reaction [3]. He reported that sodium methoxide was more effective than sodium hydroxide because generally a small amount of water is released during the mixing of methanol and sodium hydroxide which leads to hydrolysis. But sodium hydroxide is much less expensive than sodium methoxide. A

concentration of sodium hydroxide of 0.3-0.5% gave maximum activity in beef tallow transesterification [9]. Higher concentration can decrease the biodiesel yield because of the direct saponification of triglycerides [15, 21].

#### **2.2.5. The effect of free fatty acids**

The free fatty acid (FFA) content in feedstock for transesterification reaction is one of the most important parameters. The FFA content should be lower than 3 % when the base catalyzed transesterification is being used [22]. The use of vegetable oils with FFA content more than 3 % produces lower yields of biodiesel because of neutralisation of the catalyst by the FFA. Increasing the amount of catalyst then increases the possibility of soap formation which results in difficulty with ester glycerol separation [23]. The effects of FFA in biodiesel production have been studied by Ma at al. [9]. If the feedstock has FFA content higher than 3 %, the FFA must be refined either by saponification or by a pre-esterification reaction using an acid catalyst.

#### **2.2.6. The effect of mixing**

Oils and fats are immiscible with alcohol and produce a two phase liquid. In the initial stages of the reaction, the rate is diffusion controlled and poor diffusion between the two phases results in a low rate [24]. As methyl esters are formed, they act as solvent for both oil and alcohol to generate a single phase system. Once the single phase fully mixed system is established, further mixing becomes unimportant when homogeneous catalysts are used.

### 2.3. Transesterification reaction

Transesterification (alcoholysis) is the reaction of a fat or oil with an alcohol to form esters and glycerol, catalyzed by base/alkalis [18, 25], acids [26] or enzymes [13-24]. Most commonly, methanol is used but ethanol and butanol can be used effectively [27]. The general equation for the transesterification of triglycerides with alcohol is illustrated in Figure 2.2. If methanol is used in the reaction it is called methanolysis. The transesterification reaction is a reversible reaction; hence, excess alcohol is required to favour the reaction in the forward direction.

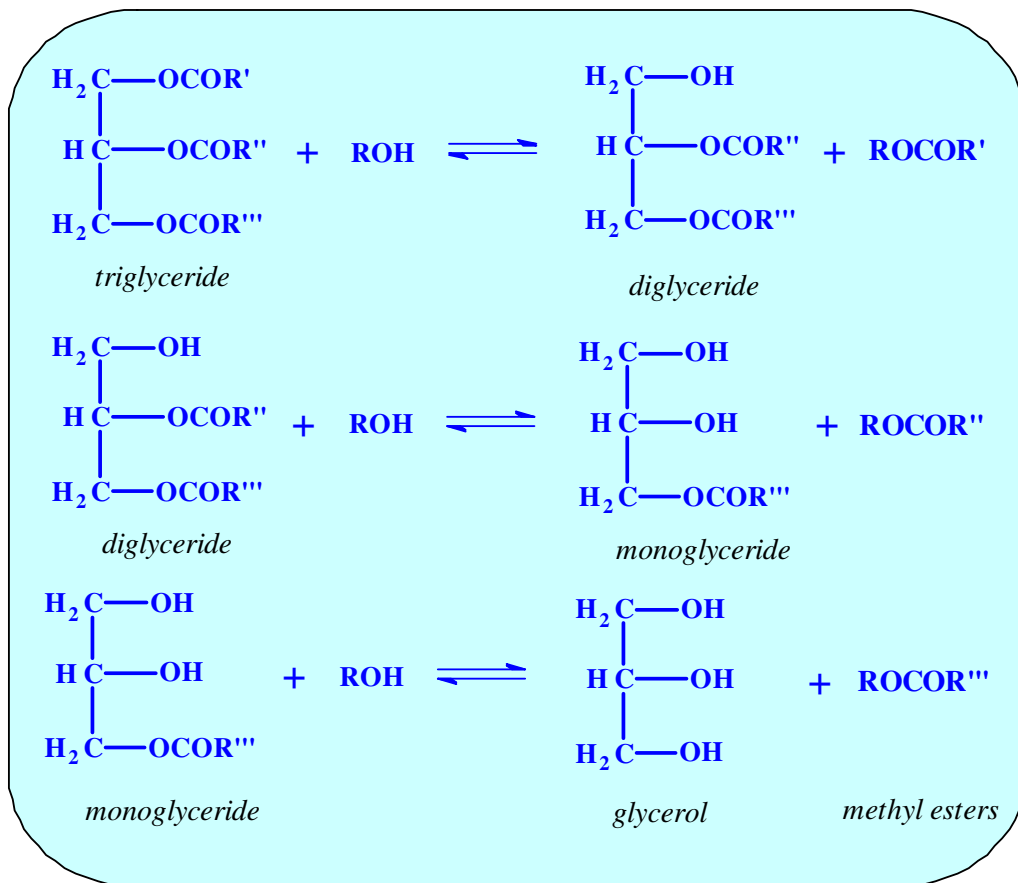


Figure.2.2. Transesterification reaction of triglycerides with alcohol in three steps.

### 2.3.1. Mechanism for acid catalysed transesterification

The acid-catalysed mechanism is illustrated in Figure 2.3. as explained by Di Serio [28]. First is the protonation of triglyceride at the carbonyl group and it is followed by nucleophilic attack by the alcohol to form a tetrahedral carbocation intermediate. Then, the tetrahedral intermediate undergoes proton migration, followed by breakdown of the tetrahedral intermediate. This process is repeated twice and three FAME (fatty acid methyl ester molecule) are formed and glycerol is the by-product. At the end of the reaction, the catalyst is regenerated.

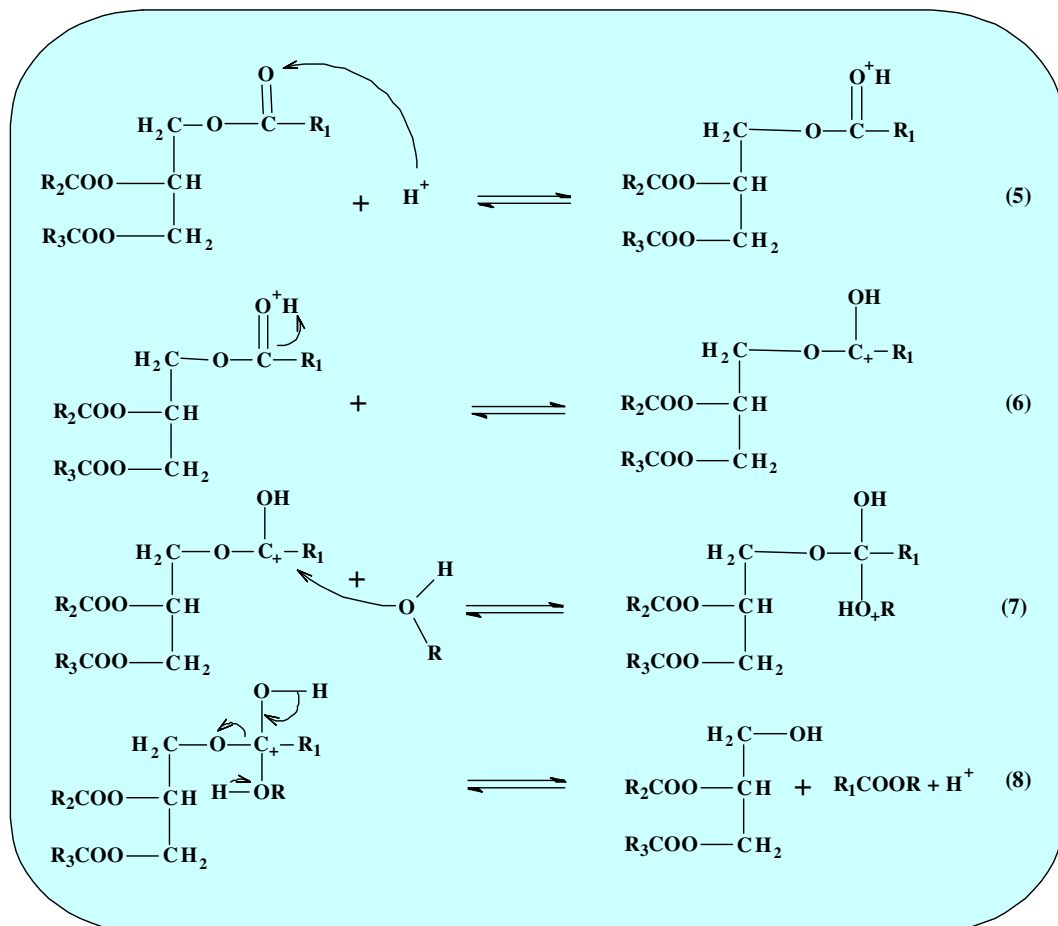


Figure 2.3. Acid-catalysed reaction mechanism for transesterification.

### 2.3.2. Mechanism of base-catalysed transesterification

In the base-catalysed reaction  $\text{OH}^-$  or  $\text{RO}^-$  are the active species. The mechanism pathways for both homogeneous and heterogeneous base-catalysed transesterification basically follow the same principle. In the heterogeneous base-catalysed transesterification, the catalytic reaction is started on the surface of the solid base. First, the reaction of the base produces alkoxide ion  $\text{RO}^-$  which is strongly basic. Nucleophilic attack on the carbonyl group of the triglyceride by  $\text{RO}^-$  occurs, forming a tetrahedral intermediate, followed by rearrangement of the intermediate forming FAME. This process is repeated twice producing three molecules of FAME (biodiesel) and one molecule of glycerol [28]. The base-catalyzed mechanism reaction is shown in Figure 2.4.

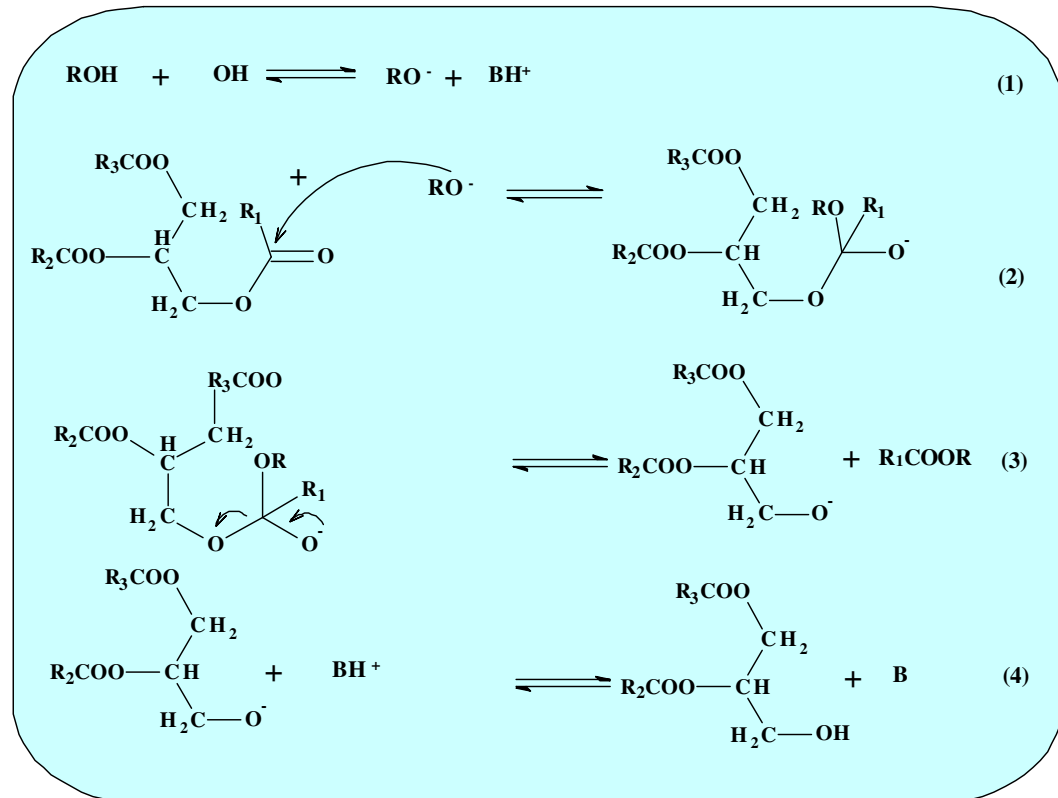


Figure 2.4. Base-catalysed reaction mechanism transesterification.

## 2.4. Homogeneous acid and base catalysis

Transesterification in the synthesis of biodiesel is commonly catalyzed by homogeneous alkaline (base) catalysts, because mild conditions are needed, catalysts are inexpensive and high yield can be achieved [22]. Acid catalyzed transesterification is very slow. It was reported that acid catalyzed transesterification is 4000 times slower than base catalyzed reaction [29]. Base catalyzed transesterification has been comprehensively studied by Nouredini [24]. The most common basic catalysts for transesterification process are sodium hydroxides and potassium hydroxide [30-31], sodium and potassium alkoxides [9]. However, base-catalyzed transesterification is limited to feedstock with low fatty acid contents less than 1% [32]. Table 2.2. shows typical limits of FFA content proposed by several authors [33].

Table 2.2. Recommended FFA contents in biodiesel feedstocks [33].

Author	Recommended FFA (%)	References
Freedman	<1	[3]
Ma and Hanna	<1	[9]
Zhang	<0.5	[18]
Ramadhas	<2	[34]
Sahoo	<2	[35]

An alternative route to biodiesel from vegetable oils is to use a homogeneous acid catalyst. Acid catalysis requires high temperature and high molar alcohol to oil ratio. It creates problem in catalyst separation and washing, corrosion of reactors and environmental concerns [36-37]. The most investigated homogeneous acid catalysts are H<sub>2</sub>SO<sub>4</sub> (sulphuric acid) and HCl (hydrochloric acid). Advantages of using a homogeneous acid catalyst is

that acid catalysts are less sensitive to the presence of FFA (free fatty acid) [30] and oils with more than 1% FFA can successfully be transesterified [18,3]. An acid catalyst has the capability to catalyse esterification of FFA and transesterification triglycerides simultaneously [36].

A study of the acid-catalysed transesterification reaction using waste cooking oil reported that the biodiesel yield was increased by increasing reaction time, molar ratio of methanol to oil and higher catalyst loading [32]. This study showed that a yield of biodiesel of 90% can be achieved after 10 h reaction using 20:1 methanol to oil ratio and 4 wt% H<sub>2</sub>SO<sub>4</sub> to oil. In a previous study, Freedman et al., reported that 99% conversion reaction was completed after 69 h, using a 30:1 methanol to oil ratio and 1 mol% H<sub>2</sub>SO<sub>4</sub> [3]. These two examples prove that the acid-catalysed reaction needs severe reaction condition compared to base-catalysed reaction. The summary of some work on homogeneous acid catalysed transesterification is shown in Table 2.3.

Table 2.3. Homogeneous acid catalysed transesterification of vegetable oil using mineral acids and sulfonic acid [33].

Raw Material	Catalyst	Alcohol	Ester yield (%)	References
Acid oil (59% FFA)	H <sub>2</sub> SO <sub>4</sub>	MeOH	85	[38]
Crude palm oil (CPO)	H <sub>2</sub> SO <sub>4</sub>	BuOH	97	[39]
Oleic Acid	p-TSA <sup>a</sup>	EtOH	79-90	[40]
Waste cooking oils	H <sub>2</sub> SO <sub>4</sub>	MeOH	97-99	[41]

## 2.5. Heterogeneous acid and base catalysis

The history of heterogeneous base catalysis is shorter than heterogeneous acid catalysis. Base catalysis by heterogeneous material was not used in the early developmental period, in part due to rapid poisoning by species such as CO<sub>2</sub>, H<sub>2</sub>O and O<sub>2</sub>. In 1970's, heterogeneous basic catalysts became more popular due to a better understanding of the reactivity of surface basic sites [42], and it was shown that thermal pre-treatment at over 450 °C removed adsorbed catalyst poisons [43]. Solid base catalysts can be classified into several categories. One description is shown in Table 2.4.

The main reasons for using solid basic catalysts in the synthesis of biodiesel are simplified operation and the reduction of waste. Under heterogeneous base catalysis, the presence of high FFA is less of a problem than with KOH or NaOH catalysts; saponification and hydrolysis are less likely

Table 2.4. Heterogeneous basic catalysts classification [42].

Single metal oxides	Alkali metal oxides
	Alkali earth oxides
	Rare earth oxides
Zeolites	Alkali metal exchanged zeolite
	Alkali metal supported on zeolite
Supported alkali metal or / alkaline earth metal	Alkali metal on alumina
	Alkali metal on silica
	Alkali metal on alkaline earth oxides
	Alkali metal and alkali metal hydroxide on alumina
Clay minerals	Hydrotalcites

Research in heterogeneous basic catalysis for biodiesel synthesis has increased quite significantly in recent years. Example of some of this work is given in Table 2.5.

Table 2.5. Heterogeneous base catalysts for biodiesel synthesis [44].

Catalyst	Temperature (°C)	Reaction Time (h)	Performance (%)	References
MgO	65	1	98	[45]
NaOH/Al <sub>2</sub> O <sub>3</sub>	50	24	86	[46]
SrO <sub>2</sub>	65	5	94.7	[47]
NaX zeolite/KOH	65	8	85.6	[48]
SrO	65	0.3	95	[49]
CaO	60	-	90	[50]
CaO	60	2	93	[51]
CaO	60	2	98	[52]
Ca(OCH <sub>3</sub> ) <sub>2</sub>	60	-	-	[53]
Li-ZnO		3	96.3	[54]
Hydrotalcite/Mg	60	3	97	[55]
KF/ZnO	-	-	-	[56]
ZnO-La <sub>2</sub> O <sub>3</sub>	-	-	-	[57]
Alkali/Al <sub>2</sub> O <sub>3</sub>	60	3	94.3	[58]
Trimethyl guanidine (TMG)/silica	80	3	86	[59]

Some of the disadvantages of homogenous acid catalysts can be overcome by using solid acid catalysts. There is an obvious attraction to using solid acid catalysts rather than solid base catalysts because the former can catalyse the esterification of any free fatty acid at the same time as catalyse the transesterification of triglycerides. The problem is the low activity of acid catalysts in general towards the transesterification reaction. Despite this, considerable effort has been devoted into solid acid catalysts for biodiesel

synthesis. Some of the heterogeneous acid catalysts that have sufficient acid strength to be effective for the transesterification are shown in Table 2.6.

Table 2.6. Solid acid catalysts for transesterification [44].

Catalyst class	Catalyst	Reaction Conditions	Yields (%)	Ref.
Metal	Zn/I <sub>2</sub>	338 K, 0.1 MPa, 26 h	96	[60]
Zeolite	KNO <sub>3</sub> /KL zeolite	473 K, 5Pa, 4h	71-77	[62]
Mesoporous Silica	SBA-SO <sub>3</sub> H	358 K, > 0.1 Mpa, 3 h	60-65	[61]
Mixed metal oxides	WO <sub>3</sub> /ZrO <sub>2</sub>	473 K, > 0.1 Mpa, 5 h	97	[63]
Superacids	SO <sub>4</sub> /ZrO <sub>2</sub>	393 K, > 0.1 Mpa, 1 h	92-98	[64]

Strong solid acids like sulfated zirconia (SZ) and similar material have been used for transesterification but even with this strong acid, activity is low. There are however, many reports of solid acids being used effectively for just the pre-esterification of free fatty acid. For example, sulfated zirconia has been used in the esterification of lauric acid with 2-ethyl hexanol to form ester 2-ethyl-hexyl dodecanoate [65].

## 2.6. Heterogeneous acid catalyst studied in this work

### 2.6.1. Ion-exchange resin catalysts

Catalysis by ion-exchange resins is one of the earliest applications of active groups on polymeric supports and has therefore been studied thoroughly [66]. Several kinds of organic synthesis involving hydrolysis, hydration, dehydration, cyclization, isomerization, polymerization, racemization, condensation, etc. can involve acid and base catalysis by ion-

exchange resins. The use of ion-exchange resins was developed mainly during the early 1950's alongside the development of methods to produce styrene and divinylbenzene (DVB) copolymers as beads. Ion-exchange resins are polymers onto which functional groups are attached. The most commonly used resins are composed of copolymers of divinyl benzene (DVB) and styrene with sulfonic acid groups grafted on the benzene rings.

The surface area and pore size distribution of a resin are characterized by the content of the crosslinking divinylbenzene (DVB) component [67]. The overall structure of the resin and its ability to swell depends on the DVB content, normally expressed as a % of the total monomer content. Some resins exhibit permanent porosity (generated by polymerizing in the presence of a porogen compound which, when vaporised after synthesis, leaves permanent pores in the structure). The polymer is reacted with sulphuric acid and it is assumed that sulfonation occurs predominantly at the para position, so the chemical structure of a polystyrene/DVB sulfonic acid resin can be represented as in Figure 2.5.

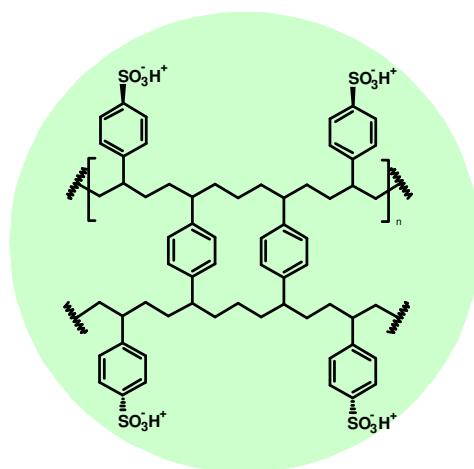


Figure 2.5. Sulfonated crosslinked polystyrene resin structure.

The use of cation exchange resins in the esterification reaction of FFA has been widely reported and studied [68-75]. Most studies of polystyrene sulfonic acid resins have been based on those with permanent macroporosity such as Amberlysts-15, 35, 36 [69]. Some gelular resin has also been reported for the same reaction, such as EBD 100 [68].

Hypercrosslinked resin catalysts: These have been studied, mainly by Tsyurupa and Davankov for many years [76]. They differ from conventional cross-linked polystyrene in having much more extensive cross-linking, by methylene groups linking neighbouring styrene units. Small angle X-ray diffraction studies have shown that this results in a three dimensional crosslinked polymer network with dramatically enhanced permanent porosity. In fact, if applied to polystyrene resins with existing permanent macroporosity, the additional crosslinking results in additional microporosity in a hierarchiral pore structure. These materials exhibit very high surface areas as measured by gas adsorption, of typically  $1000 \text{ m}^2 \text{ g}^{-1}$ . A typical structure of hypercrosslinked resin is illustrated in Figure 2.6.

Hypercrosslinked networks have been known since the 1970's [77]. These polymers can be functionalised with sulfonic acid. They tend to be functionalised at a much lower loading than conventional polystyrene sulfonic acid.

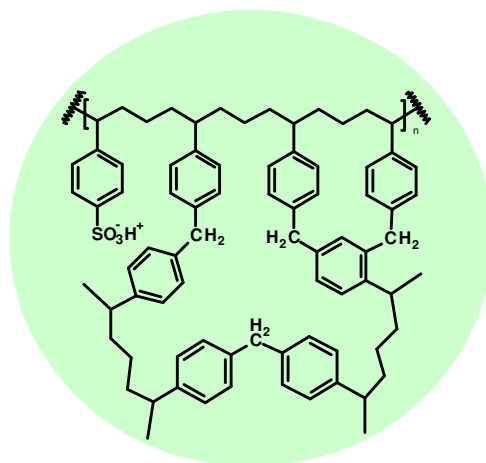


Figure 2.6. Structure model of a hypercrosslinked polystyrene resin .

Because of the high porosity, in the dry state, these materials show extremely low bulk density. The sorption capacities to both polar and non polar solvents exceed many times those of conventional polymeric sorbents and activated carbon [76, 77]. According to our knowledge, there is no published work using hypercrosslinked resins as catalysts for esterification reactions.

### 2.6.2. Sulfonated polyvinyl alcohol

Another polymer-supported acid catalyst has been reported by Castanheiro et al. who used polyvinyl alcohol (PVA), cross-linked with sulfosalicylic acid and sulfosuccinic acid to catalyse the esterification of acetic acid with isoamyl alcohol [78]. Guirero et al. evaluated the transesterification of soybean oil with methanol using sulfonated PVA [79]. The use of sulfonated PVA without any further cross-linking results in leaching of sulfonic acid groups. In this work, we have investigated the influence of

cross-linking agents such as glutaraldehyde in the catalyst preparation. This polymer can be turned into a support for sulfonic acid by reacting it with sulfosuccinic acid (SSA) or sulfosalicylic acid or a combination of both. The molecular structure of both acids is illustrated in Figure 2.7a,b, c.

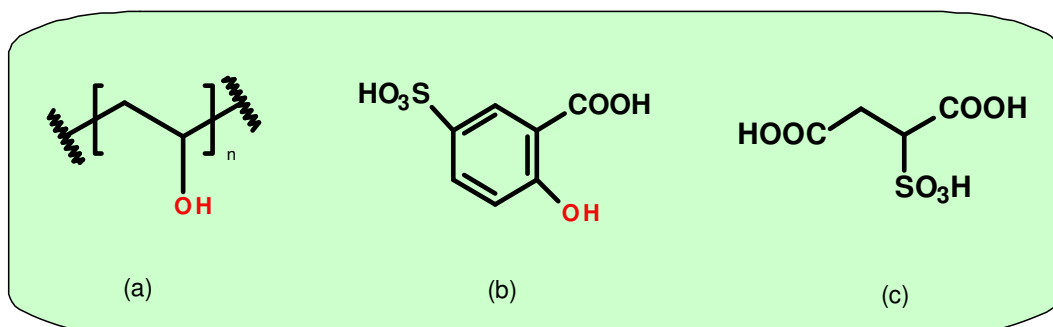


Figure 2.7. Molecular structure of (a) PVA ; (b) Sulfosalicylic acid ; (c) Sulfosuccinic acid.

The sulfosuccinic acid is quite often used because it can act as a cross-linking agent, at the same time providing the sulfonic acid species. The possible reaction between PVA and sulfosuccinic acid is explained by Rhim and Castanheiro [78, 80] as illustrated in the Figure 2.8.

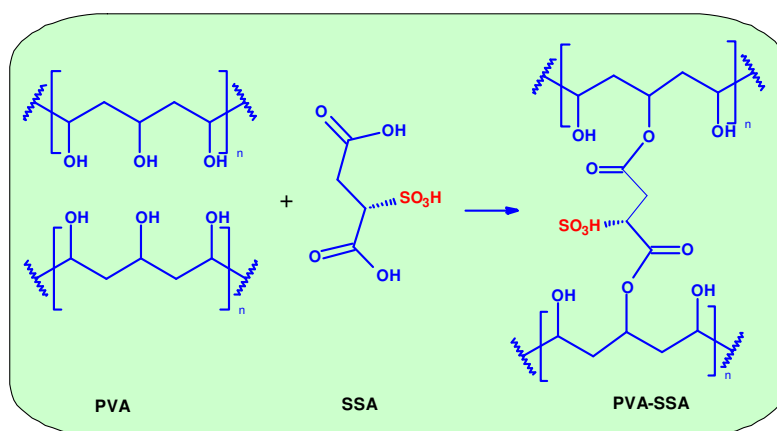


Figure 2.8. Esterification reaction of PVA with sulfosuccinic acid.

### 2.6.3. Sulfated zirconia catalysts

Many metal oxide catalysts have been studied for transesterification and esterification processes. Among those, sulfated zirconia has received considerable attention in the last 20 years due to its strong acidity [81-82]. This catalyst has shown both high catalytic activity and good stability in esterification and even transesterification reactions [83-87], and has been used for many other industrially important reactions such as: acylation, condensation, etherification, isomerisation, cracking, dehydration etc [85]. The synthesis of sulfated zirconia, its structural characterization and its catalytic properties have been reported in a review by Yadav & Nair [65]. Its catalytic performance is highly dependent on the method of preparation. The precise nature of the acidity is still uncertain. Whether these materials are mainly Lewis acids or Bronsted acid is not clear.

### 2.6.4. Sulfated zirconia preparation

#### (i) Two step method (the most common)

The preparation of the method is illustrated in Figure 2.9, based on Matsushashi's work [88]. A zirconium salt such as  $ZrOCl_2$  or  $ZrO(NO_3)_2$ , is hydrolysed to produce zirconium hydroxide. The second step is treating zirconium hydroxide with  $H_2SO_4$  or  $(NH_4)_2SO_4$  solution or by mixing zirconium hydroxide with  $(NH_4)_2SO_4$  powder (non solvent method). This forms sulfated zirconia on calcination.

## (ii) One step method

This is achieved by using a sol-gel technique [89]. For instance, zirconium n-propoxide is mixed with n-propanol, nitric acid and sulphuric acid, resulting in a gel. The gel is then aged for 2 h at room temperature and then the alcohol is removed by drying. During the subsequent calcination, sulfate is somehow expelled onto the surface and transformed into the catalytically active species.

Sulfated zirconia (SZ) has been considered a superacid. In the early work, Hammet indicators were used to determine the strength of SZ. Matsushashi showed the acid strength of SZ to be as high as  $-H_o \geq 16$ . This compares with  $H_o = -12$  for 100 %  $H_2SO_4$ . The Hammet acidity of a range of solid acid is shown in Table 2.7.

Table 2.7. The acid strength of solid acids [88].

Catalyst (calcination temperature, °C)	$H_o$
$SO_4/SnO_2$ (550)	-18.0
$SO_4/ZrO_2$ (650)	-16.1
$SO_4/HfO_2$ (700)	-16.0
$SO_4/TiO_2$ (525)	-14.6
$SO_4/Al_2O_3$ (650)	-14.6
$SO_4/Fe_2O_3$ (500)	-13.0
$SO_4/SiO_2$ (400)	-12.2
$WO_3/ZrO_2$ (800)	-14.6
$MoO_3/ZrO_2$ (800)	-13.3

Sulfated zirconia ( $\text{SO}_4/\text{ZrO}_2$ ) has been the most frequently studied of the “strong” solid acids shown here, partly because of its very strong acid sites and ease of preparation. The following features are noted.

- a. Generally, specific surface areas of sulfated zirconia are much larger than the corresponding oxide.
- b. The degree of crystallization of sulfated zirconia is much lower than zirconia without sulfate treatment.
- c. The infra-red spectrum of sulfated zirconia is distinctly different from those of conventional metal sulfates: the material shows absorption bands at 980-990, 1040, 1130-1150 and 1219-1230  $\text{cm}^{-1}$ . These bands are assigned to bidentate sulfate coordinated to metal ions.
- d. Catalysts obtained by treatment of zirconium salts with sulphuric acid are usually more active than those obtained with ammonium sulfate treatment.

The superacid sites are considered to be metal ions (Lewis acid sites) whose acid strength is enhanced by an inductive effect caused by the sulfate ions, specifically the S=O bonds. Bronsted acid sites may be generated by interaction of the Lewis acid sites with water or organic molecules. A number of models have been proposed to explain the nature of the active sites. A few of these proposed structures are described by Babou, Arata, and Clearfield [90-92]. Vadrine has proposed the structure of sulfated zirconia shown in Figure 2.9.

Babou [90] suggested that sulfation of  $\text{Zr}(\text{OH})_4$  proceeds via following steps:  
 (i)  $\text{H}_2\text{SO}_4$  dissociation in aqueous solution, (ii)  $\text{Zr}(\text{OH})_4$  surface is ionized by trapping protons, (iii) the ionized traps  $\text{SO}_4^{2-}$  anions, (iv) calcination less than  $200\text{ }^\circ\text{C}$  produces structure (iv) and more than  $200\text{ }^\circ\text{C}$  produces structure (v).

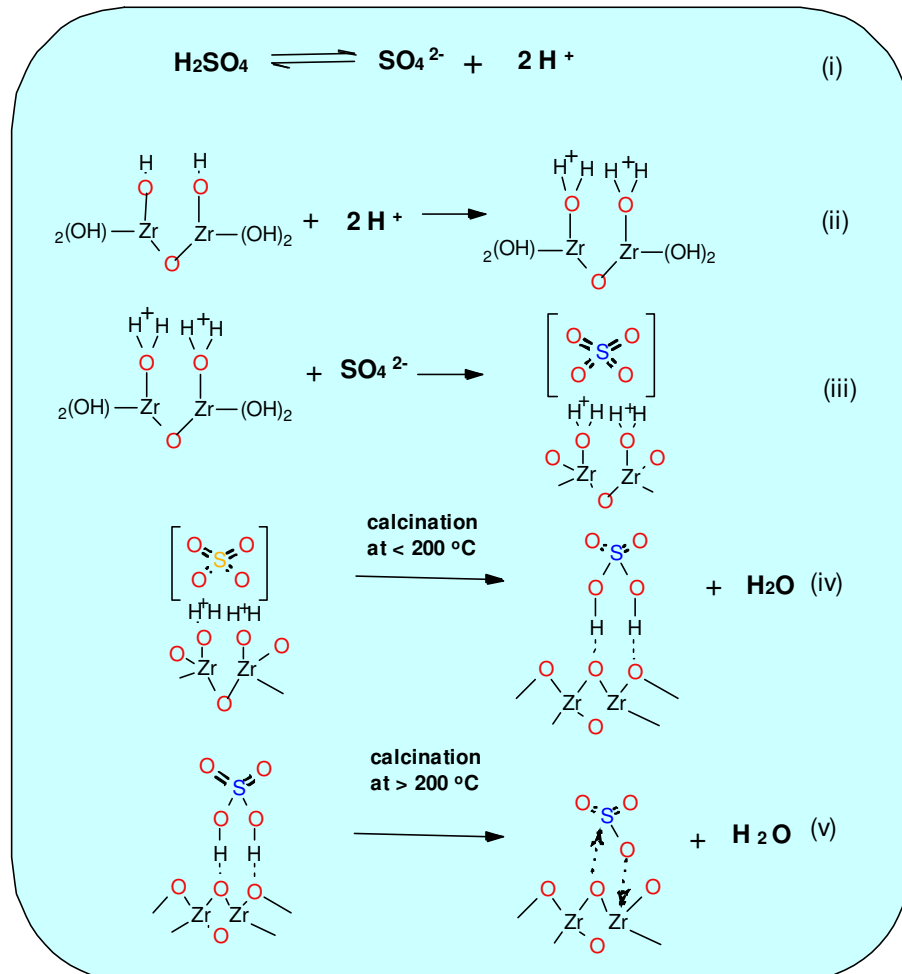
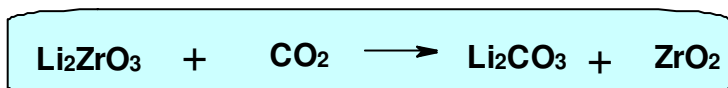


Figure 2.9. Structure model of sulfated zirconia proposed by Babou [90].

## 2.7. Solid base catalysts used in this work

### 2.7.1. Lithium zirconate

Lithium zirconate is known as an adsorbent especially for CO<sub>2</sub> separation from flue gas at high temperature, 400-700 °C [93-96]. The reaction can be reversed to regenerate the adsorbent. The reaction between Li<sub>2</sub>ZrO<sub>3</sub> and CO<sub>2</sub> produces lithium carbonate and zirconia as described in the equation below.



Lithium zirconate can be synthesized using different routes: a wet method [95], a solid state method [97] and a sol gel method [98]. The wet method involves mixing the zirconia or zirconium hydroxide with lithium carbonate/acetate in a aqueous slurry which is dried and calcined. The solid state involves mixing the solid precursors before calcination. In the sol-gel method a mixture of isopropanol (IPA) and zirconium propoxide is dissolved in water and nitric acid added. After reaction lithium carbonate solution is added. The mixture is then dried and the solid is calcined.

The use of lithium zirconate as a catalyst has not been reported to a significant extent. Related materials have been used as catalysts. For example, mesoporous zirconia doped with alkaline earth metals such as lithium have been reported by Ding as solid base catalysts for the production of biodiesel[99]. Despite the similarity of ZrO<sub>2</sub> doped with lithium, it is clearly

different from the discrete compound lithium zirconate which is studied in the work reported in this thesis.

Ding reported the CO<sub>2</sub> TPD on Mg/ZrO<sub>2</sub> and Ca/ZrO<sub>2</sub> and showed that the materials were weakly basic. When the zirconia was modified with Na and K, medium and strong basic sites were detected. Zirconia modified with Li showed the highest basic strength. The catalytic activities in the transesterification of soybean oil using methanol were in line with basicities, with lithium doped zirconia showing the highest activity. Unfortunately, the reusability of the catalyst decreased quite rapidly, and after a third run conversion was down from 98.2 % to 10.5 %. Ding assumed that this was due to leaching of lithium into the reaction medium.

In the work reported in this thesis, the objective is to synthesize Li<sub>2</sub>ZrO<sub>3</sub>, instead of doping Li metal on zirconia, and to use it as solid base catalyst in a transesterification reaction.

### **2.7.2. Calcium oxide magnetite composite**

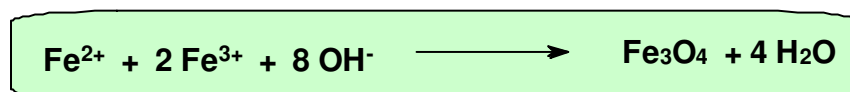
Calcium oxide is the the most studied single metal oxide for the production of biodiesel. The reason is CaO is cheap, non-toxic and readily available [25]. Gleglewicz studied the use of CaO in the transesterification reaction of rapeseed oil with methanol, comparing with Ca(OH)<sub>2</sub> and Ca(CH<sub>3</sub>O)<sub>2</sub>. The activities of these catalyst were in the order of Lewis basicity: Ca(OH)<sub>2</sub><CaO< Ca(CH<sub>3</sub>O)<sub>2</sub>. Liu showed that the transesterification reaction can be accelerated by adding water [100]. However, the water addition should be limited to 2.8 % of the oil. More than this causes the hydrolysis of

triglyceride to form free fatty acid. Kouzu investigated the mode of action of CaO, and showed that the catalyst formed calcium diglyceroxide by the reaction between calcium oxide and glycerol and that this compound was catalytically active [51]. The CaO catalyst was compared with calcium diglyceroxide made by reacting CaO with 50 % glycerol in methanol and the resultant activities were essentially similar.

The leaching of CaO was studied by Granados [50]. Calcium oxide catalyst doped with LiNO<sub>3</sub>, KNO<sub>3</sub> and NaNO<sub>3</sub> were found to give high conversions and calcination of the doped CaO increased the activities even further [101]. Lanthanum doping was also found to enhance the basic strength and, surprisingly, the surface area of the calcium oxide [57]. Base catalysis by CaO was centred on the electron-rich surface oxygen anion. Lizuka showed how to identify the basic properties of CaO using an IR method in the presence of an acidic molecular probe such as benzaldehyde [102]. The basicity of CaO can also be determined using CO<sub>2</sub> temperature programming desorption (TPD), as reported by Zheng et al. who studied CaO and other alkaline earth oxides [20]. The result showed that the basic strength follows the order of MgO < CaO < SrO < BaO.

Magnetite/CaO : magnetically recoverable catalyst materials have been widely used in many different reactions, including hydrogenation, oxidation, photocatalysis, C-C bond formation, hydration, Knoevenagel condensation and CO<sub>2</sub> cyclo addition [103-104]. Magnetite is a ferromagnetic mineral with chemical formula Fe<sub>3</sub>O<sub>4</sub>. Magnetic carrier technology (MCT), first reported by Robinson in 1973, has become an increasingly popular tool

in bio-separations, environmental and material science [105], and catalysis. Combining magnetite and CaO catalyst by impregnation or co-precipitation of the salt will produce a catalyst material that can be separated easily by application of a magnetic field, without the need of filtration. The calcium oxide base catalyst then can be reused. The basic principle of magnetite formation is described in the equation below [106] :



The preparation of genuine composites which possess both magnetic and catalytic properties in the same particle is not trivial. Variables such as composite composition and calcination temperature can influence the balance of the two properties.

## References

1. Helwani, Z.; Othman, M. R.; Aziz, N.; Fernando, W. J. N.; Kim, J., Technologies for production of biodiesel focusing on green catalytic techniques: A review. *Fuel Processing Technology* 2009, 90, (12), 1502-1514.
2. Gerpen, J. V., Biodiesel processing and production. *Fuel Processing Technology* 2005, 86, (10), 1097-1107.
3. Freedman, B.; Pryde, E.; Mounts, T., Variables affecting the yields of fatty esters from transesterified vegetable oils. *Journal of the American Oil Chemists' Society* 1984, 61, (10), 1638-1643.
4. Srivastava, A.; Prasad, R., Triglycerides-based diesel fuels. *Renewable and Sustainable Energy Reviews* 2000, 4, (2), 111-133.

5. Gui, M. M.; Lee, K. T.; Bhatia, S., Feasibility of edible oil vs. non-edible oil vs. waste edible oil as biodiesel feedstock. *Energy* 2008, 33, (11), 1646-1653.
6. Lotero, E.; Liu, Y.; Lopez, D. E.; Suwannakarn, K.; Bruce, D. A.; Goodwin, J. G., Synthesis of Biodiesel via Acid Catalysis. *Industrial & Engineering Chemistry Research* 2005, 44, (14), 5353-5363.
7. Feofilova, E.; Sergeeva, Y.; Ivashechkin, A., Biodiesel-fuel: Content, production, producers, contemporary biotechnology (Review). *Applied Biochemistry and Microbiology* 2010, 46, (4), 369-378.
8. De Filippis, P.; Giavarini, C.; Scarsella, M.; Sorrentino, M., Transesterification processes for vegetable oils: A simple control method of methyl ester content. *Journal of the American Oil Chemists' Society* 1995, 72, (11), 1399-1404.
9. Ma, F.; Hanna, M. A., Biodiesel production: a review. *Bioresource Technology* 1999, 70, (1), 1-15.
10. Chai, F.; Cao, F.; Zhai, F.; Chen, Y.; Wang, X.; Su, Z., Transesterification of Vegetable Oil to Biodiesel using a Heteropolyacid Solid Catalyst. *Advanced Synthesis & Catalysis* 2007, 349, (7), 1057-1065.
11. Canakci, M.; Van Gerpen, J., Biodiesel production from oils and fats with high free fatty acids. *Transactions of the American Society of Agricultural Engineers* 2001, 44, (6), 1429-1436.
12. Pessoa, F.; Magalhães, S.; de Carvalho Falcão, P., Production of Biodiesel via Enzymatic Ethanolysis of the Sunflower and Soybean Oils: Modeling. *Applied Biochemistry and Biotechnology* 2010, 161, (1), 238-244.
13. Du, W.; Xu, Y.-y.; Zeng, J.; Liu, D.-h., Novozym 435-catalysed transesterification of crude soya bean oils for biodiesel production in a solvent-free medium. *Biotechnology and Applied Biochemistry* 2004, 40, (2), 187-190.
14. Saka, S.; Kusdiana, D., Biodiesel fuel from rapeseed oil as prepared in supercritical methanol. *Fuel* 2001, 80, (2), 225-231.

15. Leung, D. Y. C.; Wu, X.; Leung, M. K. H., A review on biodiesel production using catalyzed transesterification. *Applied Energy* 2010, 87, (4), 1083-1095.
16. Banerjee, A.; Chakraborty, R., Parametric sensitivity in transesterification of waste cooking oil for biodiesel production : A review. *Resources, Conservation and Recycling* 2009, 53, (9), 490-497.
17. Marchetti, J. M.; Miguel, V. U.; Errazu, A. F., Heterogeneous esterification of oil with high amount of free fatty acids. *Fuel* 2007, 86, (5-6), 906-910.
18. Zhang, Y.; Dube, M. A.; McLean, D. D.; Kates, M., Biodiesel production from waste cooking oil: 1. Process design and technological assessment. *Bioresource Technology* 2003, 89, (1), 1-16.
19. Zhang, Y.; Dube, M. A.; McLean, D. D.; Kates, M., Biodiesel production from waste cooking oil: 2. Economic assessment and sensitivity analysis. *Bioresource Technology* 2003, 90, (3), 229-240.
20. Zheng, S.; Kates, M.; Dube, M. A.; McLean, D. D., Acid-catalyzed production of biodiesel from waste frying oil. *Biomass and Bioenergy* 2006, 30, (3), 267-272.
21. Eevera, T.; Rajendran, K.; Saradha, S., Biodiesel production process optimization and characterization to assess the suitability of the product for varied environmental conditions. *Renewable Energy* 2009, 34, (3), 762-765.
22. Meher, L. C.; Vidya Sagar, D.; Naik, S. N., Technical aspects of biodiesel production by transesterification" a review. *Renewable and Sustainable Energy Reviews* 2006, 10, (3), 248-268.
23. Dorado, M. P.; Ballesteros, E.; Lopez, F. J.; Mittelbach, M., Optimization of Alkali-Catalyzed Transesterification of Brassica Carinata Oil for Biodiesel Production. *Energy & Fuels* 2003, 18, (1), 77-83.
24. Nouredini, H.; Zhu, D., Kinetics of transesterification of soybean oil. *Journal of the American Oil Chemists' Society* 1997, 74, (11), 1457-1463.

25. Gryglewicz, S., Rapeseed oil methyl esters preparation using heterogeneous catalysts. *Bioresource Technology* 1999, 70, (3), 249-253.
26. Furuta, S.; Matsubishi, H.; Arata, K., Biodiesel fuel production with solid superacid catalysis in fixed bed reactor under atmospheric pressure. *Catalysis Communications* 2004, 5, (12), 721-723.
27. Bozek-Winkler, E.; Gmehling, J. r., Transesterification of Methyl Acetate and n-Butanol Catalyzed by Amberlyst 15. *Industrial & Engineering Chemistry Research* 2006, 45, (20), 6648-6654.
28. Di Serio, M.; Tesser, R.; Pengmei, L.; Santacesaria, E., Heterogeneous Catalysts for Biodiesel Production. *Energy & Fuels* 2007, 22, (1), 207-217.
29. Fukuda, H.; Kondo, A.; Noda, H., Biodiesel fuel production by transesterification of oils. *Journal of Bioscience and Bioengineering* 2001, 92, (5), 405-416.
30. Felizardo, P.; Neiva Correia, M. J.; Raposo, I.; Mendes, J. o. F.; Berkemeier, R.; Bordado, J. o. M., Production of biodiesel from waste frying oils. *Waste Management* 2006, 26, (5), 487-494.
31. Kulkarni, M. G.; Gopinath, R.; Meher, L. C.; Dalai, A. K., Solid acid catalyzed biodiesel production by simultaneous esterification and transesterification. *Green Chemistry* 2006, 8, (12), 1056-1062.
32. Wang, Y.; Ou, S.; Liu, P.; Xue, F.; Tang, S., Comparison of two different processes to synthesize biodiesel by waste cooking oil. *Journal of Molecular Catalysis A: Chemical* 2006, 252, (1-2), 107-112.
33. Lam, M. K.; Lee, K. T.; Mohamed, A. R., Homogeneous, heterogeneous and enzymatic catalysis for transesterification of high free fatty acid oil (waste cooking oil) to biodiesel: A review. *Biotechnology Advances* 2010, 28, (4), 500-518.
34. Ramadhas, A. S.; Jayaraj, S.; Muraleedharan, C., Biodiesel production from high FFA rubber seed oil. *Fuel* 2005, 84, (4), 335-340.

35. Sahoo, P. K.; Das, L. M.; Babu, M. K. G.; Naik, S. N., Biodiesel development from high acid value polanga seed oil and performance evaluation in a CI engine. *Fuel* 2007, 86, (3), 448-454.
36. Jacobson, K.; Gopinath, R.; Meher, L. C.; Dalai, A. K., Solid acid catalyzed biodiesel production from waste cooking oil. *Applied Catalysis B: Environmental* 2008, 85, (1-2), 86-91.
37. Wang, Y.; Ou, S.; Liu, P.; Xue, F.; Tang, S., Comparison of two different processes to synthesize biodiesel by waste cooking oil. *Journal of Molecular Catalysis A: Chemical* 2006, 252, (1-2), 107-112.
38. Haas, M.; Scott, K., Combined nonenzymatic-enzymatic method for the synthesis of simple alkyl fatty acid esters from soapstock. *Journal of the American Oil Chemists' Society* 1996, 73, (11), 1393-1401.
39. Crabbe, E.; Nolasco-Hipolito, C.; Kobayashi, G.; Sonomoto, K.; Ishizaki, A., Biodiesel production from crude palm oil and evaluation of butanol extraction and fuel properties. *Process Biochemistry* 2001, 37, (1), 65-71.
40. Vieville, C.; Mouloungui, Z.; Gaset, A., Esterification of oleic acid by methanol catalyzed by p-toluenesulfonic acid and the cation-exchange resins K2411 and K1481 in supercritical carbon dioxide. *Industrial & Engineering Chemistry Research* 1993, 32, (9), 2065-2068.
41. Al-Widyan, M. I.; Tashtoush, G.; Abu-Qudais, M. d., Utilization of ethyl ester of waste vegetable oils as fuel in diesel engines. *Fuel Processing Technology* 2002, 76, (2), 91-103.
42. Hattori, H., Solid base catalysts: generation of basic sites and application to organic synthesis. *Applied Catalysis A: General* 2001, 222, (1-2), 247-259.
43. Hideshi, H., Solid base catalysts: Generation, characterization, and catalytic behavior of basic sites. *Journal of the Japan Petroleum Institute* 2004, 47, (2), 67-81.
44. Semwal, S.; Arora, A. K.; Badoni, R. P.; Tuli, D. K., Biodiesel production using heterogeneous catalysts. *Bioresource Technology* 2011, 102, (3), 2151-2161.

45. Dossin, T. F.; Reyniers, M.-F. O.; Berger, R. J.; Marin, G. B., Simulation of heterogeneously MgO-catalyzed transesterification for fine-chemical and biodiesel industrial production. *Applied Catalysis B: Environmental* 2006, 67, (1-2), 136-148.
46. Arzamendi, G., et al., *Synthesis of biodiesel with heterogeneous NaOH/alumina catalysts: Comparison with homogeneous NaOH*. *Chemical Engineering Journal*, 2007. 134(1-3): p. 123-130.
47. Liu, X.; He, H.; Wang, Y.; Zhu, S., Transesterification of soybean oil to biodiesel using SrO as a solid base catalyst. *Catalysis Communications* 2007, 8, (7), 1107-1111.
48. Xie, W.; Huang, X.; Li, H., Soybean oil methyl esters preparation using NaX zeolites loaded with KOH as a heterogeneous catalyst. *Bioresource Technology* 2007, 98, (4), 936-939.
49. Liu, X.; He, H.; Wang, Y.; Zhu, S., Transesterification of soybean oil to biodiesel using SrO as a solid base catalyst. *Catalysis Communications* 2007, 8, (7), 1107-1111.
50. Granados, M. L. P.; Alonso, D. M. N.; Sadaba, I.; Mariscal, R.; Ocan, P., Leaching and homogeneous contribution in liquid phase reaction catalysed by solids: The case of triglycerides methanolysis using CaO. *Applied Catalysis B: Environmental* 2009, 89, (1-2), 265-272.
51. Kouzu, M.; Kasuno, T.; Tajika, M.; Sugimoto, Y.; Yamanaka, S.; Hidaka, J., Calcium oxide as a solid base catalyst for transesterification of soybean oil and its application to biodiesel production. *Fuel* 2008, 87, (12), 2798-2806.
52. Veljkovic, V. B.; Stamenkovic, O. S.; Todorovic, Z. B.; Lazic, M. L.; Skala, D. U., Kinetics of sunflower oil methanolysis catalyzed by calcium oxide. *Fuel* 2009, 88, (9), 1554-1562.
53. Kawashima, A.; Matsubara, K.; Honda, K., Development of heterogeneous base catalysts for biodiesel production. *Bioresource Technology* 2008, 99, (9), 3439-3443.

54. Xie, W.; Yang, Z.; Chun, H., Catalytic Properties of Lithium-Doped ZnO Catalysts Used for Biodiesel Preparations. *Industrial & Engineering Chemistry Research* 2007, 46, (24), 7942-7949.
55. Georgogianni, K. G.; Katsoulidis, A. P.; Pomonis, P. J.; Kontominas, M. G., Transesterification of soybean frying oil to biodiesel using heterogeneous catalysts. *Fuel Processing Technology* 2009, 90, (5), 671-676.
56. Hameed, B.H., L.F. Lai, and L.H. Chin, *Production of biodiesel from palm oil (Elaeis guineensis) using heterogeneous catalyst: An optimized process*. *Fuel Processing Technology*, 2009. 90(4): p. 606-610.
57. Yan, S.; Salley, S. O.; Simon Ng, K. Y., Simultaneous transesterification and esterification of unrefined or waste oils over ZnO-La<sub>2</sub>O<sub>3</sub> catalysts. *Applied Catalysis A: General* 2009, 353, (2), 203-212.
58. Benjapornkulaphong, S.; Ngamcharussrivichai, C.; Bunyakiat, K., Al<sub>2</sub>O<sub>3</sub>-supported alkali and alkali earth metal oxides for transesterification of palm kernel oil and coconut oil. *Chemical Engineering Journal* 2009, 145, (3), 468-474.
59. Faria, E. A.; Ramalho, H. F.; Marques, J. S. S.; Suarez, P. A. Z.; Prado, A. G. S., Tetramethylguanidine covalently bonded onto silica gel surface as an efficient and reusable catalyst for transesterification of vegetable oil. *Applied Catalysis A: General* 2008, 338, (1-2), 72-78.
60. Li, H.; Xie, W., Transesterification of Soybean Oil to Biodiesel with Zn/I<sub>2</sub>; Catalyst. *Catalysis Letters* 2006, 107, (1), 25-30.
61. Mbaraka, I. K.; Radu, D. R.; Lin, V. S. Y.; Shanks, B. H., Organosulfonic acid-functionalized mesoporous silicas for the esterification of fatty acid. *Journal of Catalysis* 2003, 219, (2), 329-336.
62. Jitputti, J.; Kitiyanan, B.; Rangsunvigit, P.; Bunyakiat, K.; Attanatho, L.; Jenvanitpanjakul, P., Transesterification of crude palm kernel oil and crude coconut oil by different solid catalysts. *Chemical Engineering Journal* 2006, 116, (1), 61-66.
63. Sunita, G.; Devassy, B. M.; Vinu, A.; Sawant, D. P.; Balasubramanian, V. V.; Halligudi, S. B., Synthesis of biodiesel over zirconia-supported

- isopoly and heteropoly tungstate catalysts. *Catalysis Communications* 2008, 9, (5), 696-702.
64. Garcia, C. M.; Teixeira, S.; Marciniuk, L. c. L.; Schuchardt, U., Transesterification of soybean oil catalyzed by sulfated zirconia. *Bioresource Technology* 2008, 99, (14), 6608-6613.
  65. Yadav, G. D.; Nair, J. J.; Sulfated zirconia and its modified versions as promising catalysts for industrial processes. *Microporous and Mesoporous Materials* 1999, 33, (1-3), 1-48.
  66. Sherrington, D., Preparation, structure and morphology of polymer supports. *Chemical Communications* 1998, (21), 2275-2286.
  67. Sharma, Y. C.; Singh, B.; Korstad, J., Advancements in solid acid catalysts for ecofriendly and economically viable synthesis of biodiesel. *Biofuels, Bioproducts and Biorefining* 2011, 5, (1), 69-92.
  68. Russbuedt, B. M. E.; Hoelderich, W. F., New sulfonic acid ion-exchange resins for the preesterification of different oils and fats with high content of free fatty acids. *Applied Catalysis A: General* 2009, 362, (1-2), 47-57.
  69. Ozbay, N.; Oktar, N.; Tapan, N. A., Esterification of free fatty acids in waste cooking oils (WCO): Role of ion-exchange resins. *Fuel* 2008, 87, (10-11), 1789-1798.
  70. Talukder, M. M. R.; Wu, J. C.; Lau, S. K.; Cui, L. C.; Shimin, G.; Lim, A., Comparison of Novozym 435 and Amberlyst 15 as Heterogeneous Catalyst for Production of Biodiesel from Palm Fatty Acid Distillate. *Energy & Fuels* 2008, 23, (1), 1-4.
  71. Pasiadis, S.; Barakos, N.; Alexopoulos, C.; Papayannakos, N., Heterogeneously Catalyzed Esterification of FFAs in Vegetable Oils. *Chemical Engineering & Technology* 2006, 29, (11), 1365-1371.
  72. Feng, Y.; He, B.; Cao, Y.; Li, J.; Liu, M.; Yan, F.; Liang, X., Biodiesel production using cation-exchange resin as heterogeneous catalyst. *Bioresource Technology* 2010, 101, (5), 1518-1521.

73. Grob, S.; Hasse, H., Reaction Kinetics of the Homogeneously Catalyzed Esterification of 1-Butanol with Acetic Acid in a Wide Range of Initial Compositions. *Industrial & Engineering Chemistry Research* 2006, 45, (6), 1869-1874.
74. Shibasaki-Kitakawa, N.; Tsuji, T.; Kubo, M.; Yonemoto, T., Biodiesel Production from Waste Cooking Oil Using Anion-Exchange Resin as Both Catalyst and Adsorbent. *BioEnergy Research* 2011, 4, (4), 287-293.
75. Tesser, R.; Casale, L.; Verde, D.; Di Serio, M.; Santacesaria, E., Kinetics and modeling of fatty acids esterification on acid exchange resins. *Chemical Engineering Journal* 2010, 157, (2-3), 539-550.
76. Tsyurupa, M. P.; Davankov, V. A., Hypercrosslinked polymers: basic principle of preparing the new class of polymeric materials. *Reactive and Functional Polymers* 2002, 53, (2-3), 193-203.
77. Davankov, V. A.; Tsyurupa, M. P., Structure and properties of hypercrosslinked polystyrene the first representative of a new class of polymer networks. *Reactive Polymers* 1990, 13, (1-2), 27-42.
78. Castanheiro, J. E.; Ramos, A. M.; Fonseca, I. M.; Vital, J., Esterification of acetic acid by isoamylic alcohol over catalytic membranes of poly(vinyl alcohol) containing sulfonic acid groups. *Applied Catalysis A: General* 2006, 311, (0), 17-23.
79. Guerreiro, L.; Castanheiro, J. E.; Fonseca, I. M.; Martin-Aranda, R. M.; Ramos, A. M.; Vital, J., Transesterification of soybean oil over sulfonic acid functionalised polymeric membranes. *Catalysis Today* 2006, 118, (1-2), 166-171.
80. Rhim, J.-W.; Park, H. B.; Lee, C.-S.; Jun, J.-H.; Kim, D. S.; Lee, Y. M., Crosslinked poly(vinyl alcohol) membranes containing sulfonic acid group: proton and methanol transport through membranes. *Journal of Membrane Science* 2004, 238, (1-2), 143-151.

81. Hino, M.; Arata, K., ChemInform Abstract: Superacids by Metal Oxides. Part 5. Synthesis of Highly Acidic Catalysts of Tungsten Oxide Supported on Tin Oxide, Titanium Oxide, and Iron Oxide. *ChemInform* 1994, 25, (39), 1522-2667.
82. Song, X.; Sayari, A., Sulfated Zirconia-Based Strong Solid-Acid Catalysts: Recent Progress. *Catalysis Reviews* 1996, 38, (3), 329-412.
83. Lopez, D. E.; Goodwin Jr, J. G.; Bruce, D. A.; Lotero, E., Transesterification of triacetin with methanol on solid acid and base catalysts. *Applied Catalysis A: General* 2005, 295, (2), 97-105.
84. Kiss, A. A.; Dimian, A. C.; Rothenberg, G., Biodiesel by Catalytic Reactive Distillation Powered by Metal Oxides. *Energy & Fuels* 2007, 22, (1), 598-604.
85. Garcia, C. M.; Teixeira, S.; Marciniuk, L. c. L.; Schuchardt, U., Transesterification of soybean oil catalyzed by sulfated zirconia. *Bioresource Technology* 2008, 99, (14), 6608-6613.
86. Suwannakarn, K.; Lotero, E.; Goodwin Jr, J. G.; Lu, C., Stability of sulfated zirconia and the nature of the catalytically active species in the transesterification of triglycerides. *Journal of Catalysis* 2008, 255, (2), 279-286.
87. Kansedo, J.; Lee, K. T.; Bhatia, S., Cerbera odollam (sea mango) oil as a promising non-edible feedstock for biodiesel production. *Fuel* 2009, 88, (6), 1148-1150.
88. Matsushashi, H.; Miyazaki, H.; Kawamura, Y.; Nakamura, H.; Arata, K., Preparation of a Solid Superacid of Sulfated Tin Oxide with Acidity Higher Than That of Sulfated Zirconia and Its Applications to Aldol Condensation and Benzoylation<sup>1</sup>. *Chemistry of Materials* 2001, 13, (9), 3038-3042.
89. Ward, D. A.; Ko, E. I., Sol-Gel Synthesis of Zirconia Supports: Important Properties for Generating n-Butane Isomerization Activity upon Sulfate Promotion. *Journal of Catalysis* 1995, 157, (2), 321-333.

90. Babou, F.; Coudurier, G.; Vedrine, J. C., Acidic Properties of Sulfated Zirconia: An Infrared Spectroscopic Study. *Journal of Catalysis* 1995, 152, (2), 341-349.
91. Arata, K.; Hino, M., Preparation of superacids by metal oxides and their catalytic action. *Materials Chemistry and Physics* 1990, 26, (3-4), 213-237.
92. Clearfield, A.; Serrette, G. P. D.; Khazi-Syed, A. H., Nature of hydrous zirconia and sulfated hydrous zirconia. *Catalysis Today* 1994, 20, (2), 295-312.
93. Nair, B. N.; Yamaguchi, T.; Kawamura, H.; Nakao, S.-I.; Nakagawa, K., Processing of Lithium Zirconate for Applications in Carbon Dioxide Separation: Structure and Properties of the Powders. *Journal of the American Ceramic Society* 2004, 87, (1), 68-74.
94. Ida, J.-i.; Lin, Y. S., Mechanism of High-Temperature CO<sub>2</sub> Sorption on Lithium Zirconate. *Environmental Science & Technology* 2003, 37, (9), 1999-2004.
95. Iwan, A.; Stephenson, H.; Ketchie, W. C.; Lapkin, A. A., High temperature sequestration of CO<sub>2</sub> using lithium zirconates. *Chemical Engineering Journal* 2009, 146, (2), 249-258.
96. Ochoa-Fernandez, E.; Ronning, M.; Yu, X.; Grande, T.; Chen, D., Compositional Effects of Nanocrystalline Lithium Zirconate on Its CO<sub>2</sub> Capture Properties. *Industrial & Engineering Chemistry Research* 2007, 47, (2), 434-442.
97. Kato, M.; Yoshikawa, S.; Nakagawa, K., Carbon dioxide absorption by lithium orthosilicate in a wide range of temperature and carbon dioxide concentrations. *Journal of Materials Science Letters* 2002, 21, (6), 485-487.
98. Nair, B. N.; Yamaguchi, T.; Kawamura, H.; Nakao, S.-I.; Nakagawa, K., Processing of Lithium Zirconate for Applications in Carbon Dioxide Separation: Structure and Properties of the Powders. *Journal of the American Ceramic Society* 2004, 87, (1), 68-74.

99. Ding, Y.; Sun, H.; Duan, J.; Chen, P.; Lou, H.; Zheng, X., Mesoporous Li/ZrO<sub>2</sub> as a solid base catalyst for biodiesel production from transesterification of soybean oil with methanol. *Catalysis Communications* 2011, 12, (7), 606-610.
100. Liu, X.; He, H.; Wang, Y.; Zhu, S.; Piao, X., Transesterification of soybean oil to biodiesel using CaO as a solid base catalyst. *Fuel* 2008, 87, (2), 216-221.
101. MacLeod, C. S.; Harvey, A. P.; Lee, A. F.; Wilson, K., Evaluation of the activity and stability of alkali-doped metal oxide catalysts for application to an intensified method of biodiesel production. *Chemical Engineering Journal* 2008, 135, (1-2), 63-70.
102. Iizuka, T.; Hattori, H.; Ohno, Y.; Sohma, J.; Tanabe, K., Basic sites and reducing sites of calcium oxide and their catalytic activities. *Journal of Catalysis* 1971, 22, (1), 130-139.
103. Polshettiwar, V.; Varma, R. S., Green chemistry by nano-catalysis. *Green Chemistry* 2010, 12, (5), 743-754.
104. Shylesh, S.; Schünemann, V.; Thiel, W. R., Magnetically Separable Nanocatalysts: Bridges between Homogeneous and Heterogeneous Catalysis. *Angewandte Chemie International Edition* 2010, 49, (20), 3428-3459.
105. Robinson, P. J.; Dunnill, P.; Lilly, M. D., The properties of magnetic supports in relation to immobilized enzyme reactors. *Biotechnology and Bioengineering* 1973, 15, (3), 603-606.
106. Guo, P.; Huang, F.; Zheng, M.; Li, W.; Huang, Q., Magnetic Solid Base Catalysts for the Production of Biodiesel. *Journal of the American Oil Chemists' Society* 2012, 89, (5), 925-933.
107. Kleine, K.L.; Oladosu, G.A.; Wolfe, A.K.; Perlack, R.D.; V.H.; McMahon, M.; Biofuel Feedstock assessment for selected countries. Oak ridge national laboratory 2007, 224, 163.

# CHAPTER 3

## SULFONATED HYPERCROSSLINKED RESIN AS SOLID ACID CATALYST

---

“In this chapter the use of sulfonated hypercrosslinked resins as solid catalysts for pre-esterification of free fatty acid is described. In addition, the characterization of these catalysts and comparing their activity against conventional sulfonated polystyrene resins are also discussed”.

*The contents of this chapter are summarised in a publication : “Hypercrosslinked polystyrene sulfonic acid catalysts for the esterification of free fatty acids in biodiesel synthesis”. Applied Catalysis B: Environmental, 115-6. (2012) pp. 261-268. ISSN 09263373”*

### 3.1. Overview

New sulfonic acid catalysts supported on hypercrosslinked polystyrene have been studied in the esterification of oleic acid with methanol and in the rearrangement of  $\alpha$ -pinene to camphene and limonenes. The catalysts have been characterised in terms of specific surface areas and porosities, affinities for water and for cyclohexane vapours, and both concentrations and strengths of acid sites. They have been compared with conventional macroporous polystyrene sulfonic acids (Amberlysts-15 and 35) and SAC-13, a composite between Nafion and silica. The results show that the hypercrosslinked polystyrene sulfonic acids, despite exhibiting relatively low concentrations of acid sites and acid site strengths below those of Amberlysts-15 and 35, are very much more catalytically active than conventional resins in reactions such as esterification in which high acid site strengths are not required. It is thought that this is due to the highly accessible acid sites throughout the catalyst particles. Reusability studies are reported and it appears that the temperature at which the catalyst is used is important in controlling and minimising catalyst deactivation.

### 3.2. Introduction

Biodiesel is usually produced by the transesterification of vegetable oil with methanol, converting the triglyceride in the oil to the fatty acid methyl ester (FAME), with glycerol as a by-product [1]. The reaction is conventionally carried out using sodium or potassium hydroxide homogeneous catalysts [2]. Problems arise when the raw materials are low grade oils or used cooking oils because they frequently contain relatively high concentrations of free fatty acids (FFAs). These can form intractable soaps with the catalyst, making subsequent separation of the fuel from the glycerol difficult [3,4]. To prevent this, a pre-esterification step with methanol under acid catalysis can be used to convert the FFA to FAME. Currently, sulphuric acid is often used for this step, but its use requires extensive washing to remove the catalyst [5]. The esterification of FFA, typically oleic acid, is a relative facile reaction and it is not unreasonable to assume that a solid acid catalyst could be used, removing the need for the expensive washing step.

Polystyrene-supported sulfonic acid catalysts have been extensively studied in the direct esterification of free fatty acids and similar reactions [6–12]. They are not amongst the strongest solid acids, but this is of less importance in this reaction than in some others [13]. Most studies of polystyrene sulfonic acid resins have been based on those with permanent macroporosity such as Amberlysts-15, 35 and 36 (sometimes referred to as “macroreticular” resins), although at least one report has shown, surprisingly, that some “gel” resins can exhibit slightly higher activities [6].

Sulfonic acid catalysts on a range of other supports have also been studied, including polyvinyl alcohol [14,15] and activated carbon [16]. Both amorphous and ordered porous silica have been studied extensively as supports for sulfonic acid but, in all cases, only relatively low concentrations of acid groups on the support surface have been achievable, limiting the catalytic activities of these materials [17, 18]. Overall, the relatively high sulfonic acid loadings on polystyrene sulfonic acid resins combined with their ready availability makes these materials particularly attractive as esterification catalysts.

Conventional macroporous polystyrene resins rely on polymer cross-linking with divinylbenzene and the incorporation of an inert porogen compound at the polymerisation stage to impart permanent porosity. A variation on this theme is through the so-called “hypercrosslinked” polystyrene resins. These materials have been studied, mainly by Tsyurupa and Davankov [19], for many years. They are synthesised by carrying out a second crosslinking reaction on polystyrene/divinylbenzene using typically chlorodimethylether with a suitable Friedel-Crafts catalyst. Small angle X-ray diffraction studies have shown that this results in a three dimensional crosslinked polymer network with dramatically enhanced permanent porosity. In fact, if applied to polystyrene resins with existing permanent macroporosity, the additional crosslinking results in additional microporosity in a hierarchical pore structure. These materials exhibit very high surface areas as measured by gas adsorption, of typically  $1000 \text{ m}^2 \text{ g}^{-1}$ .

Most of the reported studies have involved the use of these materials as adsorbents [20] and there is relatively little in the literature on their use as catalyst supports. However, they can be functionalised with sulphuric acid, although not to the same extent as conventional polystyrene/divinylbenzene (since functionalisation tends to be restricted to styrene residues not involved in cross linking). In the present work, two examples of sulfonated hypercrosslinked polystyrene have been studied as acid catalysts. These materials, D5081 and D5082, were made by Purolite International Ltd. and are functionalised at the relatively low levels of nominally 1 mmol g<sup>-1</sup> and 2 mmol g<sup>-1</sup>. For comparison, a standard sulfonated macroporous polystyrene/divinylbenzene resin, Amberlyst-15, has been used. The level of sulfonation is about 4.7 mmol g<sup>-1</sup>, corresponding to approximately one sulfonic acid group per phenyl group in the resin. Amberlyst-35 is similar except that it has been “over-sulfonated” by 10–20%, and this is known to increase the average strength of the supported sulfonic acid groups, through the interaction and activating effects of neighbouring sulfonic acid groups [21]. Finally, Nafion SAC-13 has been used. This is a composite material, combining Nafion (sulfonic acid supported on a fluorinated polymer) and a porous silica. This material is known to exhibit relatively very strong acid sites [22–25].

Two reactions have been used to compare these catalysts. The first is the esterification of oleic acid with methanol to form methyl oleate (Figure 3.1a), representative of the pre-esterification step that is necessary with low grade oils for biodiesel. The role of the acid catalyst is to protonate the oleic

acid and for that reason it is essential that oleic acid is able to access the active sites as well as the methanol if esterification is to occur rather than dehydration of the methanol to form dimethylether.

The second reaction is the acid-catalysed rearrangement of  $\alpha$ -pinene to camphene and limonene (Figure 3.1b). It is used to probe different properties of the catalysts because of the very different nature of the reactant. The driving force for this reaction is the alleviation of strain in the four-membered ring of  $\alpha$ -pinene. This reaction is generally regarded as requiring relatively strong acid sites for effective catalysis [26]. It involves a non-polar reactant, and therefore places quite different requirements on catalysts in terms of their compatibilities with reaction media compared to the esterification reaction which is carried out in an excess of methanol.

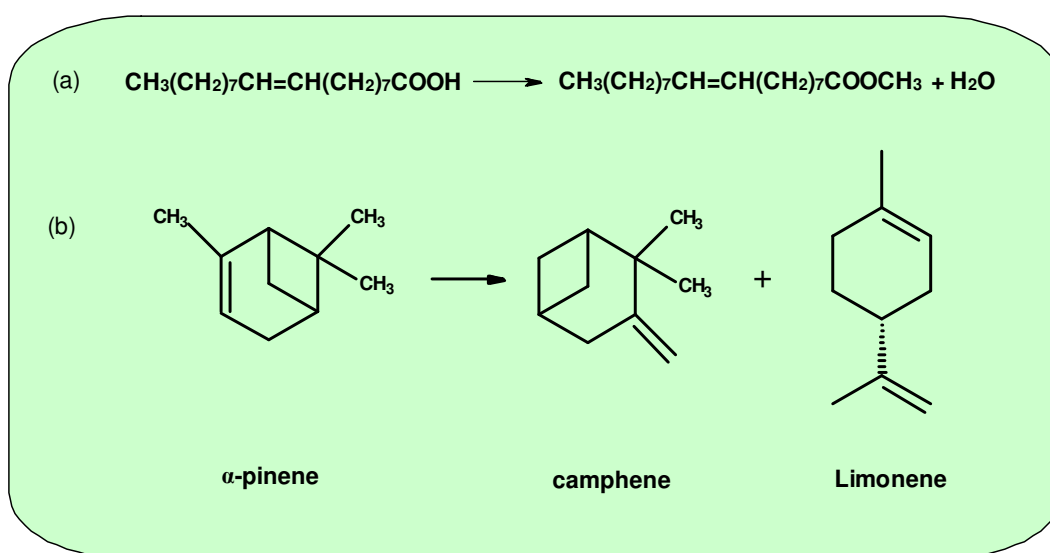


Figure 3.1. (a) Esterification of oleic acid (b) and isomerisation of  $\alpha$ -pinene.

### **3.3. Experimental methods**

#### **3.3.1. Materials**

D5082 and D5081 are sulfonated hypercrosslinked polystyrene resins and were supplied in bead form by Purolite International. Amberlyst-15 and Amberlyst-35 were supplied by Rohm and Haas. In two cases, the resins were used as powders. To prepare powder samples the beads were cooled in liquid nitrogen and, while still cold, ground with a pestle and mortar. The fractions of particle size below 125  $\mu\text{m}$  were used for catalytic testing. Nafion SAC-13 was obtained from Aldrich and is described as containing 13 % (w/w) Nafion [23]. Oleic acid and methanol were obtained from Fluka and  $\alpha$ -pinene from Aldrich.

#### **3.3.2. Catalyst characterization**

Nitrogen adsorption experiments were conducted using a Micromeritics ASAP 2020. Adsorption and desorption isotherms were recorded at 77 K after degassing at 80  $^{\circ}\text{C}$  (Picture of the apparatus and the operating conditions shown in APPENDIX-B). Surface areas were calculated from the adsorption isotherms using the BET method. Desorption isotherms were used to calculate pore volumes and mean pore diameters using the BJH method. The surface morphology of the resins was investigated using a JEOL JSM 6600 scanning electron microscope. The images were taken with 20 mA emission current and 12 kV accelerator voltages. The resins were secured on brass stubs with carbon conductive tape, and coated with gold.

Catalyst acidity was characterised by ammonia adsorption calorimetry, under flow conditions, using a system based on a flow-through Setaram 111 differential scanning calorimeter and an automated gas flow and switching system, with a mass spectrometer (Hiden HPR20) connected via a heated capillary (at 175 °C) for down-stream gas flow detection [27]. Picture of the apparatus and the operating conditions are shown in APPENDIX-C.

In a typical experiment the sample (20-50 mg) was activated under dry nitrogen (5 ml min<sup>-1</sup>) for 1 h at 100 °C. Small pulses (typically 1 ml) of the probe gas (1% ammonia in nitrogen) were then injected into the carrier gas stream from a gas sampling valve at the same temperature, monitoring the concentration of ammonia (using m/z-15) downstream of the sample. An important feature of the flow calorimetric technique is that net heat measurements relate only to ammonia bound irreversibly to the samples. Reversibly (weakly) bound ammonia desorbs immediately the gas flow reverts to the carrier gas. The net amount of ammonia irreversibly adsorbed from each pulse was determined by comparing the mass spectrometer signals with a signal recorded during a control experiment through an empty sample tube. The molar enthalpy of ammonia adsorption ( $\Delta H^{\circ}_{\text{ads}}$ ) was calculated for each pulse. Data are plotted as a profile of  $\Delta H^{\circ}_{\text{ads}}(\text{NH}_3)$  vs. amount of ammonia irreversibly adsorbed.

The concentration of acid sites on each of the catalysts was determined by aqueous titration with 0.10 or 0.010 mol dm<sup>3</sup> NaOH solution

following exchange with sodium ions from a 2.0 mol dm<sup>3</sup> sodium chloride solution. Cyclohexane and water vapour adsorption isotherms were measured on the two hypercrosslinked resins and the two Amberlyst resins, all in bead form, and the SAC-13 in its as-supplied form, using a Surface Measurement Systems Dynamic Vapor Sorption apparatus (Advantage™), using a method described by Hill et al. [28]. Adsorption isotherms were recorded at 25 °C, following activation of the catalysts at 100 °C. The apparatus and the operating conditions are shown in APPENDIX-D.

### 3.3.3. Catalyst testing

Catalytic activity measurements were conducted in a 50 ml batch reactor equipped with a reflux condenser and magnetic stirrer (APPENDIX-E). Stirrer speeds were set at 600 rpm, a speed at which the rates of reaction showed no stirrer speed dependence, verifying that they were not under mass transfer control. For the esterification reaction 4.0 g oleic acid and 20 g methanol were heated to the reaction temperature of 65 °C. Catalyst (0.20 g) was activated at 80 °C for 1 h and then added to the reactant mixture. Aliquots were taken before addition of the catalyst and during the reaction. The FFA content was measured using a standard titration method with aqueous 0.25 M NaOH solution and phenolphthalein indicator, adding anhydrous ethanol to ensure miscibility (AOCS official method Cd 3d-63).

For the isomerisation of  $\alpha$ -pinene, 10.0 g  $\alpha$ -pinene was charged to the reactor and heated to the reaction temperature of 120 °C [26]. Catalyst (0.20 g) was activated at 120 °C for 1 h and then added to the reactant. Small

aliquots were withdrawn periodically and analysed by GC using a 25 m BPI column at 2 ml min<sup>-1</sup> helium flow. The oven temperature was held at 60 °C for 15 min and then increased to 290 °C at 20 °C min<sup>-1</sup>. Gas chromatography apparatus used in the experiment shown in APPENDIX - F . The reaction was monitored in terms of the conversion of  $\alpha$ -pinene, using n-decane as an internal standard. Further studies were carried out based on the esterification of oleic acid, to test for catalyst leaching and catalyst reusability. The possibility of acid species leaching to the reactant solution was eliminated by removing catalyst (this test was performed using D5081 and D5082) from a partially converted reaction mixture and verifying that the reaction ceased. Catalyst reusability was tested for D5081 in the oleic acid esterification reaction. Used catalyst was washed in methanol, dried, re-activated and re-tested with fresh reactant mixture. Also, the activity of used catalyst after regeneration by stirring in 1.0 mol dm<sup>3</sup> H<sub>2</sub>SO<sub>4</sub> solution overnight followed by washing, drying and re-activating was measured. The specific surface areas of the used and the regenerated catalysts were measured, along with the acid site concentrations by titration. Additional reusability tests were carried out following the same reaction, but this time at the higher temperature of 85 °C, using a stirred (1000 rpm) Autoclave Engineers (APPENDIX-G) closed reactor, with the same reactant and catalyst concentrations. In these experiments, oleic acid conversion after 1 h was measured, the catalyst was washed in methanol and dried, and, using fresh reactant mixture with used catalyst, the reaction was run again. The process was repeated four times.

### 3.4. Results

#### 3.4.1. Catalyst characterization

Table 3.1 shows specific surface areas and pore volumes of the catalysts. The surface areas of the hypercrosslinked resins are very much higher than those of the simple macroporous resins. As mentioned above, the surface areas of the hypercrosslinked polymer before sulfonation, as measured by nitrogen adsorption, are even higher, approaching  $1000 \text{ m}^2 \text{ g}^{-1}$ . It is worth saying, however, that the idea of a conventional surface in an open polymer network of this type requires careful interpretation, and the link between the amount of nitrogen that can be adsorbed and a meaningful surface area is not as obvious as it might be [19]. Notwithstanding this reservation, the pore volumes and the mean pore diameters of the hypercrosslinked resin by nitrogen adsorption/desorption are similar to those of the Amberlyst resins. However, the pore size distributions for the hypercrosslinked resins, although not shown, are typically very different. They are usually bimodal, with one maximum in the macropore range and a second in the micropore range arising from the additional cross-linking [19,20].

Table 3.1. Characteristic supported resin sulfonic acid catalysts.

Catalyst	specific surface area ( $\text{m}^2 \text{ g}^{-1}$ )	Pore volume ( $\text{cm}^3 \text{ g}^{-1}$ )	Average pore diameter (nm)	acid site concentration (by titration) ( $\text{mmol g}^{-1}$ )	$\text{NH}_3$ adsorbed ( $\text{mmol g}^{-1}$ )
Amberlyt-15	53	0.4	30	4.7	4.9
Amberlyst-35	50	0.35	30	5.4	5.5
Nafion SAC-13	196	0.6	10	0.15	0.12
Purolite D5082	381	0.34	27	2.0	1.2
Purolite D5081	701	0.39	19	1.0	0.8

The SEM images of cross-sectioned beads of Amberlyst-15 and of D5082 in Figure 3.2 illustrate the different surface textures of the conventional macroporous and the hypercrosslinked polystyrene resins. Even on the scale of the micrographs, some pores can be seen on the surface of the hypercrosslinked resin where none is visible on the conventional macroporous resin. This supports the notion of a much broader pore size distribution in the hypercrosslinked material, although it is somewhat surprising to see pores of quite such large diameters (100–300 nm) when conventional macroporous resins exhibit a relatively narrow distribution of pore size centred around 30–40 nm diameter.

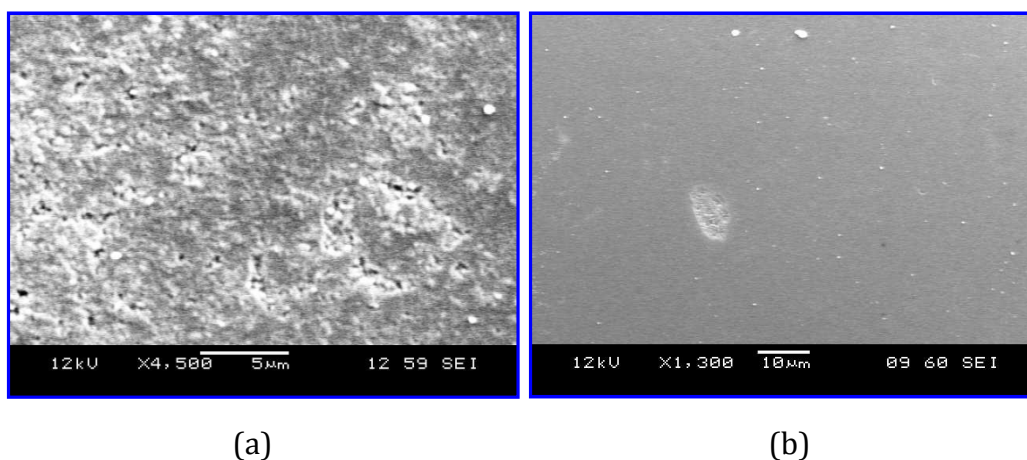


Figure 3.2. Scanning electron microscope images of: (a) D5082 (hypercrosslinked resin) and (b) Amberlyst-35 (macroporous resin).

The relative concentrations of acid sites on each of the catalysts are also shown in table 3.1, as measured by aqueous titration and by ammonia adsorption. There is broad agreement between concentrations determined in

the two ways and the values are all close to the sulfonic acid concentrations quoted by the manufacturers. The acid concentrations vary from 5.40 mmol g<sup>-1</sup> for the over-sulfonated Amberlyst-35 down to 0.15 mmol g<sup>-1</sup> for the SAC-13 composite material, in line with the known acid site concentration on pure Nafion of 0.89 mmol g<sup>-1</sup> and the Nafion loading in the composite of 13% (w/w) [23]. These differences in acid site density have to be taken into account when considering catalytic activities, which have initially been compared based on the weight of catalysts.

### 3.4.2. Catalyst testing

Figures 3.3 and 3.4 show the rate plots for the two test reactions with the five catalysts. Initial turnover frequencies (TOFs) are given in Table 3.2. These are based on the concentrations of active sites determined by aqueous titration.

Table 3.2. TOF for the catalysts in isomerisation and esterification reactions.

Catalyst	TOF (h <sup>-1</sup> )	
	Isomerisation	Esterification
Purolite D5081	37	65
Purolite D5082	52	26
Amberlyst-15	113	4.8
Amberlyst-35	118	2.4
Nafion SAC-13	740	80

Note: TOF calculation, see APPENDIX-H

The important point to note is that the order of the catalysts in terms of activity is reversed in the two reactions. In the more demanding  $\alpha$ -pinene reaction the two Amberlyst resins with relatively high concentrations of acid sites are the most active, with the over-sulfonated Amberlyst-35 more active

than Amberlyst-15. The two hypercrosslinked materials are very much less active and show lower turnover frequencies. The catalyst with the highest turnover frequency is SAC-13, with a value six times higher than any of the other.

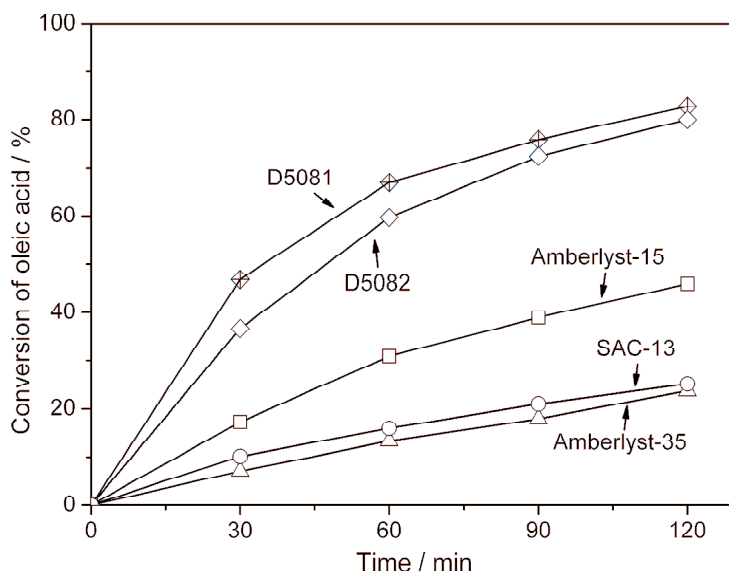


Figure 3.3. Esterification of oleic acid using solid acids catalyst at 65 °C.

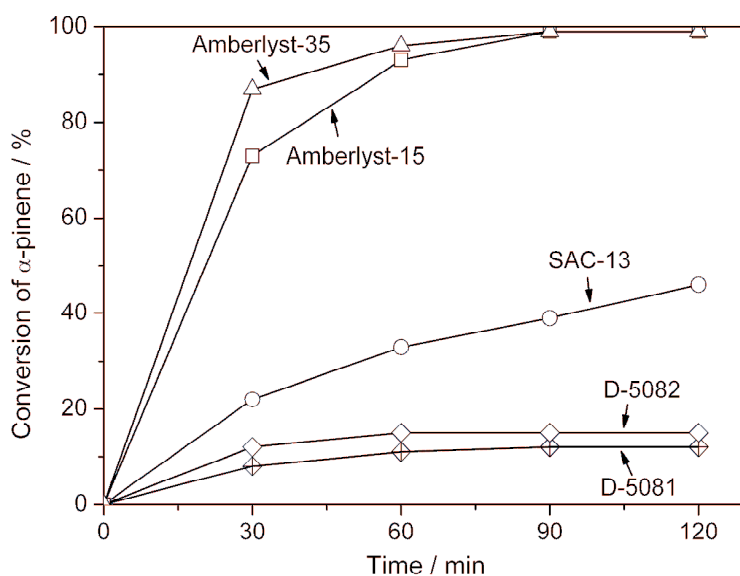


Figure 3.4. Isomerisation reaction of  $\alpha$ -pinene using solid acid catalysts.

In the more facile esterification reaction, the highest activities are exhibited by the hypercrosslinked materials and, in terms of turnover frequencies they show very much higher activities than the macroporous Amberlyst resins. D5081, with the lower concentration of acid sites, is the more active of the two. In this reaction even SAC-13 shows a turnover frequency only slightly higher than that of this hypercrosslinked resin.

In Figures 3.5 and 3.6 the effect of reducing the particle size of the resin catalysts on their activities in the esterification reaction is shown for hypercrosslinked D5081 and for macroporous Amberlyst-15, through comparisons between bead and powder forms of the catalysts. No dependence on particle size is seen for the hypercrosslinked resin, confirming the absence of reaction rate diffusion control, but a significant increase in rate is seen when the Amberlyst resin is used in powder form compared to bead form. This has been observed before for conventional macroporous resins. It is worth saying however that in bead form their catalytic properties are not generally found to be consistent with a diffusion controlled reaction rate, and this is thought to be because catalysis is dominated by acid sites close to the surface of the resins and, even though in bead form only a fraction of the sites are easily accessible in this way, the kinetics of reaction at this limited number of sites is not diffusion limited [13].

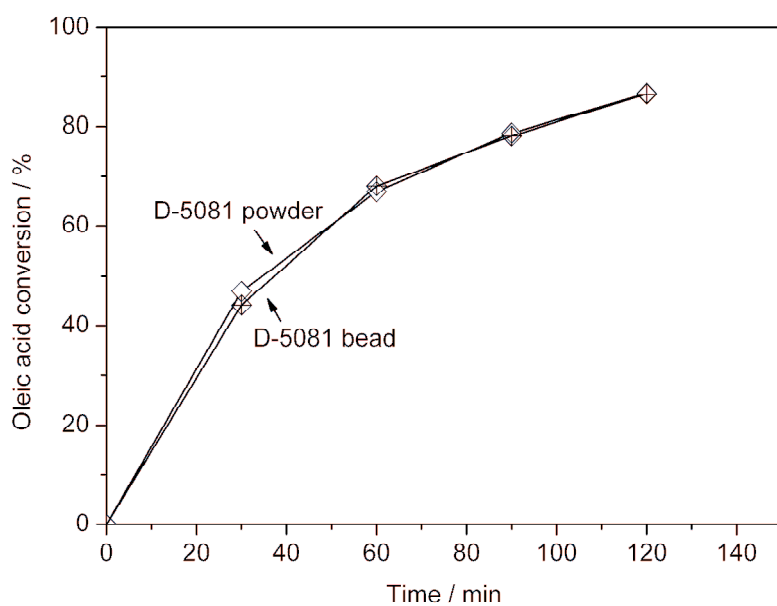


Figure 3.5. The effect of reducing the particle size of the resin catalysts on their activities in the esterification reaction for the hypercrosslinked resin D5081 at 65 °C.

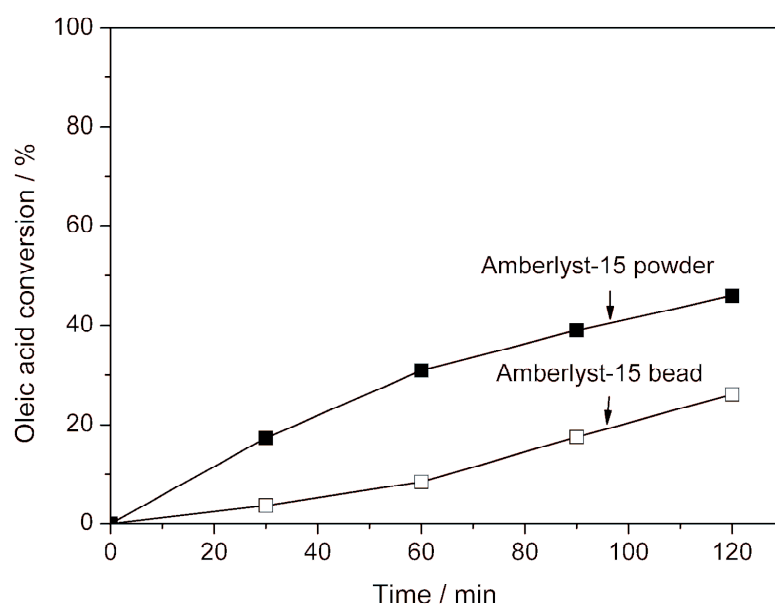


Figure 3.6. The effect of reducing the particle size of the resin catalysts on their activities in the esterification reaction for Amberlyst-15.

### 3.3.3. Catalyst reusability

A summary of the results of the reusability tests carried out on D5081 in the oleic acid esterification reaction appear in Figure 3.7. When the reaction is carried out at 65 °C, catalytic activity is substantially lost after one reaction. The used catalyst has a reduced surface area and reduced acid site concentration. Regeneration with H<sub>2</sub>SO<sub>4</sub> solution results in the recovery of about 90% of the surface area and complete recovery of acid concentration, but catalytic activity remains slightly reduced. In remarkable contrast to this, if the reaction is carried out at the higher temperature of 85°C, washing in methanol results in almost complete recovery of original activity, and, most importantly, the activity remains stable on repeated use (Figure 3.8).

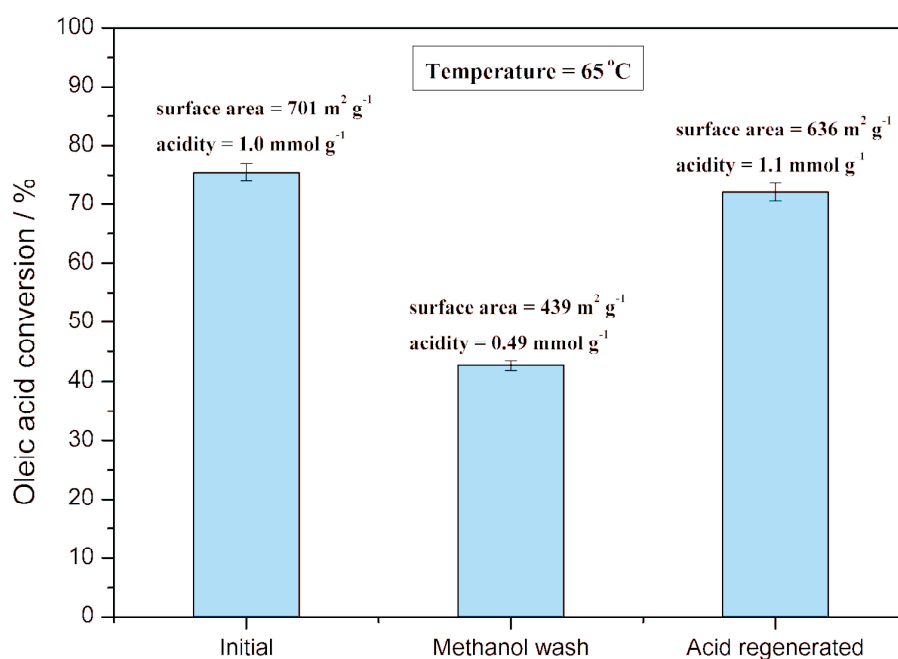


Figure 3.7. Reusability tests carried out on D5081 in the oleic acid esterification reaction at 65 °C with different reaction conditions.

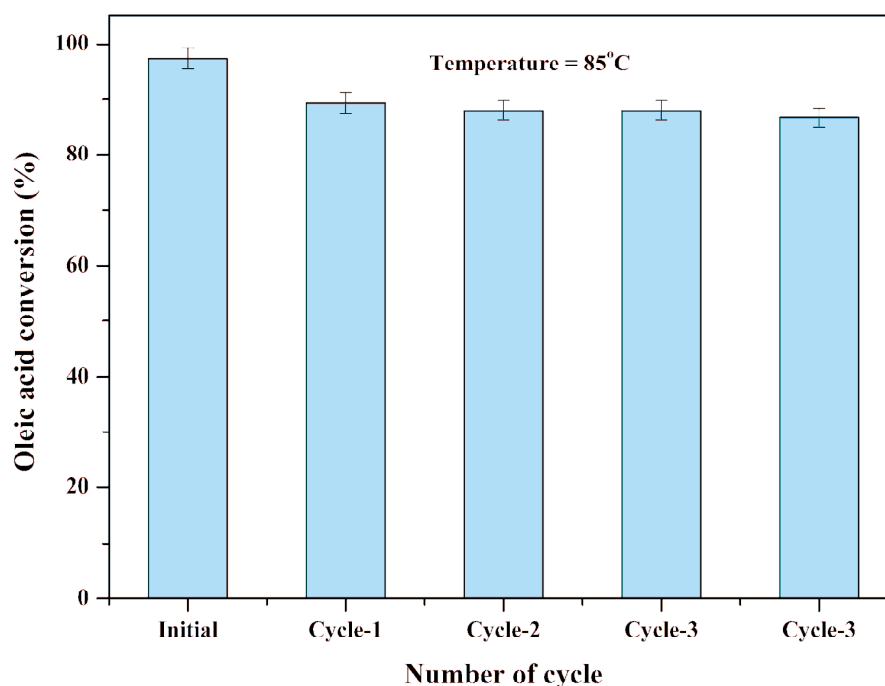


Figure 3.8. Reusability tests carried out on D5081 in oleic acid esterification reaction at 85 °C.

### 3.3.4. Vapour sorption

Figures 3.9 and 3.10 show the adsorption isotherms for cyclohexane and for water vapours for the catalysts. Water uptake is generally higher than cyclohexane uptake, not surprisingly given the presence of hydrophilic sulphonate groups on all catalysts. But the important feature of this data is that the order of catalysts in terms of their adsorption capacities is reversed for the two solvent vapours. There is a broad correlation between the level of sulfonation and water uptake and an inverse relationship with cyclohexane uptake suggesting, as expected, that the hydrophilicity/hydrophobicity of these resins is directly dependent on the degree of sulfonation.

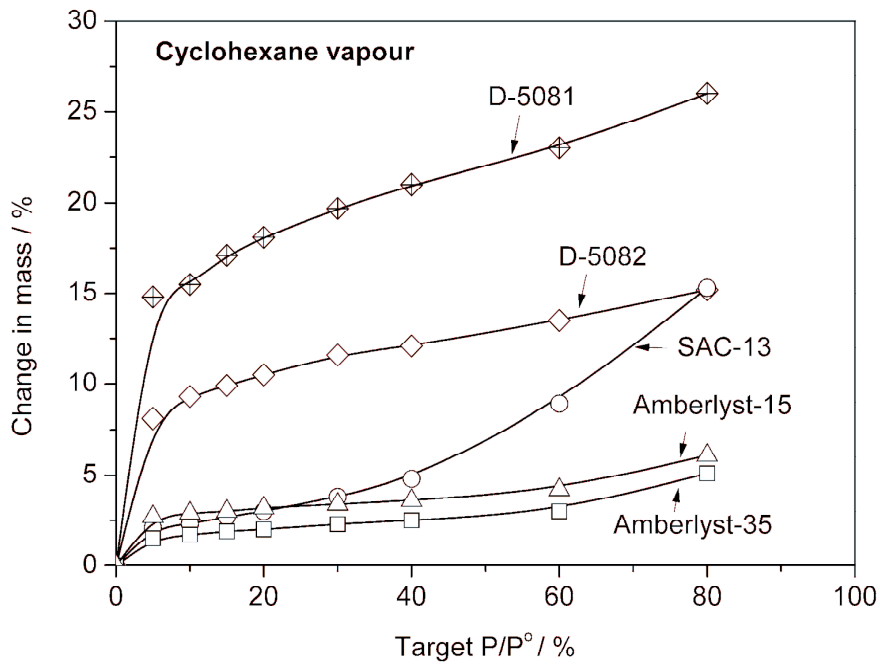


Figure 3.9. The adsorption isotherms for cyclohexane vapours for the catalysts.

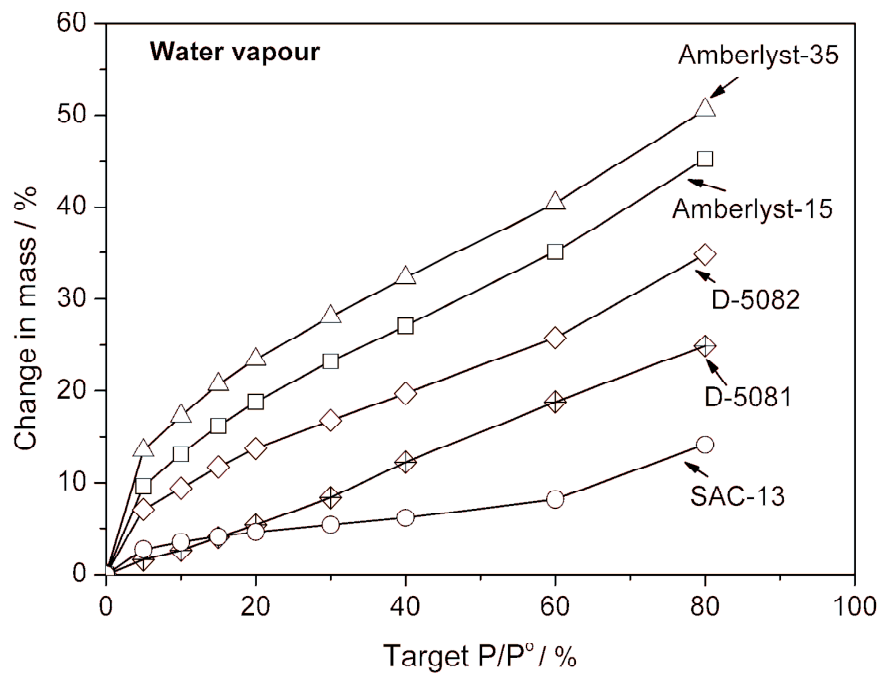


Figure 3.10. The adsorption isotherms for water vapours for the catalysts.

### 3.3.5. Ammonia adsorption calorimetry

Figure 3.11 shows the molar enthalpy of ammonia adsorption plotted against the amount of adsorbed ammonia for all the catalysts. On the assumption that ammonia adsorbs stoichiometrically on acid sites and that only sites that adsorb with enthalpies greater than  $80 \text{ kJ mol}^{-1}$  are significantly acidic, the concentrations of acid sites can be determined [29,30]. These values appear in Table 3.1 and can be compared with the acid site concentrations determined by aqueous titration. The values determined by the two methods are similar for the two Amberlyst resins and for Nafion SAC-13, justifying this assumption and confirming that if a Bronsted acid site is able to exchange with sodium ions from aqueous solution (as in the NaOH titration method), it is also accessible to ammonia adsorbed on a dry catalyst from the gas phase. This is not entirely expected for the macroporous Amberlyst 15 and 35 resins, for which most of the acid groups must be within the polymer matrix and not on the immediate surface. Evidently ammonia is able to diffuse into the polymer matrix, even in its anhydrous state, to react with all the acid sites. This is significant in reviewing these macroporous resins as catalysts in terms of the facility with which other reactant compounds might diffuse to acid sites within the polymer.

It is surprising that the acid site concentrations determined by ammonia adsorption for the two hypercrosslinked resins are, in contrast, significantly lower than the concentrations determined by aqueous titration, especially in view of the enhanced acid site accessibilities in these resins discussed later. It would have been reasonable to expect that ammonia could

react with all acid sites. Indeed, it seems highly unlikely that reaction between acid sites and ammonia would be restricted in any way. A rather speculative explanation for these apparently low acid site concentrations for D5081 and D5082 is that some of the acid sites in these resins may be weaker than expected and, although they react with ammonia, the enthalpies of reaction fall below the  $80 \text{ kJ mol}^{-1}$  cut-off that we have used to define acid sites.

In terms of acid strength, it is assumed that the differential enthalpy of adsorption is a measure of acid site strength and that the profile of this value plotted against the amount of ammonia adsorbed is related to the acid site strength distribution for the catalyst. On this basis, Amberlyst-35 exhibits significantly stronger acid sites than Amberlyst-15. This has been observed before and has been put down to close-neighbour sulfonic acid groups activating each other to a greater extent on the over-sulfonated resin than on the stoichiometrically sulfonated material. This results in enhanced activity for Amberlyst-35 in reactions requiring strong acid sites for catalysis. In contrast, the hypercrosslinked polystyrene sulfonic acid resins exhibit significantly weaker acid sites than the two Amberlyst resins, with D5081 showing weaker sites than D5082. This is consistent with the relatively large separations between acid groups in the hypercrosslinked resins and reduced interactions between neighbouring sulfonic acid groups. Similar observations have been made for sulfonic acids on other supports at high and low loadings [31]. The Nafion composite material exhibits a relatively low concentration of acid sites, as expected, but they are significantly stronger than those of the

other catalysts, as a consequence of the electron withdrawing properties of the fluorinated polymer support.

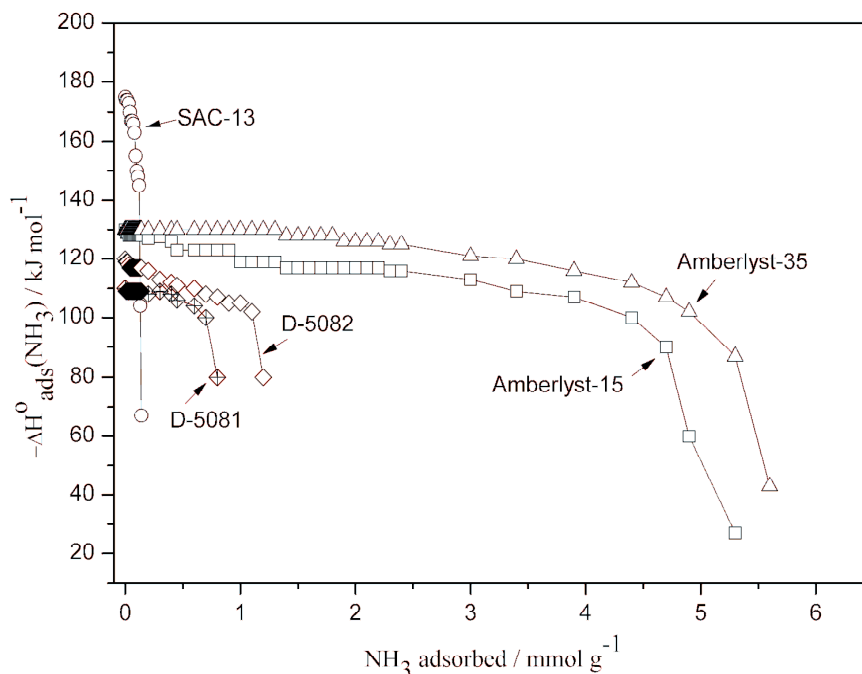


Figure 3.11. The molar enthalpy of ammonia adsorption plotted against the amount of adsorbed ammonia for all the catalysts.

### 3.5. Discussion

Comparing catalytic activities as turnover frequencies with acidity data shows that there is a broad correlation between activity and acid site strength for the  $\alpha$ -pinene reaction, with the significantly stronger acid sites on Nafion resulting in dramatically higher activity than for any of the other catalysts. The two Amberlyst catalysts show similar activities in line with their intermediate acid strengths, and the sulfonated hypercrosslinked resins show the lowest turnover frequencies and the weakest acid sites.

It appears that the strength of acid sites is a major factor in controlling activity in this reaction. The other factor that might have been expected to be important is the hydrophobicity of the catalyst, since  $\alpha$ -pinene is a completely non-polar hydrocarbon. But, on the basis that cyclohexane vapour adsorption is an indicator of hydrophobicity, it is clear that this is a less important factor than catalyst acid strength; indeed, the most active catalysts are the least hydrophobic.

For the esterification reaction the order is very different. Nafion SAC-13 again exhibits the highest turnover frequency, but only just. The surprising observation is that the hypercrosslinked resin catalysts are almost as active, with D5081 with the lower level of sulfonation showing the higher activity of this pair. The turnover frequencies for the hypercrosslinked catalysts are dramatically higher than those for the macroporous Amberlysts-15 and 35 and, even based on catalyst weight, D5081 and D5082 are much more active than the Amberlysts. There is no correlation between activity of the catalysts and their acid site strengths. The catalyst with the weakest acid sites shows the second highest activity, only slightly lower than that of SAC-13. It is striking that the turnover frequency for D5081 in this reaction is comparable with those of a series of cesium-exchanged silicotungstic heteropolyacids acid catalysts studied earlier for the esterification of palmitic acid [32]. These heteropolyacids are regarded as relatively strong solid acids but with relatively low concentrations of acid sites compared to the catalysts studied in this work.

The reaction is carried out in excess methanol and the catalytic step is the protonation of oleic acid, so it would not be unreasonable to expect a correlation between activity in the esterification reaction and catalyst hydrophilicity. However, based on the data in Figure 3.8, there is no apparent relationship between these two. Furthermore, the pronounced particle size dependence of esterification activity for Amberlyst-15, one of the two most hydrophilic resins, suggests that the accessibility of its catalytic sites to methanol is not as might be expected from its affinity for water. Evidently Amberlyst-15 is not sufficiently hydrophilic to render all acid sites accessible to methanol, in bead form at least. In contrast, the activity of the most hydrophobic resin, hypercrosslinked D5081, shows no dependence on particle size, suggesting that, even in bead form, all the acid sites on this resin are accessible to methanol. Evidently the hypercrosslinked structure of D5081 (and D5082) results in significantly better accessibility for reactant molecules to sulfonic acid groups than exists in conventional sulfonated macroporous polystyrene (Amberlyst-15 and 35).

It appears that only a fraction of the sulfonic acid groups in Amberlyst resins are readily accessible to methanol, even when fully solvated. This fraction is increased when the material is used in powder rather than in bead form. Now, the initial esterification reaction rates in the presence of Amberlyst-15 in bead and in powder form can be estimated from Figure 3.5 and, roughly, the powder seems to be about ten times more active than the bead form. If this is the case then it means that ten times more acid sites are accessible in the powder form. It follows that a maximum of 10% of the acid

sites on Amberlyst-15 are accessible to methanol when in bead form. Amberlyst-15 contains a total of 4.7 mmol g<sup>-1</sup> acid sites so this means that catalysis relies on a sulfonic acid concentration of, at most, only 0.47 mmol g<sup>-1</sup> when used in bead form. The behaviour of the hypercrosslinked polystyrene catalyst contrasts with this. If, as seems the case from the absence of any particle size dependence of the activity, all the acid sites are accessible, then it is obvious why the activity of these resins is higher than the Amberlysts, at least in reactions where the strength of acid sites is not a crucial factor. It is simply down to the accessibilities of all acid sites to reactant compounds, even when the catalyst is used in bead form.

A comparison between the two hypercrosslinked catalysts shows D5081 to exhibit a very much higher turnover frequency than D5082 in the esterification reaction, but a lower value in the  $\alpha$ -pinene rearrangement. The TOFs in the  $\alpha$ -pinene broadly correlate with the strengths of the acid sites as mentioned above. But in the esterification reaction, the much higher TOF for D5081 could be linked to the higher specific surface area of this catalyst, which is almost twice that of D5082. Based on these two materials, it appears that progressive functionalisation reduces the available surface area. This may be a result of acid groups, or solvated acid groups, blocking some of the network of micropores in the hypercrosslinked structure but, whatever the reason, it clearly points to the need for a careful balance between surface area and sulfonic acid loading if optimum catalytic activity is to be achieved. The data for the two test reactions used here suggests that optimum loadings

differ depending on the reaction to be catalysed and the reaction medium in which the catalyst is to be used.

Catalyst reusability is addressed for D5081 in the oleic acid esterification reaction and we show that activity is significantly and irreversibly reduced after just one use when the reaction temperature is 65 °C, but activity is maintained when reaction temperature of 85 °C is used. The reason for loss in activity is not certain but it could be related to the blockage of the fine pores in the hypercrosslinked resin by large fatty acid molecules, possibly even oligomerised forms of the acid. It is suggested that at 65 °C these molecules deposit in the pores. They are not effectively removed by methanol washing but prolonged washing with mineral acid does indeed have some effect. It is tempting to think that the reduction in measureable acidity in the resins after use is an indication of ion-exchange from the reactant mixture but the reactants used in this work were essentially free of contaminant cations so this possibility cannot explain the loss in acid concentration. It is more likely that the low measureable acidity in used resins is also a result of pore blockage and reduced accessibility of a proportion of the acid sites. Russbuel and Hoelderich studied the deactivation of sulfonic acid ion-exchange resin catalysts for similar esterification reactions in some detail, but largely using natural vegetable oils spiked with additional fatty acids [6]. These workers proposed that it was ion-exchange of  $\text{Na}^+$ ,  $\text{K}^+$ ,  $\text{Mg}^{2+}$  and  $\text{Ca}^{2+}$  from the oils that was responsible for loss in activity but, even when using cation-free oils, some activity was lost, so this result is not inconsistent with our findings.

At the higher temperature of 85 °C, we suggest that pore blockage does not occur, or at least not to the same extent, and activity is retained for multiple cycles without the need for catalyst regeneration. It is possible that fatty acid diffusion is now fast enough to prevent deposition. We note that Banavali et al. reported the use of Amberlyst BD20 for the esterification of free fatty acids in oils with methanol at the same temperature of 85 °C [33]. Using temperatures above the boiling point of methanol adds complication to the process, so we wonder whether this too may be linked to possible deactivation of catalysts at lower temperatures.

For practical application of sulfonated hypercrosslinked polystyrene catalysts for the esterification of free fatty acids in biodiesel synthesis, reaction conditions must be set to avoid significant catalyst deactivation. We show here that running the reaction at elevated temperature is one solution. However, we observe that, in a single reaction, the oleic acid conversion vs time plot at the more practical reaction temperature of 65 °C (Figure 3.3) does not show that the catalyst is losing significant activity during the course of the reaction. And yet, on re-use, activity is massively diminished. It is possible that catalyst poisoning occurs when the reaction is stopped, the mixture cooled, and the catalyst removed. If this is the case, then using these new resin catalysts in a continuous flow reactor, rather than under batch conditions, may allow for better activity retention, without having to resort to elevated reaction temperatures.

### **3.6. Conclusions**

Acid site accessibility in sulfonated hypercrosslinked polystyrene resins appear to be significantly higher than for conventional polystyrene/divinylbenzene sulfonic acids, and facile diffusion to these sites is possible even for large reactant molecules such as oleic acid. The level to which these hypercrosslinked polymer supports can be functionalised with sulfonic acid is lower than for conventional cross-linked polystyrene, and the acid strengths are lower than those of typical conventional sulfonated polystyrene. But in acid-catalysed reactions where very high acid strengths are not required, the advantages of excellent acid site accessibility can result in higher activity than other typical solid acid catalysts. The high activity exhibited by these catalysts towards oleic acid esterification points to their possible use in many reactions, including the pre-treatment step in the synthesis of biodiesel from low grade oils with high free fatty acid contents.

### ***Acknowledgements***

The help over of Dr Jim Dale of Purolite International, who passed away early in 2011, is most gratefully acknowledged. The help from Liz Dawson for vapour sorption analysis is also most appreciated.

## References

1. Melero, J. A.; Iglesias, J.; Morales, G., Heterogeneous acid catalysts for biodiesel production: current status and future challenges. *Green Chemistry* 2009, 11, (9), 1285-1308.
2. Ma, F.; Hanna, M. A., Biodiesel production: a review. *Bioresource Technology* 1999, 70, (1), 1-15.
3. Wang, Y.; Ou, S.; Liu, P.; Xue, F.; Tang, S., Comparison of two different processes to synthesize biodiesel by waste cooking oil. *Journal of Molecular Catalysis A: Chemical* 2006, 252, (1-2), 107-112.
4. Canakci, M.; Van Gerpen, J., Biodiesel production from oils and fats with high free fatty acids. *Transactions of the American Society of Agricultural Engineers* 2001, 44, (6), 1429-1436.
5. Zhang, Y.; Dube, M. A.; McLean, D. D.; Kates, M., Biodiesel production from waste cooking oil: 1. Process design and technological assessment. *Bioresource Technology* 2003, 89, (1), 1-16.
6. Russbueltdt, B. M. E.; Hoelderich, W. F., New sulfonic acid ion-exchange resins for the preesterification of different oils and fats with high content of free fatty acids. *Applied Catalysis A: General* 2009, 362, (1-2), 47-57.
7. Ozbay, N.; Oktar, N.; Tapan, N. A., Esterification of free fatty acids in waste cooking oils (WCO): Role of ion-exchange resins. *Fuel* 2008, 87, (10-11), 1789-1798.
8. Marchetti, J. M.; Miguel, V. U.; Errazu, A. F., Heterogeneous esterification of oil with high amount of free fatty acids. *Fuel* 2007, 86, (5-6), 906-910.
9. Talukder, M. M. R.; Wu, J. C.; Lau, S. K.; Cui, L. C.; Shimin, G.; Lim, A., Comparison of Novozym 435 and Amberlyst 15 as Heterogeneous Catalyst for Production of Biodiesel from Palm Fatty Acid Distillate. *Energy & Fuels* 2008, 23, (1), 1-4.

10. Pasiás, S.; Barakos, N.; Alexopoulos, C.; Papayannakos, N., Heterogeneously Catalyzed Esterification of FFAs in Vegetable Oils. *Chemical Engineering & Technology* 2006, 29, (11), 1365-1371.
11. Kouzu, M.; Kasuno, T.; Tajika, M.; Sugimoto, Y.; Yamanaka, S.; Hidaka, J., Calcium oxide as a solid base catalyst for transesterification of soybean oil and its application to biodiesel production. *Fuel* 2008, 87, (12), 2798-2806.
12. Lundquist E., *Catalyzed esterification process*. US Patent 5,426,199, 1999.
13. Siril, P. F.; Davison, A. D.; Randhawa, J. K.; Brown, D. R., Acid strengths and catalytic activities of sulfonic acid on polymeric and silica supports. *Journal of Molecular Catalysis A: Chemical* 2007, 267, (1-2), 72-78.
14. Caetano, C. S.; Guerreiro, L.; Fonseca, I. M.; Ramos, A. M.; Vital, J.; Castanheiro, J. E., Esterification of fatty acids to biodiesel over polymers with sulfonic acid groups. *Applied Catalysis A: General* 2009, 359, (1-2), 41-46.
15. Pito, D. S.; Fonseca, I. M.; Ramos, A. M.; Vital, J.; Castanheiro, J. E., Methoxylation of  $\alpha$ -pinene over poly(vinyl alcohol) containing sulfonic acid groups. *Chemical Engineering Journal* 2009, 147, (2-3), 302-306.
16. Mo, X.; Lotero, E.; Lu, C.; Liu, Y.; Goodwin, J., A Novel Sulfonated Carbon Composite Solid Acid Catalyst for Biodiesel Synthesis. *Catalysis Letters* 2008, 123, (1), 1-6.
17. Mbaraka, I. K.; McGuire, K. J.; Shanks, B. H., Acidic Mesoporous Silica for the Catalytic Conversion of Fatty Acids in Beef Tallow. *Industrial & Engineering Chemistry Research* 2006, 45, (9), 3022-3028.
18. Melero, J. A.; Bautista, L. F.; Morales, G.; Iglesias, J.; Sánchez-Vázquez, R., Biodiesel production from crude palm oil using sulfonic acid-modified mesostructured catalysts. *Chemical Engineering Journal* 2010, 161, (3), 323-331.

19. Tsyurupa, M. P.; Davankov, V. A., Porous structure of hypercrosslinked polystyrene: State-of-the-art mini-review. *Reactive and Functional Polymers* 2006, 66, (7), 768-779.
20. Oh, C.-G.; Ahn, J.-H.; Ihm, S.-K., Adsorptive removal of phenolic compounds by using hypercrosslinked polystyrenic beads with bimodal pore size distribution. *Reactive and Functional Polymers* 2003, 57, (2-3), 103-111.
21. Siril, P.F., Cross, H.E., and Brown, D.R., *New polystyrene sulfonic acid resin catalysts with enhanced acidic and catalytic properties*. *J. Molec. Catal. A.*, 2008. 279: p. 63-68.
22. Siril, P. F.; Cross, H. E.; Brown, D. R., New polystyrene sulfonic acid resin catalysts with enhanced acidic and catalytic properties. *Journal of Molecular Catalysis A: Chemical* 2008, 279, (1), 63-68.
23. Harmer, M.A., Farneth, W.E., and Sun, Q., *High Surface Area NafionResin/Silica Nanocomposites: A New Class of Solid Acid Catalyst*. *Journal of the American Chemical Society*, 1996. 118(33): p. 7708-7715.
24. Harmer, M. A.; Farneth, W. E.; Sun, Q., High Surface Area Nafion Resin/Silica Nanocomposites: A New Class of Solid Acid Catalyst. *Journal of the American Chemical Society* 1996, 118, (33), 7708-7715.
25. Harmer, M. A.; Sun, Q.; Vega, A. J.; Farneth, W. E.; Heidekum, A.; Hoelderich, W. F., Nafion resin-silica nanocomposite solid acid catalysts. Microstructure-processing-property correlations. *Green Chemistry* 2000, 2, (1), 7-14.
26. Hart, M. P.; Brown, D. R., Surface acidities and catalytic activities of acid-activated clays. *Journal of Molecular Catalysis A: Chemical* 2004, 212, (1-2), 315-321.
27. Felix, S. P.; Savill-Jowitt, C.; Brown, D. R., Base adsorption calorimetry for characterising surface acidity: a comparison between pulse flow and conventional techniques. *Thermochimica Acta* 2005, 433, (1-2), 59-65.

28. Hill, C.; Norton, A.; Newman, G., The water vapour sorption properties of Sitka spruce determined using a dynamic vapour sorption apparatus. *Wood Science and Technology* 2010, 44, (3), 497-514.. *J. Appl.Polym. Sci.*, 2009. 112: p. 1524-1537.
29. Meziani, M. J.; Zajac, J.; Jones, D. J.; Partyka, S.; Roziare, J.; Auroux, A., Number and Strength of Surface Acidic Sites on Porous Aluminosilicates of the MCM-41 Type Inferred from a Combined Microcalorimetric and Adsorption Study. *Langmuir* 2000, 16, (5), 2262-2268.
30. Auroux, A., Acidity characterization by microcalorimetry and relationship with reactivity. *Topics in Catalysis* 1997, 4, (1), 71-89.
31. Dacquin, J.-P.; Cross, H. E.; Brown, D. R.; Duren, T.; Williams, J. J.; Lee, A. F.; Wilson, K., Interdependent lateral interactions, hydrophobicity and acid strength and their influence on the catalytic activity of nanoporous sulfonic acid silicas. *Green Chemistry* 2010, 12, (8), 1383-1391.
32. Pesaresi, L.; Brown, D. R.; Lee, A. F.; Montero, J. M.; Williams, H.; Wilson, K., Cs-doped  $H_4SiW_{12}O_{40}$  catalysts for biodiesel applications. *Applied Catalysis A: General* 2009, 360, (1), 50-58.
33. Banavali, R.; Hanlon, R.T.; Jerabek, K.; Schultz A.K., *Heterogeneous Catalyst and Process for the Production on Biodiesel from High Free-Fatty Acid-Containing Feedstocks*. (Eng) In: *Catalysis of Organic Reactions:Twenty-second Conference (Chemical Industries)*. (Prunier, M.L., Ed.), 2008. p. 279-289.

## **Chapter 4**

### **SULFONATED POLYVINYL ALCOHOL AS SOLID ACID CATALYST**

---

“In this chapter the synthesis, characterization and testing of sulfonated polyvinyl alcohol is described. The catalyst is used for esterification of oleic acid with methanol in liquid phase. The parameters which affect the conversion of oleic acid are also reported”.

#### 4.1. Overview

In this chapter, the synthesis, characterization and testing of polyvinyl alcohol (PVA) supported sulfonic acid catalyst was studied. The synthesized catalyst was prepared, characterized and tested towards two types of reactions: the esterification of oleic acid and the isomerization of  $\alpha$ -pinene. The activity of synthesized catalyst was compared with other commercially available solid acid catalysts. The synthesized catalyst was made by reacting PVA and sulfosuccinic acid (SSA) to form PVA-SSA polymer matrix with sulfonic groups bonded to hydroxyl group of PVA. The PVA-SSA catalyst was then further cross-linked using glutaraldehyde (GA) to form a hydrophobic protective layer in order to reduce swelling and leaching of sulfonic groups into reaction media and denoted as PVA-SSA-GA.

The esterification reaction was performed using oleic acid and methanol as starting material and the reaction was carried out at 60 °C. The isomerization reaction was performed at 120 °C, converting  $\alpha$ -pinene to camphene. The catalyst was characterized using FTIR, nitrogen adsorption and simple titration methods to measure the acid capacity. The catalytic activity test for isomerization was monitored using GC, and the kinetics of the esterification reaction was followed using acid-base titration.

## 4.2. Introduction

Polyvinyl alcohol (PVA) is the biggest volume, synthetic water soluble polymer produced in the world [1]. Polyvinyl alcohol was synthesized by Herman and Haenel in 1924 by hydrolyzing polyvinyl acetate in alcohol (ethanol/methanol) with potassium hydroxide. The physical properties and its specific functional uses depend on the degree of polymerization and the degree of hydrolysis [2]. Polyvinyl alcohol is categorized into two categories: partially hydrolyzed and fully hydrolyzed. The excellent adhesion capacity of PVA to cellulosic materials makes this polymer useful for many applications, as an adhesive, film, coating, etc [3]. It is a film coating agent particularly in applications where moisture barrier/protection properties are required. Unfortunately, polyvinyl alcohol film undergoes swelling when soaked in water or alcohol. Therefore, crosslinking of the film is required to tune the hydrophilicity and hydrophobicity properties to meet a special application such as membranes for fuel cell (PEMFC) or catalysts.

The use of PVA as a catalyst support for sulfosuccinic acid (SSA) or sulphosalicylic acid has been reported by many researchers [4-6]. PVA can be crosslinked with carboxylic acid or dialdehydes [7-8]. The hydroxyl group of PVA and the carboxylic acid of polymers or monomers form a network structure via dehydration that contributes to strong bonding on heating (Figure 4.1) [9]. The hydroxyl groups of PVA and dialdehyde-containing monomers are crosslinkable by acetal reactions under acid conditions [8].

Polyvinyl alcohol cross-linked with sulfosuccinic acid (SSA) to form polyvinyl alcohol-sulphosuccinate (PVA-SSA) shown in Figure 4.1 has been

studied thoroughly by Rhim et al. [10]. PVA-SSA catalyst for transesterification of soybean oil has been reported by Guerreiro et al. [5]. The esterification of palmitic, stearic and oleic acid using PVA sulfonated with sulfosuccinic acid was also reported by Caetano et al. [11].

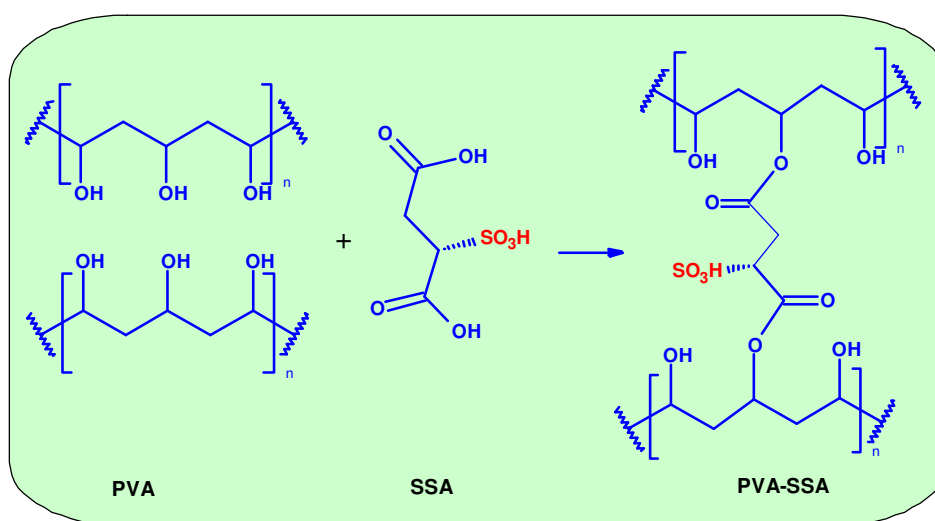


Figure 4.1. Reaction of polyvinyl alcohol and sulfosuccinic acid to form PVA-SSA.

Sulfosuccinic acid (SSA) as a cross-linking agent increases the acid capacity of the polymer and also reduces water permeability. However, the cross-linking through ester bond formation is quite easily hydrolyzed under acid condition. This can happen in an esterification reaction where water is produced as a by-product. For this reason, further cross-linking to the catalyst is required to prevent hydrolysis.

Many papers discussed the cross-linking process of PVA using aldehydes [12-13]. Glutaraldehyde is one of the common cross-linking

agents among aldehydes [14-16]. The crosslinking reaction between PVA-SSA and glutaraldehyde may affect the mechanical strength and hydrophilicity of PVA-SSA catalyst. Swelling characteristics and surface properties of PVA-SSA can be changed according to the degree of cross-linking.

Figure 4.2 shows the use of glutaraldehyde as a second crosslinking agent for PVA-SSA. The reaction of PVA-SSA and glutaraldehyde is performed at 70 °C in acetone [17]. The use of acetone instead of water as solvent is to avoid any swelling and losing the SSA into the water phase. Sulphuric acid is used as a catalyst during the second cross-linking reaction and the reaction is carried out for 4 h. The glutaraldehyde will react with unused OH groups within the PVA-SSA matrix to form an acetal ring to form PVA-SSA-GA which is expected to be more stable towards hydrolysis.

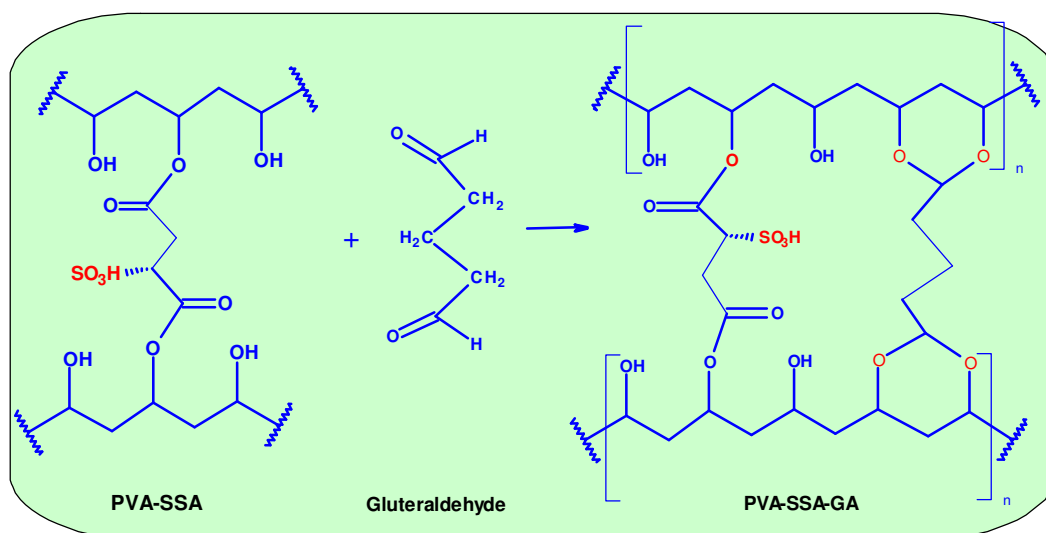


Figure 4.2. Crosslinking reaction of PVA-SSA with glutaraldehyde to form PVA-SSA-GA.

Two reactions have been used to monitor catalytic activities: esterification of free fatty acid and isomerisation of  $\alpha$ -pinene. The isomerisation reaction involves a non-polar reactant which has different requirements on catalyst properties and compatibilities compared to the esterification reaction which is carried out in methanol.

In this work, PVA-SSA-GA has been compared with two other solid acid catalysts: Nafion SAC 13 which is a composite between silica gel and the perfluorinated polymer supported sulfonic acid and Amberlyst-35 which is a sulfonated polystyrene resin, described in detail in chapter 3.

### **4.3. Experimental methods**

#### **4.3.1. Materials**

Polyvinyl alcohol (PVA) (99 mol % hydrolyzed; MW=88,000) was purchased from Fluka and the sulfosuccinic acid (SSA) (70 percent in water) was purchased from Aldrich. Glutaraldehyde and oleic acid were purchased from Fluka, and methanol was purchased from Fisher Scientific. Nafion SAC-13 was supplied by Aldrich, and Amberlyst-35 (Rohm and Hass) was purchased from Sigma Aldrich.

#### **4.3.2. Catalyst preparation**

##### a) Preparation of PVA/SSA polymeric film

PVA/SSA polymeric film was prepared according to Rhim et al. [18]. Typical preparation is as follows: Aqueous 10% PVA solutions were prepared by dissolving the 10 g of PVA to 90 ml water at 90 °C for 6 h by constant

agitation. The PVA solutions were mixed with various amount of SSA by weight PVA/SSA (17%, 29%, 50%) and the mixtures were mixed vigorously for 24 h at 70 °C to obtain cast solution. For example, PVA-SSA-GA17 was made by adding 17 % w/w (1.7 g) of sulfosuccinic acid to the solution containing 10 g of PVA. The cast solution was then cast onto a plexiglass plate. The cast film was allowed to dry at at 40 °C until visually dry in oven with controlled temperature. The film is then peeled from the flexiglass and further heated in oven under vacuum at 120 °C for 2h.

#### b) Chemical crosslinking of PVA/SSA and glutaraldehyde

The crosslinking process for PVA/SSA was conducted according to the method described by Chun at al. [17]. For the crosslinking reaction with glutaraldehyde, PVA film was immersed in 0.5 M glutaraldehyde/acetone reaction solution at 70 °C for 4 h. The crosslinked catalyst was then dried in the oven at 50 °C for 24 h.

#### **4.3.3. Catalyst characterization**

FTIR was used to monitor the sulfosuccinic acid crosslinked to the PVA membrane catalyst. An FTIR single reflection Nicolet spectrometer recording attenuated total reflectance infrared (ATR IR) spectra of the membrane catalyst was used (APPENDIX-I). The nitrogen adsorption isotherm was used to determine the BET surface area and the desorption isotherm was used to determine the pore volume of the catalyst.

#### **4.3.4. Ion exchange capacity (IEC) measurement**

The ion exchange capacities of the catalyst membranes were determined using a titration method. A sample membrane catalyst was soaked in 25 ml of 2 M NaCl solution and equilibrated for at least 24 h, to exchange the protons by sodium ions. The solution was then titrated with 0.01 M NaOH with phenolphthalein as indicator. Ion exchange capacities (IEC) are quoted on the basis that they are equal to the concentration of H<sup>+</sup> in the resin and in units of mmol g<sup>-1</sup>.

#### **4.3.5. Catalytic testing**

Catalytic testing was conducted for the esterification of oleic acid with methanol and for the isomerisation of  $\alpha$ -pinene. The esterification was conducted in a 50 ml three necked round bottom flask at 60 °C. The experiment was run using 20 g of methanol and 4.0 g of oleic acid and 0.2 g of catalyst cut in small pieces 2-3 mm<sup>2</sup> (dried at 60 °C before use). Samples were taken at regular intervals ( $\pm 1.0$  g) and 25 ml anhydrous ethanol was added to ensure miscibility. To the mixture, two drops of phenolphthalein was added as indicator.

The mixture was then titrated using 0.25 M of NaOH and the percentage of unreacted free fatty acid (FFA) was calculated.

$$\text{FFA (\%)} = \frac{[C_{\text{NaOH}} \times V_{\text{NaOH}} \times \text{MW}_{\text{OA}}] \times 100}{\text{Weight of sample (g)} \times 1000}$$

C NaOH = concentration of NaOH used

V NaOH = Volume NaOH used (endpoint titration)

FFA = Free fatty acid (unreacted oleic acid)

MW<sub>OA</sub> = Molecular weight of oleic acid

For the isomerisation reaction, 10.0 g of  $\alpha$ -pinene was charged to a 50 ml glass reactor and heated to reaction temperature of 120 °C using oil bath. 0.50 g (5% w/w) catalyst was used. Small aliquots were withdrawn through the reaction and analyzed by GC (Clarus 500m Perkin Elmer) using a 25m BP1 column at 2ml min<sup>-1</sup> helium flow. The oven temperature was held at 60 °C for 15 min and then increased at 20 °C min<sup>-1</sup> to 290 °C. The reaction was monitored in terms of the conversion of  $\alpha$ -pinene using n-decane as internal standard.

#### **4.4. Results and discussion**

##### **4.4.1. Catalyst characterization**

Figure 4.3 shows the FTIR spectra of PVA-SSA-GA catalysts with different compositions. PVA-SSA-GA17 is the catalyst with SSA content of 17% in the polymer. PVA-SSA-GA29, PVA-SSA-GA50 are the catalysts with SSA content of 29% and 50% w/w to the polymer respectively. It was previously

reported by Rhim et al. that the absorption band for the PVA-SSA at  $1714\text{ cm}^{-1}$  was due to ester ( $-\text{COO}-$ ) groups and this indicates that crosslinking between the  $-\text{OH}$  group on the PVA with  $-\text{COOH}$  on the sulfosuccinic acid was successful [10]. The  $1714\text{ cm}^{-1}$  band is strong for the PVA-SSA-GA samples and absent for unreacted PVA. The absorption bands at  $2850\text{ cm}^{-1}$  to  $2950\text{ cm}^{-1}$  correspond to the  $-\text{CH}$  vibrations of the acetal and  $-\text{CH}$  in the SSA and PVA structures [18]. The absorption bands at  $1240\text{ cm}^{-1}$  is the C-O stretch mode in ester group and the adsorption band at  $1037\text{ cm}^{-1}$  is associated with  $-\text{SO}_3\text{H}$  group [11, 18]. This peak is the evidence of the presence of sulfonic acid groups in the PVA matrix and therefore further evidence of incorporation of sulfosuccinic acid in the polymer.

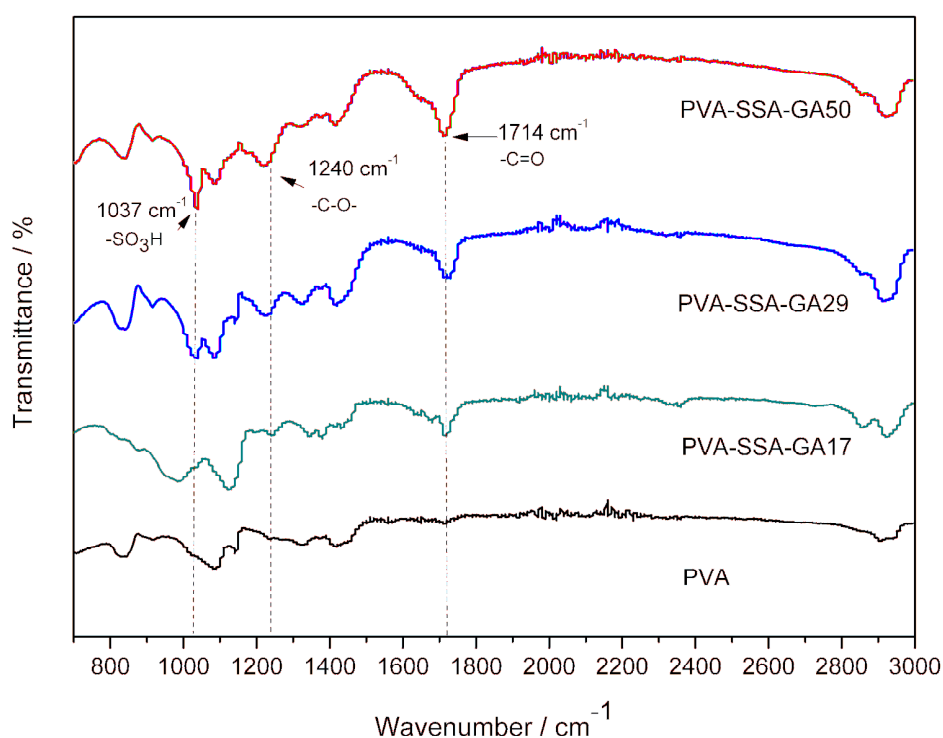


Figure 4.3. FTIR spectra of the catalysts: pure PVA (99%) and PVA-SSA-GA Catalysts.

Table 4.1. Properties of PVA-SSA-GA and resins catalysts.

<b>Catalyst</b>	<b>Pore size (nm)</b>	<b>Surface Area (m<sup>2</sup>/g)</b>	<b>IEC (mmol/g)</b>
PVA-SSA-GA17	-	-	1.01
PVA-SSA-GA29	-	-	1.37
PVA-SSA-GA50	-	-	2.70
Nafion SAC-13	10	196	0.15
Amberlyst-35	30	50	5.40

Table 4.1 shows the properties of catalysts studied. Two different polymer-supported sulfonic acid resins were used for comparison, Nafion SAC-13 and Amberlyst-35. The ion exchange capacities (IEC) vary from 5.5 mmol g<sup>-1</sup> for Amberlyst-35 down to 0.15 mmol g<sup>-1</sup> for the Nafion SAC-13 composite material. The IEC value for SAC-13 is in line with known acid site concentration for pure Nafion of 0.89 mmol g<sup>-1</sup> and the Nafion loading in the composite of 13% w/w [19]. PVA-SSA-GA29 exhibits no permanent porosity and has an IEC value of 1.47 mmol g<sup>-1</sup> which is almost ten times higher than SAC 13.

The ion exchange capacity (IEC) value of the PVA-SSA-GA catalysts plotted against SSA (% w/w) content of the polymer is shown in Figure 4.4. There is a good correlation between the ion exchange capacity (IEC) values and sulfosuccinic acid (SSA) content, confirming incorporation of the SSA in the polymer as expected.

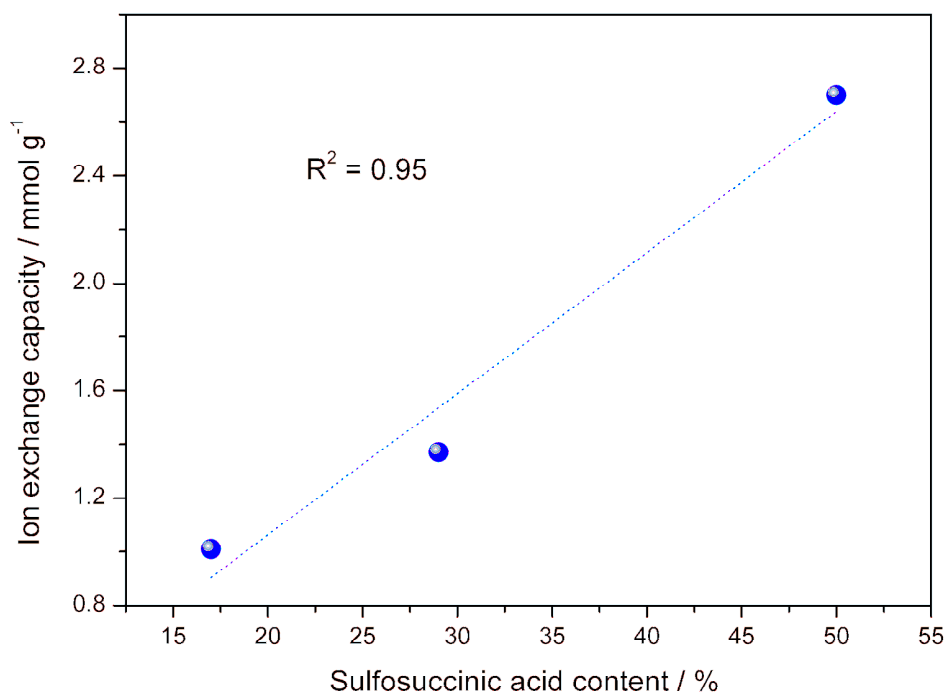


Figure 4.4. Relation between the IEC and the SSA content of PVA-SSA-GA.

#### 4.4.3. Catalyst testing

Figure 4.5 shows the conversion of oleic acid as a function of time for the three catalysts. As we expect, an increase in the sulfonic acid content results in increased reaction rate. PVA-SSA-GA17 (17%) with less SSA content shows an induction period, as is common for the solid acid catalysts, especially in esterification and transesterification reactions. This induction period is smaller with increasing SSA content in the polymer matrix.

This behavior is possibly related to the increasing of the number active sites in the catalyst. The higher of the SSA content in the polymer, the faster the diffusion of reactants into the active sites and this reduces the induction period for PVA-SSA-GA50 (50).

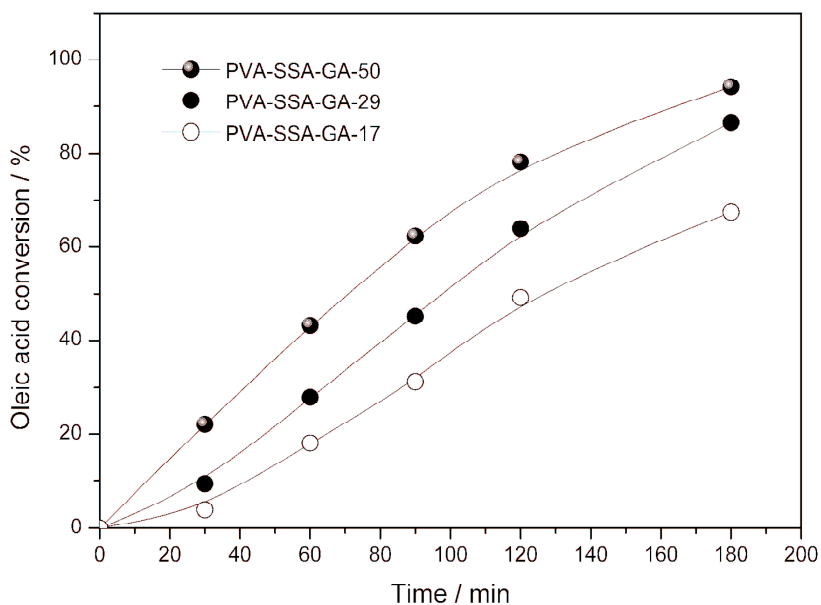


Figure 4.5. Effect of SSA content on the conversion of oleic acid at 60 °C.

The catalytic activity of the catalyst is better expressed as the rate constant. If we assume that the reaction rate is first order in oleic acid (methanol is in excess), a first order plot of  $\ln[\text{oleic acid}]$  against time can be used to calculate a rate constants as shown in Figure 4.6.

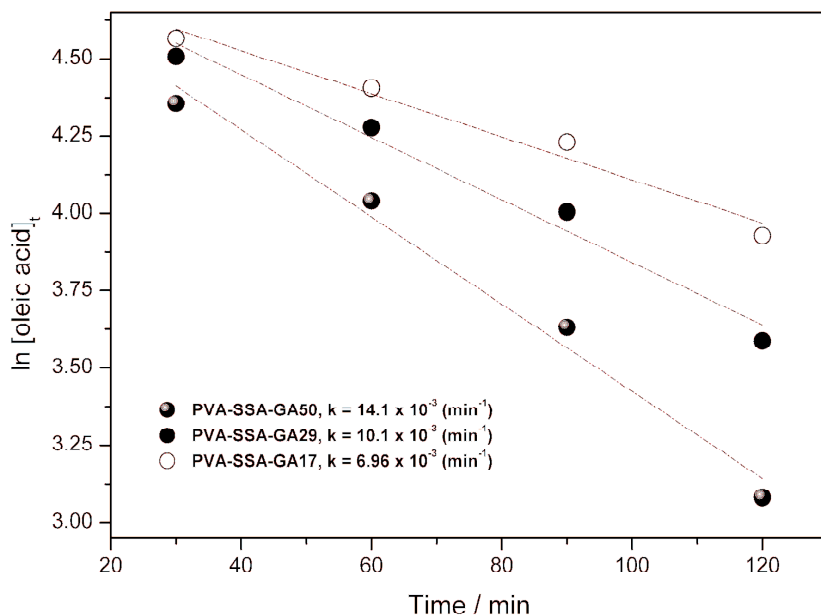


Figure 4.6. First order plots for the conversion of oleic acid with PVA-SSA-GA catalysts.

The rate constant for PVA-SSA-GA50 is double ( $14.1 \times 10^{-3} \text{ min}^{-1}$ ) than PVA-SSA-GA17 ( $6.96 \times 10^{-3} \text{ min}^{-1}$ ), this is consistent with the relative concentration of active sites. The relation of SSA content and the rate constant is shown in Figure 4.7. The linear relationship between rate constant and SSA content suggests that, in these catalysts, all sulfonic acid groups are accessible to reactants. This mean that diffusion through the methanol expanded polymer matrix is facile. It is worth noting that increasing the molar ratio of alcohol to acid above the level used here had no significant effect on the yield of ester.

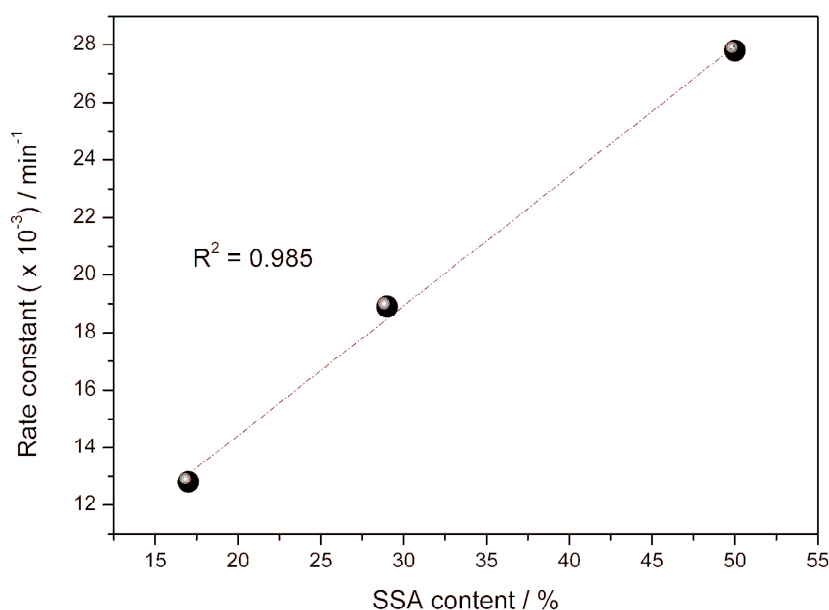


Figure 4.7. Correlation between the rate constant and the amount of SSA in the catalysts.

The effect of temperature on the conversion of oleic acid was followed using conditions as above but with a molar ratio of methanol to oleic acid of 46:1. The higher molar ratio used was to shift the equilibrium to complete conversion to the methyl ester. In Figure 4.8, it can be seen that by

increasing the temperature from 40 to 50 and to 60 °C, the rate of conversion of oleic acid is increased. It is not easy to determine rate constants from this data because all plots show an induction period. This is almost certainly restricted mass transfer which occurs as the catalyst swells in methanol. The conversion is very slow over the first 2 h at temperature 40 °C, but at 50 °C and 60 °C the effect is increasingly less marked, presumably as the swelling and diffusion of reactants to the active sites is accelerated.

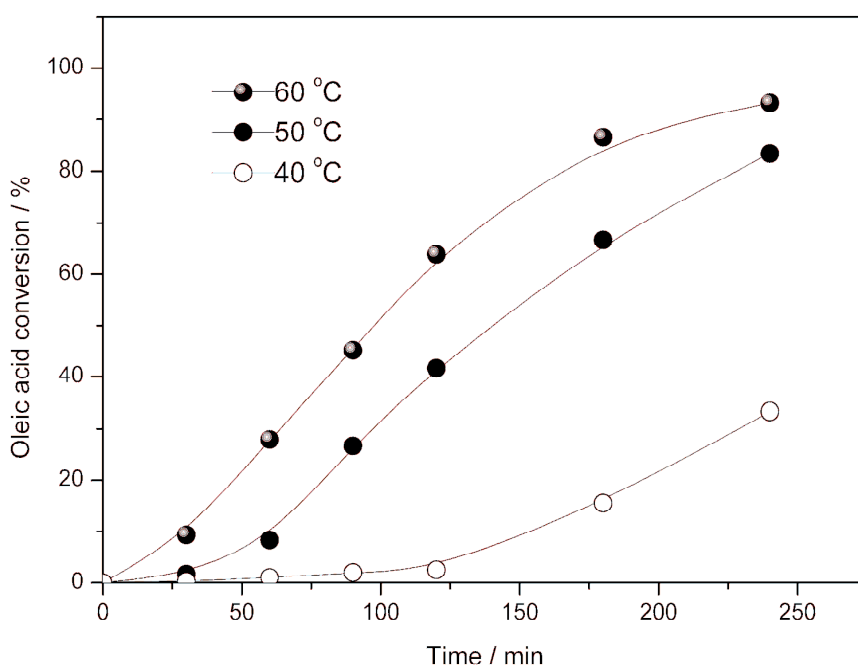


Figure 4.8. The effect of temperature on the conversion of oleic acid using PVA-SSA-GA29 catalyst.

The effect of catalyst amount of PVA-SSA-GA29 on conversion of oleic acid esterification with methanol at 60 °C is shown in Figure 4.9. It can be seen that by increasing the catalyst loading from 2.5 % to 5 % and 7.5 % w/w based on oleic acid, there is a substantial increase in the conversion of oleic

acid. In fact, the most noticeable feature of these plots is that the induction period is reduced as the catalyst loading is increased. A possible explanation is that there are active sites on these catalysts with varying accessibility to reactant, and by increasing the overall amount of catalyst, the number of readily accessible sites in the non-swollen catalysts is high enough to reduce the observable induction period to an almost undetectable level.

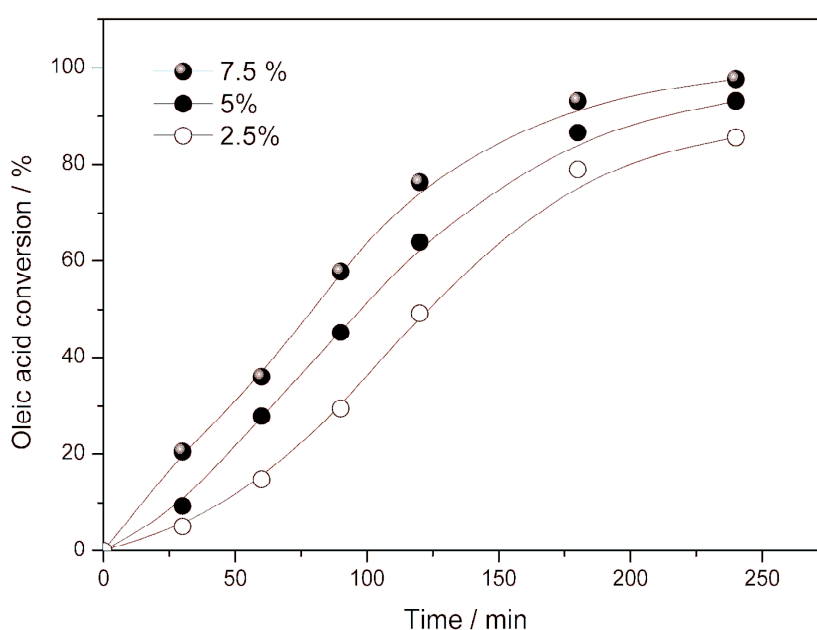


Figure 4.9. The effect of catalyst loading on conversion of oleic acid at 60 °C using PVA-SSA-GA29 catalyst.

The catalyst was also tested with different free fatty acids: palmitic, stearic and oleic acids. The reaction was carried out at 60 °C, using a molar ratio of 46.5:1 and catalyst amount of 5% w/w of fatty acids. Palmitic has 16 carbon atoms whereas stearic and oleic have 18 carbon atoms. Figure 4.10 shows that there are no significant differences in the reaction rates and the conversions.

The esterification of oleic acid with methanol was carried out at 60 °C, with molar ratio of methanol to oleic acid of 46:1 and catalyst loading of 5 % w/w on the acid. The catalyst PVA-SSA-GA29 was compared with the sulfonic acid polystyrene-divinyl benzene- resin Amberlyst-35 and Nafion SAC-13. Figure 4.11 shows that conversion of oleic acid as a function of time with three different catalysts was used.

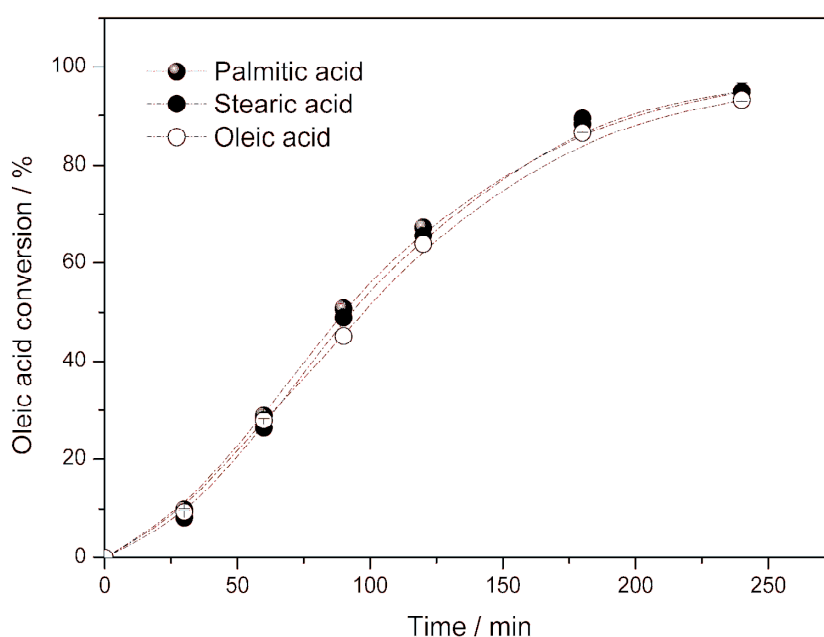


Figure 4.10. Activity of PVA-SSA-GA29 catalyst with different fatty acids using PVA-SSA-GA29.

The initial turnover frequencies (TOFs) of the catalysts are tabulated in Table 4.2. The catalytic activities of the three different catalysts in the esterification and isomerisation are in reversed order. In esterification reaction, the highest activities are exhibited by the PVA-SSA-GA29 followed by Nafion SAC-13 and Amberlyst-35. In term of TOF, PVA-SSA-GA29 with lower concentration of active sites is almost 15 fold higher than Amberlyst-

35. The isomerisation of  $\alpha$ -pinene was used as an example of a non-polar reactant that would not be capable of swelling the polar material in the sulfonated polymer catalysts, and would therefore rely on active sites being accessible on the surface, or very close to the surface of the polymer.

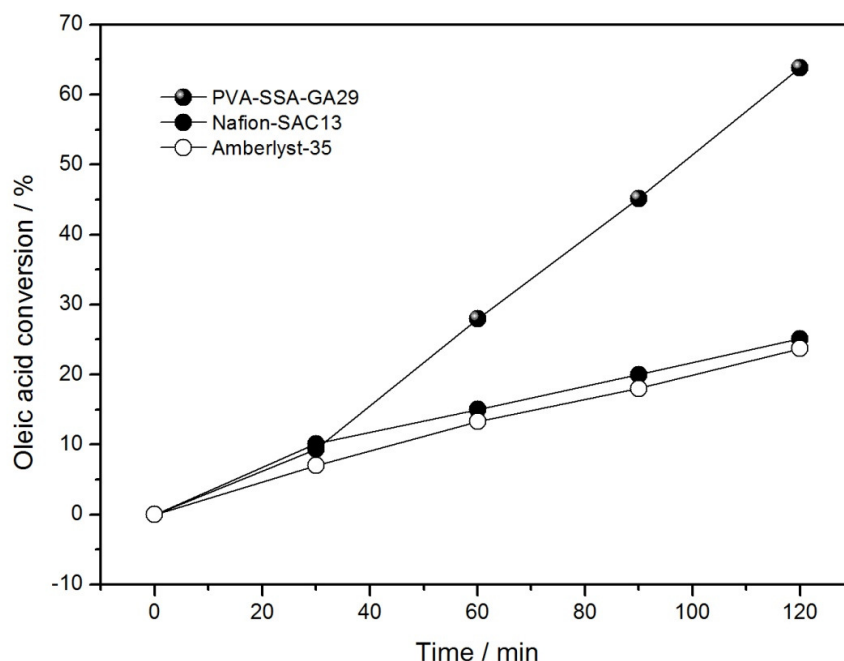


Figure 4.11. Esterification of oleic acid and methanol using different solid catalysts.

Figure 4.12 shows Amberlyst-35 with high concentration of active sites (5.5 mmol/g) is the most active catalyst in isomerisation reaction than Nafion SAC-13 and PVA-SSA-GA29. PVA-GA-SSA29 catalyst shows extremely low activity as shown in Figure 4.12, perhaps consistent with their very low nominal surface areas. Pito et al. [6] explained that the behavior could be due to the high mobility restriction of  $\alpha$ -pinene as hydrophobic molecule in the PVA-SSA matrix with hydrophilic property, the result is decreasing of diffusivity of  $\alpha$ -pinene through the polymeric matrix of PVA-SSA-GA29.

Table 4.2. Turnover frequencies of three different catalysts.

Catalyst	TOF (h <sup>-1</sup> )	
	Esterification	Isomerisation
PVA-SSA-GA29	32	2.4
NAfion SAC-13	80	740
Amberlyst-35	2.4	118

In term of TOF, Nafion SAC-13 shows the highest activity which is almost 6 times higher than Amberlyst-35 and surprisingly 300 times higher than PVA-SSA-GA29. This catalyst has been formulated by blending the polymer supported sulfonic acid with silica to give a reasonably high surface area so it is not surprising that it shows activity with non-swelling reactants.

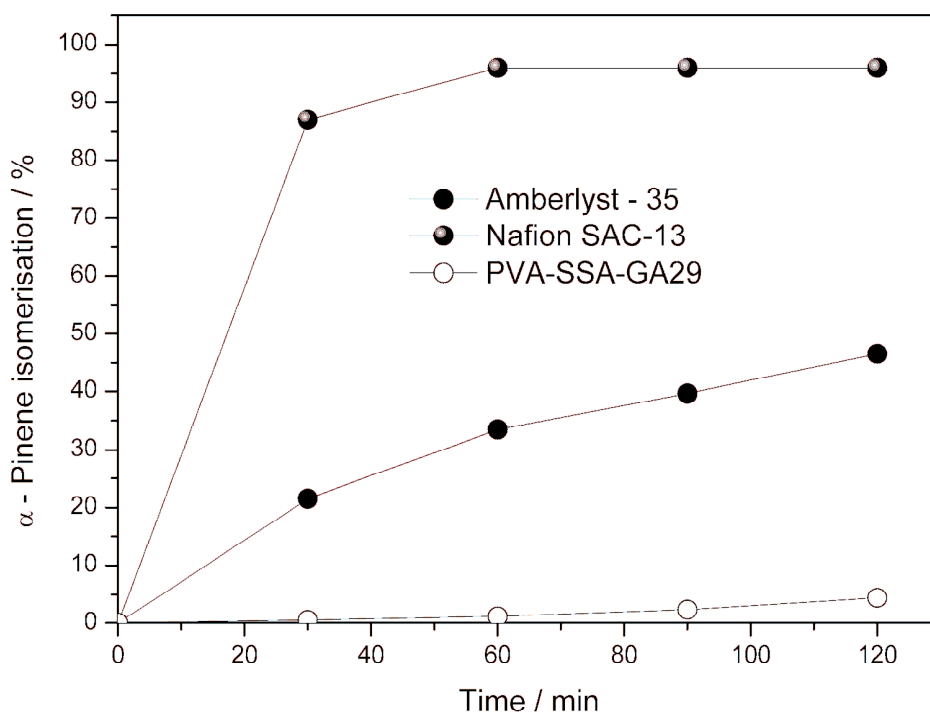


Figure 4.12. Isomerisation of  $\alpha$ -pinene using different solid acid catalysts.

#### 4.4.4. Catalyst reusability

The activity of catalysts was tested in consecutive batch runs (oleic acid esterification) with the same operating condition. Two catalysts were tested: PVA-SSA29 and PVA-SSA-GA29 that is one with and without glutaraldehyde cross-linking. Data for conversion of oleic acid after 4 h reaction is shown in Figure 4.13. Both catalysts show significant loss in activity on use. Nevertheless, it is observed the presence of glutaraldehyde inhibits the catalyst from losing its activity. The reason for loss in activity is not certain especially when it is run at low temperature (60 °C) as it happened in hypercrosslinked resin catalyst (chapter 3). The speculation is that this could lead to blockage by oleic acid molecules or oligomerised forms of acids.

The speculation is supported by the fact that the FTIR spectra of the PVA-SSA-GA29 taken before and after each run show the carbonyl group still present in the catalyst structure after each use (Figure 4.14). The spectra do not show any differences. The peak at 1714  $\text{cm}^{-1}$  (carbonyl groups) which shows the carbonyl group belonging to succinic acid retains intensity on catalyst re-use. This present of absorption bands at 1037  $\text{cm}^{-1}$ , usually assigned to the O=S=O asymmetric and symmetric vibrations respectively also confirmed the retention of active group in the polymeric matrix.

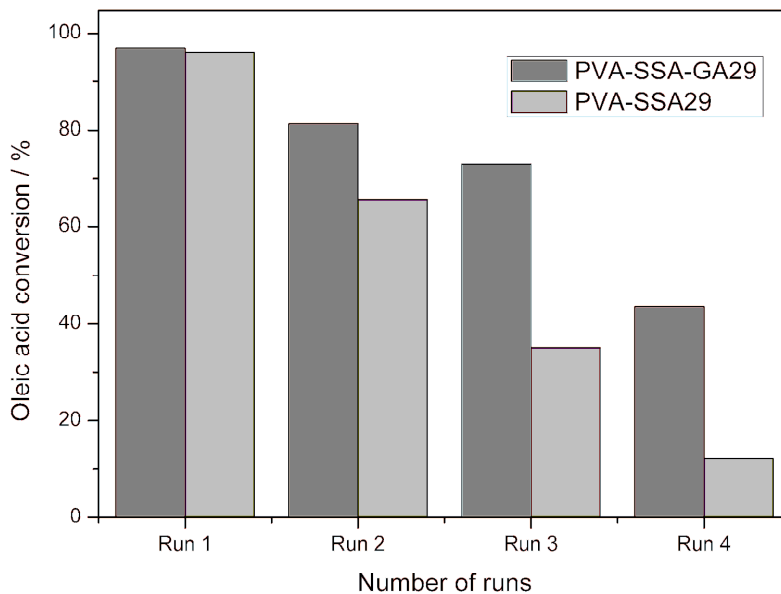


Figure 4.13. Reusability test of PVA-SSA29 and PVA-SSA-GA29 in the esterification of oleic acid after 4 h.

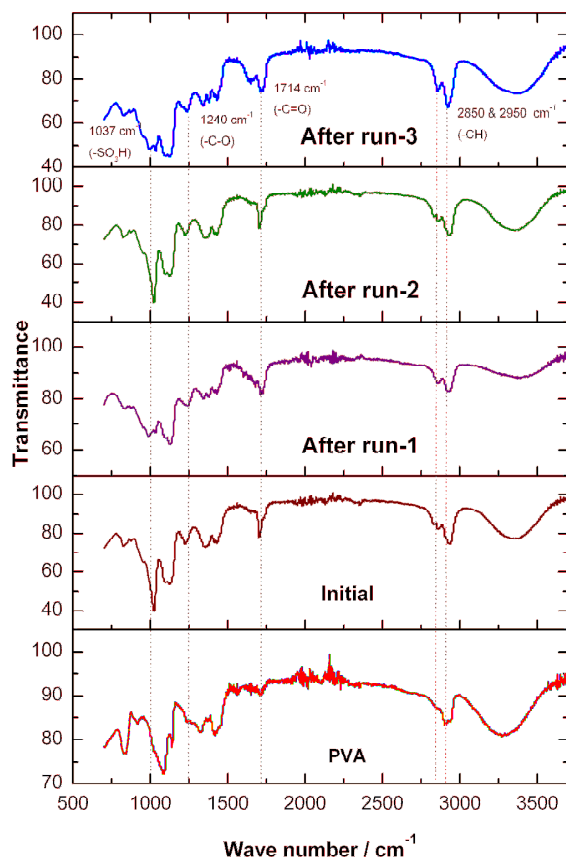


Figure 4.14. FTIR spectra of PVA-SSA-GA29 before and after being re-used.

#### 4.4.5. Kinetic study

Using PVA-SSA-GA, the activation energy for the oleic acid esterification has been determined using an Arrhenius Plot (Figure 4.16). First order plots (pseudo-first order) in oleic acid were drawn for the reaction (using fresh catalyst in each case) at 40, 50, and 60 °C as shown in Figure 4.15. The resulting rate constants from the gradients appear in the figure. An Arrhenius plot using this data in Figure 4.16 gives a gradient of -7701 which in turns gives activation an energy of 64 kJ mol<sup>-1</sup>. A large uncertainty is associated with the results so it might be quoted as 64 (± 20) kJ mol<sup>-1</sup>. This value is not significantly different that reported elsewhere for typical sulfonated polystyrene resin catalyst, Amberlyst-15, for the same reaction, of 70.3 kJ mol<sup>-1</sup>[20].

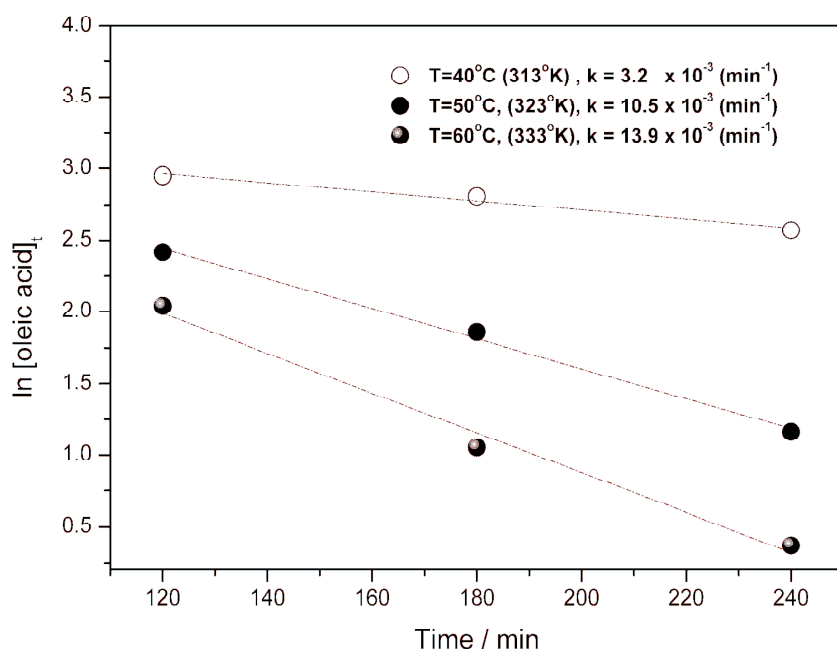


Figure 4.15. First order plots for conversion of oleic acid using PVA-SSA-GA29 at different temperature.

These values are both higher than would be expected if the reaction were under diffusion control and suggest that, in both cases, reactions are under kinetic control and the mechanism and acidities of sulfonic acid group in the two environment are similar. The absence of diffusion control in the PVA-SSA-GA catalyst is especially significant, given the very low surface area of the catalyst and the supposed need for essentially all reaction to occur at sites within the matrix to which diffusion of reactant is necessary.

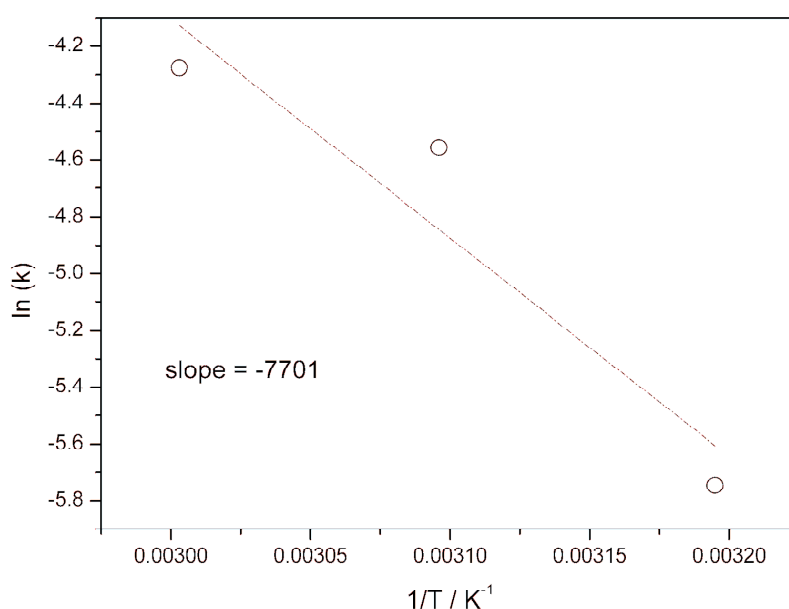


Figure 4.16. Arrhenius plot  $\ln(k)$  vs  $1/T$  of PVA-SSA-GA29.

#### 4.5. Conclusions

PVA-SSA-GA catalyst was successfully synthesized and characterized and also tested for esterification and isomerization reactions. The synthesized catalyst PVA-SSA-GA29 is more active in esterification of oleic acid than Nafion SAC-13 and conventional macroreticular resin Amberlyst-35

catalyst. This order of activities is PVA-SSA-GA29 > Nafion SAC-13 > Amberlyst-35. The relative activity of the PVA-SSA-GA catalyst in the esterification reaction suggests that the catalyst swells very effectively in polar solvents such methanol. In the  $\alpha$ -pinene isomerisation reaction the order of activity is in reversed: Amberlyst-35 > Nafion SAC-13 > PVA-SA-GA29. In this reaction, level of compatibility of this reactant with the catalyst, surface area and overall acid concentration is important in determining the activity of the catalyst.

## References

1. Ye, Y.-S.; Rick, J.; Hwang, B.-J., Water Soluble Polymers as Proton Exchange Membranes for Fuel Cells. *Polymers* 2012, 4, (2), 913-963.
2. S.K.Saxena, Polyvinyl alcohol (PVA) Chemical and Technical Assessment (CTA), Chemical and Technical Assessment 61, 2004, 3-7.
3. Hansen, E. W.; Holm, K. H.; Jahr, D. M.; Olafsen, K.; Stori, A., Reaction of poly(vinyl alcohol) and dialdehydes during gel formation probed by <sup>1</sup>H n.m.r. a kinetic study. *Polymer* 1997, 38, (19), 4863-4871.
4. Castanheiro, J. E.; Ramos, A. M.; Fonseca, I. M.; Vital, J., Esterification of acetic acid by isoamylic alcohol over catalytic membranes of poly(vinyl alcohol) containing sulfonic acid groups. *Applied Catalysis A: General* 2006, 311, (0), 17-23.
5. Guerreiro, L.; Castanheiro, J. E.; Fonseca, I. M.; Martin-Aranda, R. M.; Ramos, A. M.; Vital, J., Transesterification of soybean oil over sulfonic acid functionalised polymeric membranes. *Catalysis Today* 2006, 118, (1-2), 166-171.

6. Pito, D. S.; Fonseca, I. M.; Ramos, A. M.; Vital, J.; Castanheiro, J. E., Methoxylation of  $\alpha$ -pinene over poly(vinyl alcohol) containing sulfonic acid groups. *Chemical Engineering Journal* 2009, 147, (2-3), 302-306.
7. Yeom, C.-K.; Lee, K.-H., Pervaporation separation of water-acetic acid mixtures through poly(vinyl alcohol) membranes crosslinked with glutaraldehyde. *Journal of Membrane Science* 1996, 109, (2), 257-265.
8. Bolto, B.; Tran, T.; Hoang, M.; Xie, Z., Crosslinked polyvinyl alcohol membranes. *Progress in Polymer Science* 2009, 34, (9), 969-981.
9. Silva, R.; Muniz, E. C.; Rubira, A. F., Multiple hydrophilic polymer ultra-thin layers covalently anchored to polyethylene films. *Polymer* 2008, 49, (19), 4066-4075.
10. Rhim, J.-W.; Yeom, C.-K.; Kim, S.-W., Modification of poly(vinyl alcohol) membranes using sulfur-succinic acid and its application to pervaporation separation of water-alcohol mixtures. *Journal of Applied Polymer Science* 1998, 68, (11), 1717-1723.
11. Caetano, C. S.; Guerreiro, L.; Fonseca, I. M.; Ramos, A. M.; Vital, J.; Castanheiro, J. E., Esterification of fatty acids to biodiesel over polymers with sulfonic acid groups. *Applied Catalysis A: General* 2009, 359, (1-2), 41-46.
12. De Souza Costa-Júnior, E.; Pereira, M.; Mansur, H., Properties and biocompatibility of chitosan films modified by blending with PVA and chemically crosslinked. *Journal of Materials Science: Materials in Medicine* 2009, 20, (2), 553-561.
13. Kim, J. H.; Kim, J. Y.; Lee, Y. M.; Kim, K. Y., Properties and swelling characteristics of cross-linked poly(vinyl alcohol)/chitosan blend membrane. *Journal of Applied Polymer Science* 1992, 45, (10), 1711-1717.
14. Hirai, T.; Maruyama, H.; Suzuki, T.; Hayashi, S., Shape memorizing properties of a hydrogel of poly(vinyl alcohol). *Journal of Applied Polymer Science* 1992, 45, (10), 1849-1855.

15. Hirai, T.; Maruyama, H.; Suzuki, T.; Hayashi, S., Effect of chemical cross-linking under elongation on shape restoring of poly(vinyl alcohol) hydrogel. *Journal of Applied Polymer Science* 1992, 46, (8), 1449-1451.
16. Immelman, E.; Sanderson, R. D.; Jacobs, E. P.; Van Reenen, A. J., Poly(vinyl alcohol) gel sublayers for reverse osmosis membranes. I. Insolubilization by acid-catalyzed dehydration. *Journal of Applied Polymer Science* 1993, 50, (6), 1013-1034.
17. Tsai, C.-E.; Lin, C.-W.; Hwang, B.-J., A novel crosslinking strategy for preparing poly(vinyl alcohol)-based proton-conducting membranes with high sulfonation. *Journal of Power Sources* 2010, 195, (8), 2166-2173.
18. Rhim, J.-W.; Park, H. B.; Lee, C.-S.; Jun, J.-H.; Kim, D. S.; Lee, Y. M., Crosslinked poly (vinyl alcohol) membranes containing sulfonic acid group: proton and methanol transport through membranes. *Journal of Membrane Science* 2004, 238, (1-2), 143-151.
19. Siril, P. F.; Cross, H. E.; Brown, D. R., New polystyrene sulfonic acid resin catalysts with enhanced acidic and catalytic properties. *Journal of Molecular Catalysis A: Chemical* 2008, 279, (1), 63-68.
20. Pasiadis, S.; Barakos, N.; Alexopoulos, C.; Papayannakos, N., Heterogeneously Catalyzed Esterification of FFAs in Vegetable Oils. *Chemical Engineering & Technology* 2006, 29, (11), 1365-1371.

# **CHAPTER 5**

## **SULFATED ZIRCONIA AS SOLID ACID CATALYST**

---

“In this chapter the synthesis, characterization and testing of sulfated zirconia for simultaneous esterification and transesterification reactions is described. In addition, the parameter affecting its activity such as calcination temperature is also discussed. Finally, a comparison of its activity with other polystyrene resins catalysts in simultaneous esterification of oleic acid and transesterification of tributyrin is reported”.

## 5.1. Overview

In this work, the activity of sulfated zirconia for simultaneous esterification and transesterification reactions was investigated. Mixtures of oleic acid and tributyrin were chosen as model compounds mimicking waste vegetable oil with high free fatty acid content. The reaction was performed at 120 °C in a pressurized reactor. Two different sulfated zirconia catalysts XZO-1720 and SZ-01 were investigated and their activities were compared with sulfonated polystyrene resin catalysts, Amberlyst-15, Amberlyst-35 and Purolite D5081. The effect of calcination temperature on catalyst activity was investigated. The optimum calcination temperature for the sulfated zirconia was found to be 600 °C for both reactions. The results reveal that sulfated zirconia catalyses both esterification and transesterification reactions and is promising as a solid acid catalyst for processing low grade vegetable oils for biodiesel production.

## 5.2. Introduction

Biodiesel is made from renewable resources such as vegetable oil and animal fats [1]. Vegetable oils and fats are converted to fatty acid methyl ester (FAME) through a transesterification reaction with low molecular weight alcohols such as methanol. This is generally catalyzed by homogeneous basic catalysts such as NaOH or KOH. However, the homogeneous catalysts that are widely used have disadvantages such as producing large amount of waste, and low purity glycerol and the catalyst cannot be recycled. In contrast, the use of heterogeneous catalysts has attracted many researchers due to the ease of catalyst recovery, purity of the product and also it offers a simple process operation. Zabety at al. [2] reviewed the potential use of heterogeneous catalysts for refining biodiesel for vegetable oil and compared published papers concerned with inorganic catalysts used in biodiesel synthesis.

The transesterification reaction can be catalyzed by acidic, basic or enzyme catalysts. This choice depends on the amount of free fatty acid (FFA) in the triglyceride. For triglyceride with low free fatty acid content, the base catalyzed reaction is usually fastest [3]. In contrast, for triglyceride with higher FFA content, acid catalyzed esterification followed by base catalyzed transesterification is more suitable.

Homogeneous acid or base catalysts bring problems of reactor corrosion as well as those related to catalyst recovery and product purification. For these reasons, heterogeneous catalysts for biodiesel

synthesis, especially when low grade quality of oil is used, are receiving more attention. It would be particularly advantageous if a single solid acid catalyst can be used for both the (relatively facile) pre-esterification of free fatty acids, and the (more demanding) transesterification of the triglyceride component. The objective of this work is to evaluate sulfated zirconia catalyst for this application.

Sulfated zirconia has shown catalytic activity in reactions such as isomerisation, alkylation, acylation, etherification, esterification, condensation, nitration etc [4]. Sulfated zirconia is classified as a “*superacid*”, which is defined as being stronger than 100 % sulphuric acid [5-6]. The catalytic properties of sulfated zirconia are also related to the crystal structure. Zirconia crystallises in three different polymorphs, with tetragonal, monoclinic, and cubic symmetry. These three structures, only the tetragonal structures show catalytic properties [7-8]. However, synthesis of the pure tetragonal structure is difficult. It requires control of various parameters, especially the calcination temperature.

The use of sulfated zirconia for biodiesel production has been reported by Furuta [9], who compared the activity of sulfated zirconia (SZ), tungstated zirconia (WZ) and sulfated tin oxide (STO) in the transesterification of soybean oil, and in the esterification reaction of octanoic acid with methanol. The transesterification was conducted at 200-300 °C and the esterification at 170-200 °C. Lopez at al. [10] studied the activities of sulfated and tungstated zirconia and titania/zirconia for the

transesterification of triglycerides and the esterification of carboxylic acids with ethanol. The use of sulfated zirconia for the esterification of dodecanoic acid with 2-ethyl hexanol was reported by Kiss [11]. Jitputti also studied the transesterification of crude palm kernel oil (CPKO) and crude coconut oil (CCO) with methanol at 200 °C in an alcohol:oil molar ratio of 6:1 and catalyst loading of 3 % w/w based on the oil, producing methyl ester for both oils with higher than 90% yield [12]. Study of the activity and stability of commercial sulfated zirconia catalyst (SZ) in transesterification has been reported by Suwannakarn et al. [13].

The aim of this present investigation is to study the effect of the calcination temperature on the catalytic activity of a synthesised sulfated zirconia (SZ-01) in the transesterification reaction and in the simultaneous esterification-transesterification reactions. Transesterification was performed using tributyrin as a model compound for triglycerides. The simultaneous esterification and transesterification used a mixture of tributyrin and oleic acid. Commercial sulfated zirconia XZO-1720 (MEL Chemicals) and sulfonated resins were used for comparison purposes.

The solid acid resins used were Amberlyst-15, Amberlyst-35 and Purolite D5081. These are all polystyrene sulfonic acid resins. Amberlyst-15 is a conventional macroporous polystyrene sulfonic acid. Amberlyst-35 is similar but has been “over- sulfonated”, so the concentration of acid sites is higher than for Amberlyst-15. Purolite D5081 is a so-called hypercrosslinked resin, which differs from other two in that it has a more porous structure

much greater surface area, and it is sulfonated at a relatively low level (chapter 3).

### **5.3. Experimental methods**

#### **5.3.1. Materials**

Precursor zirconium hydroxide (hydrated zirconia) was provided by MEL Ltd. Sulfated zirconia XZO 1720 was provided by MEL International, UK in powder form. Amberlyst-15 and Amberlyst-35 were purchased from Rohm and Haas, and Purolite D5081 was provided by Purolite International Ltd. Tributyrin was purchased from Acros organics at 98% purity. Oleic acid (analytical grade-99%) was purchased from Fluka. Anhydrous methanol 99.99% was supplied by Fisher Scientific.

#### **5.3.2. Catalysts preparation**

The synthesized sulfated zirconia (SZ) was prepared by the method of Miao and Gao [14]. Typically, 1 g of hydrated zirconia was impregnated with 15 ml of 0.5 M H<sub>2</sub>SO<sub>4</sub> solution for 30 min at room temperature. The solid was filtered and dried at 110 °C for 24 h to yield the sulfated zirconia (SO<sub>4</sub><sup>2-</sup>/ZrO<sub>2</sub>). For catalytic activity tests, the powder was calcined (APPENDIX-K) at the desired temperatures for 4 h in air. A temperature ramp of 10 °C min<sup>-1</sup> was used.

#### **5.3.3. Catalyst characterization**

Sulfated zirconia samples were characterized using powder X-ray diffraction on a Bruker D8 diffractometer operated at 40 kV and 20 mA using

nickel-filtered Cu K $\alpha$  radiation (1.5406 Å), The apparatus and the operating conditions are shown in APPENDIX-J. The peaks were taken over  $2\theta = 15^\circ - 70^\circ$ . Samples were calcined in the muffle furnace and all XRD patterns were run on sample at room temperature. FT-IR measurements were performed on a Nicolet 380 spectrometer. The spectrum was measured in the range 4000 to 400  $\text{cm}^{-1}$ . Nitrogen adsorption/desorption isotherm analysis to determine surface areas and pore sizes were performed on a ASAP 2020 Micrometrics instrument at  $-196^\circ\text{C}$ . Prior to surface area analysis, the sulfated zirconia catalysts were degassed at  $310^\circ\text{C}$  for 4h.

The acid concentration or ion exchange capacities (IEC) of the catalysts were measured by acid-base titration. The procedure was described by Tsai et al. [20] and the typical procedure was: 0.1 g of sample was soaked in 30 ml of 2M NaCl solution and equilibrated for 24 h to replace the protons by sodium ions. The remaining solution was then titrated with a 0.1 M NaOH solution using phenolphthalein as an indicator. The value of IEC is in mmol of sulfate groups per gram of dried sample.

#### **5.3.4. Catalyst testing**

##### **a) Transesterification reaction**

Transesterification reactions tests were performed in a 50 ml pressurised reactor (Autoclave Engineer). The reactor was equipped with controllable temperature and stirrer. The molar ratio of tributyrin to methanol was 1:20. The catalyst used for each reaction was 5 % by weight of tributyrin, the catalyst was activated at  $150^\circ\text{C}$  before use. The reaction

mixture was agitated at 600 rpm and heated at 120 °C. Samples were taken and analyzed by gas chromatography GC (Perkin Elmer Clarus 500) with 50 m BP1 capillary column and FID detector. N-decane was used as an internal standard. The tributyrin conversion was calculated from the peak area and compared to the peak area for the internal standard (n-decane).

#### **b) Simultaneous reaction of esterification and transesterification**

The simultaneous reaction was performed in the same reactor, using a mixture of the oleic acid and tributyrin. The oleic acid content was set to 10% by weight of tributyrin and the catalyst used was 5% w/w of the oleic acid. The temperature of reaction was set to 120 °C. The reaction was stopped after 2 h. The amount of oleic acid conversion was determined using acid base titration. A certain amount of sample was taken and 25 ml of anhydrous ethanol was added to ensure miscibility. Aqueous 0.1 NaOH solution was used as titrant and phenolphthalein was used as an indicator. Tributyrin concentration was analysed using GC as described in point (a) above.

### **5.4. Results and discussions**

#### **5.4.1. Catalyst characterization**

Table 5.1 shows the properties of the commercial and the synthesised sulfated zirconias studied following calcination at temperatures 400-900 °C. The table shows that the increasing the calcination temperature from 400 °C to 900 °C decreases the surface area from 220 to around 6 m<sup>2</sup> g<sup>-1</sup>, both for the synthesised catalyst and the commercial XZO-1720. Figure 5.1 shows the

influence of calcination temperature on the concentration of active sites on the catalysts. The two samples show broadly similar behaviour, with acid concentration increasing with calcination temperature up to 600 °C and then decreasing dramatically on calcination at high temperature. At high calcination temperatures, at 800 and 900 °C the acidity drops almost to zero. It is thought that above 700 °C the catalyst loses the sulfate group due to decomposition into SO<sub>2</sub> [4] and this may be responsible for the loss of acidity.

The table 5.1 lists the dominant phases present after calcination at each temperature. These phases were identified through the powder XRD patterns of the calcined samples. The link between the phase present, and physical and catalytic properties is discussed later.

Table 5.1. Properties of the sulfated catalyst following calcination at 400-900 °C.

Calcination Temp. °C	BET surface area (m <sup>2</sup> g <sup>-1</sup> )		Acidity (mmol g <sup>-1</sup> )		XRD phases
	XZ-1720	SZ-01	XZO-1720	SZ-01	
<b>400</b>	220	<b>232</b>	0.45	0.59	Amorphous
<b>500</b>	207	<b>212</b>	0.49	0.67	Amorphous
<b>600</b>	119	<b>116</b>	0.67	0.69	t-ZrO <sub>2</sub>
<b>700</b>	68	<b>85</b>	0.18	0.21	t-ZrO <sub>2</sub>
<b>800</b>	11	<b>22</b>	0.03	0.05	m,t-ZrO <sub>2</sub>
<b>900</b>	6.0	<b>6.0</b>	0.03	0.05	m,t-ZrO <sub>2</sub>

t=tetragonal phase, m=monoclinic phase.

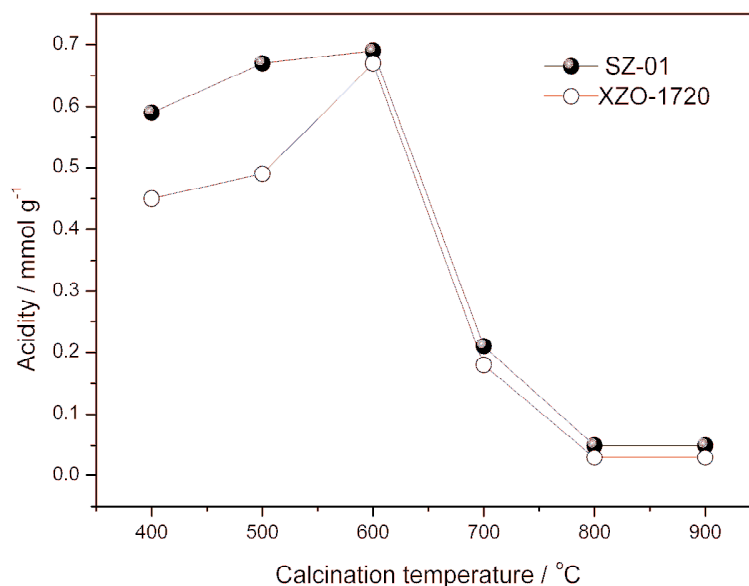


Figure 5.1. Effect of calcination temperature on acidities of sulfated zirconia catalyst.

Table 5.2 shows the five different catalysts studied in this research. The polystyrene sulfonic acid catalysts were dried at 80 °C for one hour before characterization. The Amberlyst-35 and 15 show the highest acidities. However, the BET surface area of Purolite D5081 is the highest. The value is close to 12 times higher than the other resins and six times higher than sulfated zirconia.

Table 5.2. Properties of sulfated zirconias and resins catalysts.

Catalyst	Calcination (°C)	BET Surface Area (m <sup>2</sup> .g <sup>-1</sup> )	Acidity (mmol g <sup>-1</sup> )
XZO-1720	600	119	0.67
SZ-01	600	116	0.69
Amberlyst-15	n.c	53	4.7
Amberlyst-35	n.c	50	5.4
Purolite D5081	n.c	702	1.0

n.c. not calcined

Figures 5.2a and 5.2b show powder XRD patterns for sulfated zirconia SZ-01 and XZO-1720 calcined at 400–900 °C. The powder XRD patterns of the two catalysts are similar. Calcination at 400 °C gives an amorphous (to XRD) zirconia structure. This can be seen from the broad peaks at  $2\theta = 20^\circ - 40^\circ$  and  $2\theta = 40^\circ - 70^\circ$ . When the temperature is increased to 500 °C for the SZ-01, the tetragonal phase, characterized by strong reflectance at  $2\theta = 30^\circ$  starts to develop. In contrast, the commercial sample XZO-1720 remains in the amorphous form as signalled by the broad peak at  $2\theta = 20^\circ - 40^\circ$ . On calcination at 600 °C and 700 °C the tetragonal structure for both catalysts becomes dominant, as indicated by reflections at  $2\theta = 30, 35$  and  $50^\circ$ . On further increase in temperature to 800 °C, the peaks associated with the tetragonal phase of  $ZrO_2$  are still detected but with some associated with monoclinic  $ZrO_2$  appearing at  $2\theta = 28^\circ$  and  $31.5^\circ$  in both catalysts.

On calcination at 900 °C, more monoclinic phase is seen and the intensities are higher at  $2\theta = 28^\circ$  and  $31.5^\circ$ . The strong peak at  $2\theta = 30^\circ$  due to the tetragonal phase decreases. On heating to 900 °C, the diffraction pattern for the sulfated zirconia sample is characteristic of the monoclinic zirconia structure with very little tetragonal material present. The pattern is very similar to that exhibited by zirconia (unsulfated) on calcination at 600 °C as seen at the top of Figure 5.2b.

Evidently, the presence of sulfate ions in zirconia changes the crystal structure from a mixture of the monoclinic and tetragonal phases to only tetragonal on 600 °C and 700 °C calcination. The sulfate ions tend to inhibit

the formation of the monoclinic structure, stabilizing the tetragonal phase up to 800 °C. On further increase to 900 °C, the sulfate ions decompose to form SO<sub>2</sub> as explained by Yadav [4]. Following decomposition, the material behaves like the original zirconia, converting to the monoclinic structure.

The two sulfated zirconia, SZ-01 and XZO-1720, behaves similarly but the former retain reflection due to the tetragonal phase to slightly high temperature. Whether this means that sulphatation is more effective for SZ-01 than for XZO-1720 is uncertain.

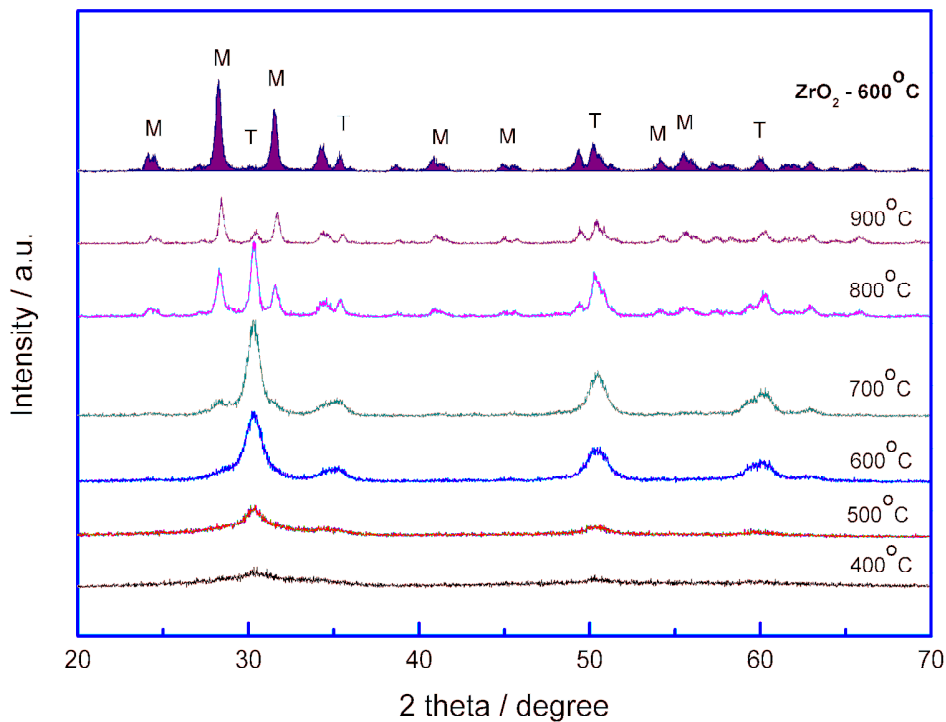


Figure 5.2a. Powder XRD patterns of sulfated zirconia (SZ-01) calcined at 400-900 °C and zirconia ZrO<sub>2</sub> at 600 °C. T = Tetragonal and M=Monoclinic.

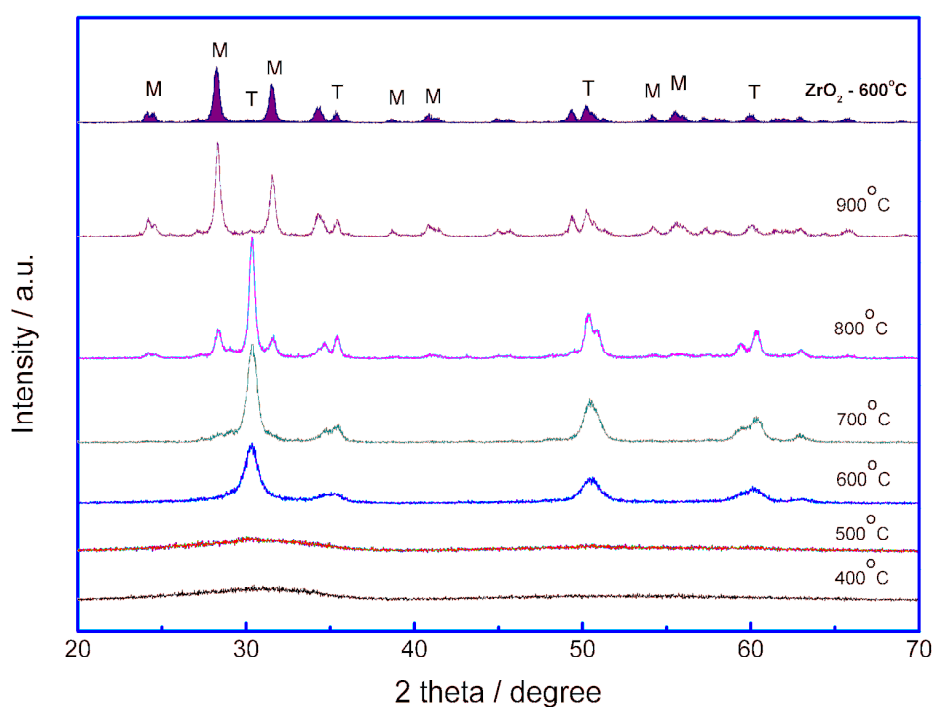


Figure 5.2b. Powder XRD patterns of sulfated zirconia (XZO-1720) calcined at 400-900 °C and zirconia  $ZrO_2$  at 600 °C. T = Tetragonal and M=Monoclinic.

The changes in the IR spectra caused by heating the catalyst to 400-900 °C for XZO-1720 and SZ-01, are shown in Figures 5.3a and 5.3b, concentrating on the band associated with S=O vibration. The bands between 1000-1100  $cm^{-1}$  are typical of sulfate ions coordinated to zirconium cations as suggested by Garcia at al. [15] and Sun at al.[16]. The detection of these bands verifies the effective sulfation of the zirconia substrate. The intensities of the bands for the two samples, while not quantified, are broadly similar, suggesting that the extent of sulfation on the SZ-01 sample was broadly similar to that of the commercial sample XZO-1720. With both samples, the intensity of the coordinated sulfate bands remains almost constant through calcination to 500-600 °C. Above this temperature the bands get smaller,

effectively disappearing by 900 °C. This is consistent with the idea that sulfate ions decompose and are lost from the solid over this temperature range. As the calcination temperature is increased, the band at 1000-1100  $\text{cm}^{-1}$  becomes sharper and the peak maximum shifts in frequency, unpredictably for the two samples. It is not clear what gives rise to this behaviour.

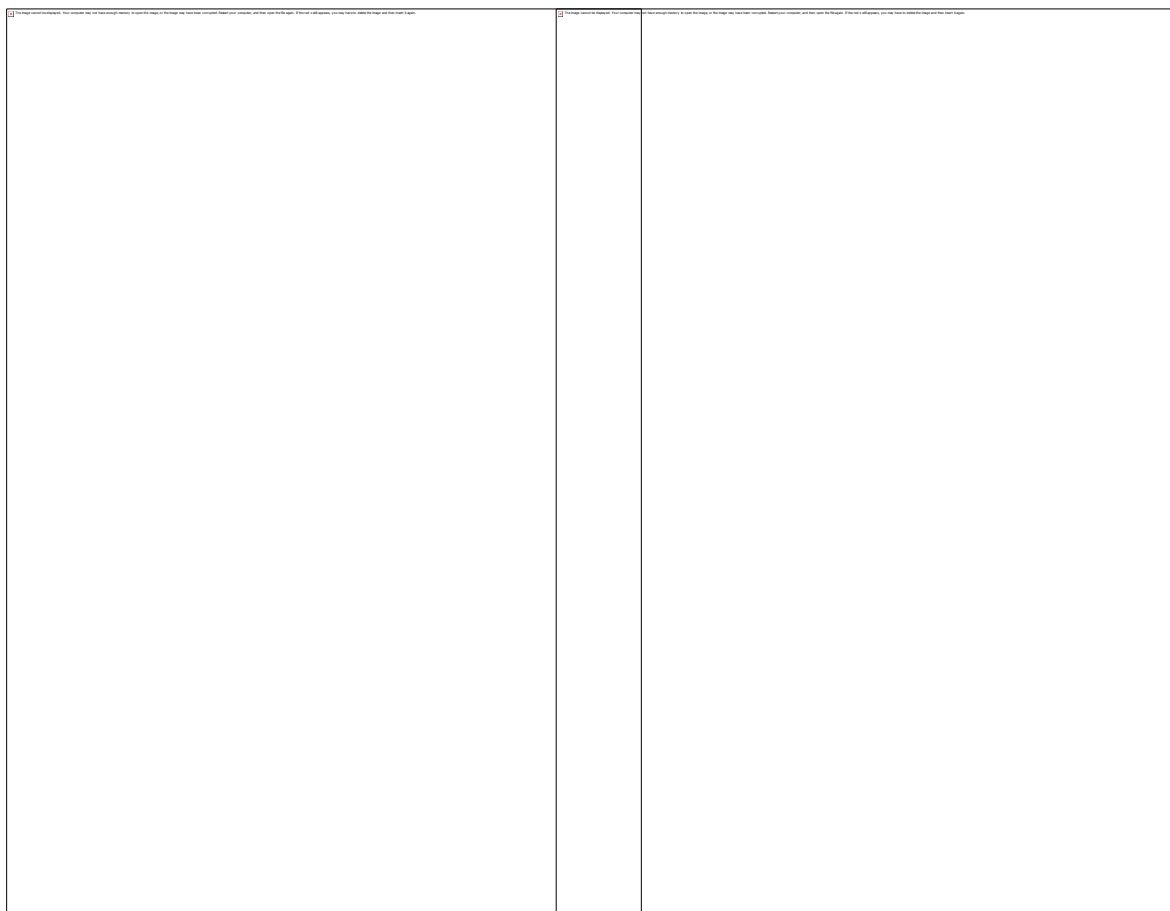


Figure 5.3. FTIR spectra of sulfated zirconia (a) XZO-1720 and (b) SZ-01 as function of calcination temperature.

### 5.4.2. Catalytic activities

Figure 5.4 shows the conversion/time profiles for both catalysts SZ-01 and XZO-1720 in the transesterification reaction of tributyrin with methanol at 120 °C in the 50 ml autoclave reactor. The catalyst was previously calcined at the optimum calcination temperature of 600 °C (see later). Figure 4.4 shows that SZ-01 exhibits 80 % conversion after 2 h, compared to 65 % with XZO-1720. This general level of activity is similar to that reported by Lopez at al.[10], who reported the transesterification of tricaprylin (TCP) with methanol using the same amount of sulfated zirconia catalyst gave 84 % yield after 2 h.

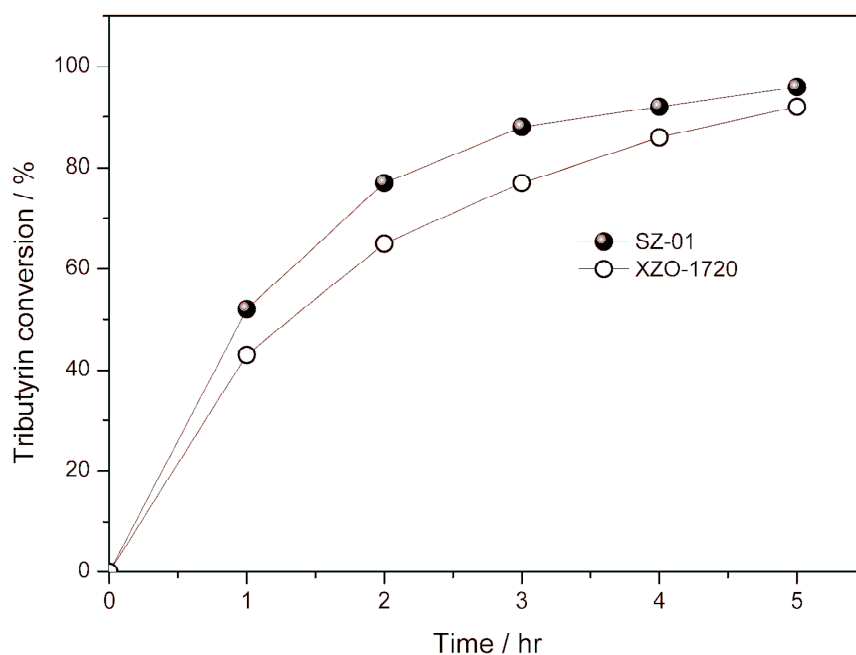


Figure 5.4 catalytic activity comparisons of SZ-01 and XZO-1720 in the transesterification of tributyrin at 120 °C.

The rate constants of the two catalysts were calculated assuming pseudo-first order kinetics, since the amount of methanol used was in excess, by

plotting  $\ln[\text{tributyrin}]$  vs time (h), as shown in Figure 5.5. The rate constant for SZ-01 is  $0.63 \text{ h}^{-1}$  and for XZO-1720 it is only  $0.49 \text{ h}^{-1}$ . Figure 5.5 shows that SZ-01 is faster than XZO-1720, this is due to the number of active sites of SZ-01 is higher ( $0.69 \text{ mmol g}^{-1}$ ) than the XZO-1720 which is  $0.67 \text{ mmol g}^{-1}$  as shown in Table 5.2.



Figure 5.5. First order plot for SZ-01 and XZO-1720 catalysts in the transesterification reaction of tributyrin.

The calcination temperature affects the catalyst surface area and acidity as shown previously (Figure 5.1). In Figures 5.6 and 5.7, the activity of sulfated zirconia SZ-01 and XZO-1720, expressed as the % conversion of tributyrin after 2 h reaction time, is plotted against calcination temperature.

On the same graph, the acid site concentration is plotted against calcination temperature (data from Table 5.1).



Figure 5.6. The effect of calcination temperature on acidity and catalyst activity for SZ-01

There is an excellent correlation between surface acidity and catalytic activity and both figures show very pronounced maxima on calcination at 600 °C. Both acidity and activity fall at higher calcination temperature. This decrease occurs because significant loss in  $\text{SO}_4^{2-}$  which, from XRD and IR results, is thought to occur at 800-900 °C. Our conclusion is that the maximum acidity and maximum activity correspond to the optimum temperature for the formation of the tetragonal zirconia structure, as opposed to the amorphous phase and the monoclinic phase.

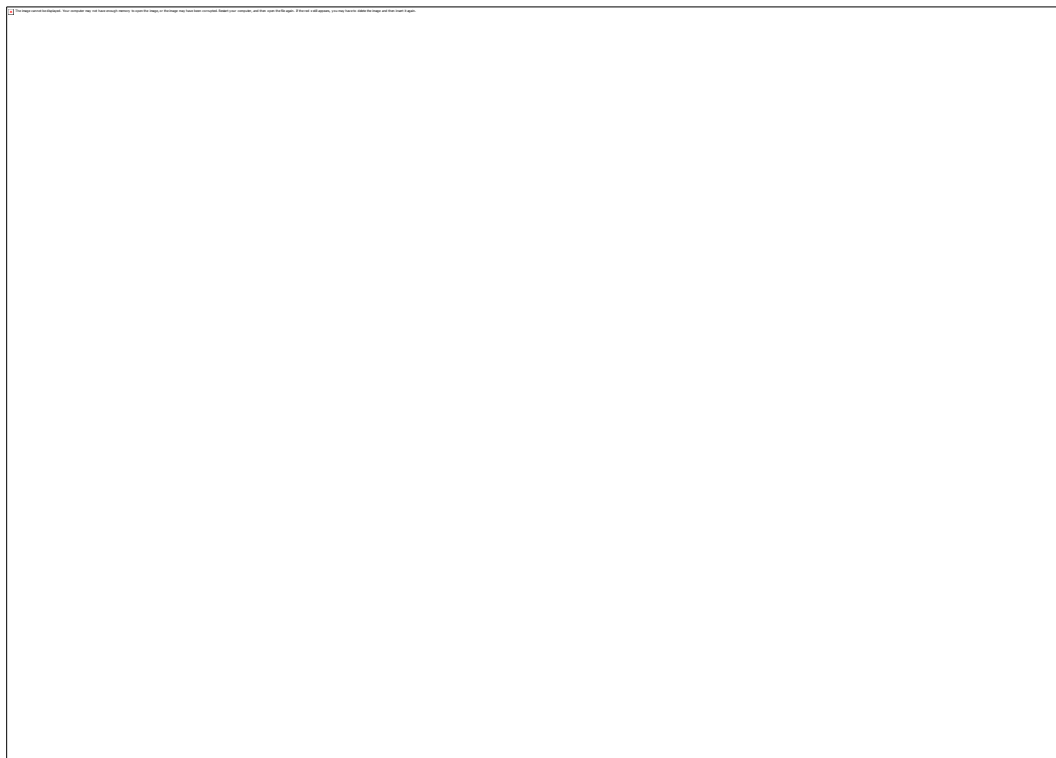


Figure 5.7. The effect of calcination temperature on acidity and catalyst activity for XZO-1720.

Table 5.3 shows the catalytic activity results for all the catalysts studied in the simultaneous esterification of oleic acid and the transesterification of tributyrin. It has already been shown that the transesterification reaction follows simple first order kinetics for reaction over 4-5 h. This justifies the use here of reactant conversion at a single reaction time of 2 h as a measure of catalytic activity. Experimentally, this was very much simpler than collecting data for full conversion/time plots.

We found that the oleic acid (free fatty acid) esterification reaction also followed first order kinetics (not shown), so activities in this reaction are also expressed as a single % conversion of reactant at a reaction time of 2 h. Using this mixture of reactant, the highest activity in the transesterification is

shown by SZ-01 followed by XZO-1720, D5081, Amberlyst-15 and Amberlyst-35. In the oleic acid esterification reaction, taking place alongside, the catalytic activities follows the order: Amberlyst- 15 > Amberlyst- 35 > SZ-01 = XZO-1720 > Purolite D5081.

Table 5.3. Catalyst activities in transesterification and esterification reactions.

Catalyst	BET Surface area (m <sup>2</sup> g <sup>-1</sup> )	Acidity (mmol g <sup>-1</sup> )	Transesterification <sup>a</sup> Conversion (%)	Esterification <sup>a</sup> Conversion (%)
XZO-1720	119	0.67	59	86
SZ-001	116	0.69	77	86
Purolite D5081	702	1.0	50	82
Amberlyst 35	50	5.4	37	91
Amberlyst 15	50	4.7	50	95

<sup>a</sup>The reaction was run for 2 h.

Figure 5.8 shows the esterification and transesterification results as a bar chart. Some conclusions can be drawn from the activities of the resin catalysts. In the esterification of oleic acid, Amberlyst-15 is more active than Amberlyst-35. This is in agreement with the result reported by Andrijanto et al. [17] (Chapter 3). In this paper, in which based simply on the single reaction between oleic acid and methanol (no triglyceride present), Purolite D5081 was shown to be even more active than Amberlyst. In marked contrast, the activity of D5081 in the same reaction studied here is very much lower. The difference is that here the reaction is carried out in the presence

of excess of triglycerides. We suggest that tributyrin could block the micropores of D5081, so the access of oleic acid to the active site become more difficult and the activity of Purolite D5081 in esterification is reduced.

In these simultaneous reactions, for the transesterification reactions, sulfated zirconia catalysts exhibit higher activities than the resin catalysts, even though the acidities are much lower. It therefore seems that, in the transesterification reaction, the number of active sites is not important. It is possible that the strength of acid sites is a more important factor in this reaction.



Figure 5.8. Catalytic activities of solid acid catalysts in simultaneous esterification and transesterification reactions at 120 °C expressed as reactant conversion after 2h.

### 5.4.3. Catalyst reusability

Catalyst reusability was tested in the transesterification reaction. The reusability test was conducted under the same conditions as described earlier and activity is expressed as conversion after 2 h. After each reaction, the catalyst was washed with methanol and recalcined at 600 °C before re-use. Figure 5.9 shows the results for SZ-01 after two consecutive additional cycles. Activity is reduced significantly after two cycles.



Figure 5.9. Reusability test on SZ-01 in transesterification of tributyrin at 120 °C.

There are several possible explanations. One is that pores in the sulfated zirconia become blocked by triglyceride and that calcination forms carbon which reduces access to the active sites. Another is that water in the

oil and methanol could bring about deactivation due to leaching of sulfate ions to the reaction mixture. In theory, water could react with sulfate ion in the catalyst to form  $H_2SO_4$ , resulting in leaching [18]. However, Kiss et al. suggested that deactivation of sulfated zirconia is not effected by water in small quantities. Fu et al. [19] also reported that no sulfate ions were observed in solution on reacting sulfated zirconia with aqueous  $BaCl_2$  and  $KOH$ . Unfortunately we did not measure sulphur leaching in this study. Lopez [10] suggested that possible leaching of sulfate ion from sulfated zirconia is due to the formation of dialkyl sulfates from sulphuric acid with alcohol. She conducted a study of this leaching process to prove the presence of alkyl-sulfate compounds by analyzing alcohol residue after sulfated zirconia was washed with alcohol. The solution was analyzed using proton-NMR and the result shows trace amounts of dimethyl sulfate confirming the presence of the species in leachate solution. She then proposed a deactivation mechanism for sulfated zirconia in alcohol at temperature above  $100\text{ }^\circ\text{C}$  as shown in Figure 5.10.

The mechanism of deactivation proposed by Lopez is shown in Figure 5.10 [10].

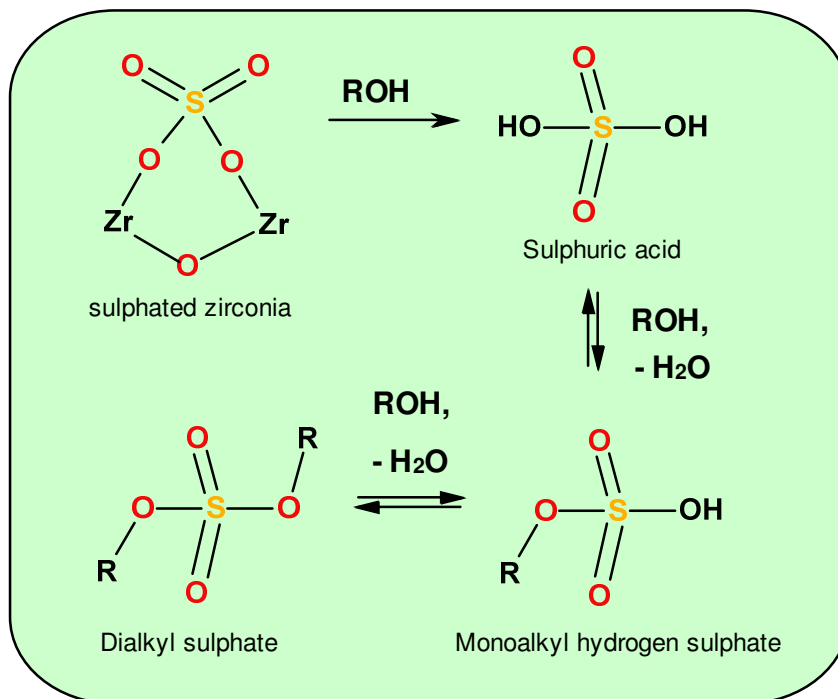


Figure 5.10. Possible sulfate leaching mechanism in sulfated zirconia.

## 5.5. Conclusions

The investigation of the effect of calcination temperature on the catalytic activity of  $\text{SO}_4^{2-}/\text{ZrO}_2$  shows that the optimum temperature for both SZ-01 and XZO-1720 is 600 °C. Evaluation in the transesterification reaction of tributyrin with methanol showed that SZ-01 is more active than XZO-1720. Evaluation in simultaneous transesterification and esterification reactions showed that the sulfated zirconia catalysts are better in the transesterification part than resin catalysts. In the esterification reaction, sulfonic acid resins catalyst show higher activity than sulfated zirconia.

Despite the reasonable catalytic activities of sulfated zirconia in the transesterification reaction, reusability is poor, suggesting that this type of catalyst may not be a practical alternative to homogeneous caustic catalysts. It seems quite likely that the deactivation of sulfated zirconia could be due to  $\text{SO}_4^{2-}$  leaching, since re-calcination did not help to recover the activity, as might have been expected if pore blocking was responsible.

By comparing resins with sulfated zirconia, it is concluded that transesterification requires relatively strong acid sites for catalysis, and that is why sulfated zirconia catalyst are more active. Esterification does not require particularly strong sites and so resins, with their higher concentration of acid sites, are more active. The dependence of sulfated zirconia activity on calcination temperature suggests that it is the tetragonal phase of sulfated zirconia that is most active.

## References

1. Ma, F.; Hanna, M. A., Biodiesel production: a review. *Bioresource Technology* 1999, 70, (1), 1-15.
2. Zabeti, M.; Wan Daud, W. M. A.; Aroua, M. K., Activity of solid catalysts for biodiesel production: A review. *Fuel Processing Technology* 2009, 90, (6), 770-777.
3. Helwani, Z.; Othman, M. R.; Aziz, N.; Fernando, W. J. N.; Kim, J., Technologies for production of biodiesel focusing on green catalytic techniques: A review. *Fuel Processing Technology* 2009, 90, (12), 1502-1514.

4. Yadav, G. D.; Nair, J. J., Sulfated zirconia and its modified versions as promising catalysts for industrial processes. *Microporous and Mesoporous Materials* 1999, 33, (1-3), 1-48.
5. Shishido, T.; Tanaka, T.; Hattori, H., State of Platinum in Zirconium Oxide Promoted by Platinum and Sulfate Ions. *Journal of Catalysis* 1997, 172, (1), 24-33.
6. Hattori, H.; Takahashi, O.; Takagi, M.; Tanabe, K., Solid super acids: Preparation and their catalytic activities for reaction of alkanes. *Journal of Catalysis* 1981, 68, (1), 132-143.
7. Hino, M.; Kurashige, M.; Matsushashi, H.; Arata, K., The surface structure of sulfated zirconia: Studies of XPS and thermal analysis. *Thermochimica Acta* 2006, 441, (1), 35-41.
8. Chen, C.-L.; Cheng, S.; Lin, H.-P.; Wong, S.-T.; Mou, C.-Y., Sulfated zirconia catalyst supported on MCM-41 mesoporous molecular sieve. *Applied Catalysis A: General* 2001, 215, (1-2), 21-30.
9. Furuta, S.; Matsushashi, H.; Arata, K., Catalytic action of sulfated tin oxide for etherification and esterification in comparison with sulfated zirconia. *Applied Catalysis A: General* 2004, 269, (1-2), 187-191.
10. Lopez, D. E.; Goodwin Jr, J. G.; Bruce, D. A.; Furuta, S., Esterification and transesterification using modified-zirconia catalysts. *Applied Catalysis A: General* 2008, 339, (1), 76-83.
11. Kiss, A. A.; Dimian, A. C.; Rothenberg, G., Biodiesel by Catalytic Reactive Distillation Powered by Metal Oxides. *Energy & Fuels* 2007, 22, (1), 598-604.
12. Jitputti, J.; Kitiyanan, B.; Rangsunvigit, P.; Bunyakiat, K.; Attanatho, L.; Jenvanitpanjakul, P., Transesterification of crude palm kernel oil and crude coconut oil by different solid catalysts. *Chemical Engineering Journal* 2006, 116, (1), 61-66.
13. Suwannakarn, K.; Lotero, E.; Goodwin Jr, J. G.; Lu, C., Stability of sulfated zirconia and the nature of the catalytically active species in the transesterification of triglycerides. *Journal of Catalysis* 2008, 255, (2), 279-286.

14. Gao, Z.; Xia, Y.; Hua, W.; Miao, C., New catalyst of  $\text{SO}_4^{2-}/\text{Al}_2\text{O}_3\text{-ZrO}_2$  for n-butane isomerization. *Topics in Catalysis* 1998, 6, (1/4), 101-106.
15. Garcia, C. M.; Teixeira, S.; Marciniuk, L. c. L.; Schuchardt, U., Transesterification of soybean oil catalyzed by sulfated zirconia. *Bioresource Technology* 2008, 99, (14), 6608-6613.
16. Sun, Y.; Ma, S.; Du, Y.; Yuan, L.; Wang, S.; Yang, J.; Deng, F.; Xiao, F.-S., Solvent-Free Preparation of Nanosized Sulfated Zirconia with Bronsted Acidic Sites from a Simple Calcination. *The Journal of Physical Chemistry B* 2005, 109, (7), 2567-2572.
17. Andrijanto, E.; Dawson, E. A.; Brown, D. R., Hypercrosslinked polystyrene sulfonic acid catalysts for the esterification of free fatty acids in biodiesel synthesis. *Applied Catalysis B: Environmental* 2012, 115-116, (0), 261-268.
18. Omota, F.; Dimian, A. C.; Bliet, A., Fatty acid esterification by reactive distillation: Part 2 : kinetics-based design for sulfated zirconia catalysts. *Chemical Engineering Science* 2003, 58, (14), 3175-3185.
19. Fu, B.; Gao, L.; Niu, L.; Wei, R.; Xiao, G., Biodiesel from waste cooking oil via heterogeneous superacid catalyst  $\text{SO}_4^{2-}/\text{ZrO}_2$ . *Energy and Fuels* 2009, 23, (1), 569-572.
20. Tsai, C.-E.; Lin, C.-W.; Hwang, B.-J., A novel crosslinking strategy for preparing poly (vinyl alcohol)-based proton-conducting membranes with high sulfonation. *Journal of Power Sources* 2010, 195, (8), 2166-2173.

# **CHAPTER 6**

## **LITHIUM ZIRCONATE AS SOLID BASE CATALYST**

---

“This chapter describes the study of lithium zirconate as a new solid base catalyst. The effect of calcination temperature on the catalytic activity in the transesterification of tributyl glycerate (tributylin) is discussed. Moreover, the parameters effecting the conversion of tributyrin, such as molar ratio, amount of catalyst, are also described”.

## 6.1. Overview

In the present work, the synthesis, characterization and the catalytic activity of the lithium zirconate as solid base catalyst for the liquid phase synthesis of the methylester of tributyrin at 63 °C was studied. Lithium zirconate catalysts have been successfully synthesized using traditional solid state synthesis with lithium acetate as precursor. They are labelled as LIZA-500, LIZA-700 and LIZA-900, depending on calcination temperature. The catalytic activities of the catalysts were compared with that of commercially available lithium zirconate MEL-1597/03 and the catalyst synthesised using lithium carbonate precursor LIZ-700, in transesterification of tributyrin with methanol. The catalyst properties were characterized using X-ray diffraction, nitrogen adsorption-desorption and scanning electron microscopy. The synthesised catalysts and commercial lithium zirconate exhibit very high activity in the transesterification of tributyrin. The effect of calcination temperature, molar ratio and the amount of catalyst to the conversion of tributyrin were also studied. It was found that lithium zirconate synthesised with different precursors yield almost the same activities.

## 6.2. Introduction

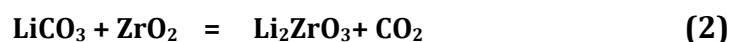
Biodiesel is usually produced via transesterification of triglyceride with alcohol catalysed by acids, bases or enzymes [1]. Base-catalyzed transesterification reaction are the most common, usually with sodium or potassium hydroxide as a homogeneous catalyst [2,3]. One problem with these catalysts is that they are limited to feedstock with low free fatty acid contents [4], and that large amounts of water are needed to wash the catalyst from the biodiesel [5].

The use of solid base catalyst would overcome these difficulties. The solid base catalyzed transesterification reaction of triglycerides has been extensively studied recently [6]. Calcium oxide is probably the most studied solid base for this reaction [7-11]. Mixed metal oxides have also been paid attention. Examples are  $\text{Al}_2\text{O}_3\text{-SnO}$  ,  $\text{Al}_2\text{O}_3\text{-ZnO}$  [12] and Mg-La oxides [13]. Alkali metal salts on alumina have also been used [7].

Recently Georgogianni has reported the use of potassium-doped zirconia in the transesterification of soybean oil with methanol at 60 °C [14]. Rekha reported high catalytic activity of mixed oxides of zirconium and magnesium. Hamad recently reported zirconia modified by cesium for the transesterification of rapeseed oil with methanol which showed reasonable activity at a practical reaction temperature of 60 °C [16].

In the present work, we describe a study of lithium zirconate as a solid base catalyst for the transesterification reaction. Lithium zirconate has been widely studied in other application and is one of the most promising

materials for CO<sub>2</sub> capture from flue gas at high temperature [17-19]. But it has not been much explored as a catalyst. In related work, lithium doped mesoporous zirconia has been shown to be active for the transesterification of soybean oil with methanol [20]. The catalyst was synthesized using a sol gel method. Unfortunately it suffered from poor reusability. After three repeat cycles the triglyceride conversion dropped from 97.9 % to 10.5 %. Zirconia promoted by Caesium (Cs) was also reported through cation exchange of zirconium hydroxide by Hamad et al. [21]. Unfortunately, no reusability data was presented by Hamad. The other problem is the cost of caesium is more expensive than lithium, and it is not practical for industrial catalyst. The synthesis of lithium zirconate has been reported in the literature [18, 19]. The reaction of zirconia and lithium precursor to form lithium zirconate is described in equations 1 and 2 below.



Scheme 1. Synthesis of lithium zirconate from 1) lithium acetate and 2) lithium carbonate.

This work is reporting the synthesis, characterization and application of lithium zirconate as an efficient heterogeneous base catalyst for the transesterification of tributyl glycerate (tributyryn) illustrated in Figure 6.1. Tributyrin was used as a mimic for vegetable oil triglycerides, in part because it is miscible with methanol, simplifying the catalytic testing.

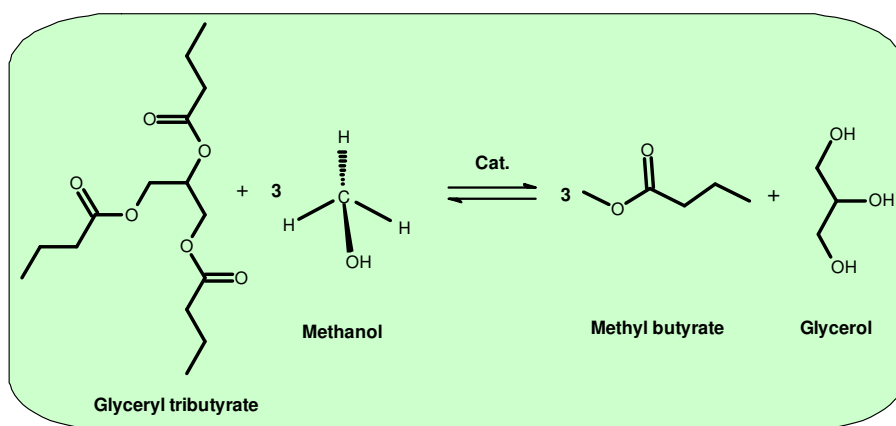


Figure 6.1. Transesterification reaction of tributyrin with methanol.

## 6.2. Experimental

### 6.2.1. Materials

Lithium acetate was purchased from Aldrich. Zirconium hydroxide, lithium carbonate and commercial Li<sub>2</sub>ZrO<sub>3</sub> were kindly given by MEL Chemicals UK. Tributyrin (98 %) was purchased from Acros Organics. Methanol (99.9 %) was purchased from Fluka. The internal standard n-decane was purchased from Fisher Scientific.

### 6.2.2. Catalyst preparation

Lithium zirconate was synthesized using a standard solid state synthesis method [18]. Lithium zirconate powder was prepared from lithium acetate (CH<sub>3</sub>COOLi) and zirconium hydroxide. The molar ratio of the starting materials was 2:1 (Li/Zr). The materials were weighed and ground in a mortar with a suitable amount of acetone. The reaction mixture was then dried at 100 °C for 24 h and the powder was ground for further calcination at various temperatures (500, 700 and 900 °C) for 6 h in dense alumina crucible

with heating rates of 1 °C min<sup>-1</sup>. These catalysts are indicated as LIZA-500, LIZA-700 and LIZA-900. The LIZC is lithium zirconate synthesized using the same method as LIZA, but lithium carbonate precursor was used to replace lithium acetate. MEL-1597 is lithium zirconate given by MEL Chemicals, UK. This lithium zirconate was synthesised using a different route, the sample was prepared by slurring a zirconium hydroxide in deionised water. Lithium carbonate was added slowly followed by potassium carbonate, and the resultant mixture was stirred for 30 min prior to calcination at 700 °C for 4 h in static air using ramp rate 3 °C min<sup>-1</sup> [22].

### **6.2.3. Catalyst characterization**

Scanning electron microscope (SEM) images were taken using a JEOL 6600 SEM instrument, at 20 mA emissions current and 12 kV accelerator voltages to study changes during the calcination.

Catalyst specific surface areas (BET) and pore volumes were measured by nitrogen adsorption/desorption at 77 K using a Micrometrics ASAP 2020 instrument. The samples were degassed at 350 °C for 6 h prior to the adsorption experiments. The surface areas were calculated from adsorption isotherms using the BET method and the desorption isotherms were used to calculate pore volumes using the BJH (Barret Joyner Halenda) method.

The concentration and strength of catalyst basic sites of the catalysts were measured using CO<sub>2</sub> adsorption calorimetry. A Setaram C80 differential microcalorimeter coupled to an evacuable glass-handling system was used to

monitor CO<sub>2</sub> adsorption and associated enthalpies of adsorption. Catalyst samples (ca. 20-30 mg dry weight) were conditioned in the calorimeter at 100 °C under vacuum for two hours, with an empty reference cell. Successive pulses of CO<sub>2</sub> were introduced to the sample at 100 °C. Enthalpy changes associated with each dose were converted to molar enthalpies of adsorption and are expressed as a function of catalyst CO<sub>2</sub> coverage. Detail of this technique has been reported in chapter 3 [23].

The powder XRD patterns of the catalysts were recorded using a Bruker D8 diffractometer using Cu K $\alpha$  radiation ( $\lambda = 1.5418 \text{ \AA}$ ) at 40 kV and 20 mA. The patterns were collected over the range 15-70 ° for  $2\theta$  with a resolution of 0.02 °, at a scanning speed of 2 ° min<sup>-1</sup>. This study was to examine phase transformations and dominant phases during calcination and following calcination at set temperatures.

#### **6.2.4. Catalytic activity**

The transesterification of tributyrin was performed in a 50 ml glass reactor equipped with a reflux condenser and magnetic stirrer. A known mass of tributyrin, methanol ( 4 g tributyrin + 20 g methanol) and internal standard (n-decane) were charged to the reactor and the temperature was elevated to 63 °C unless stated different. After the temperature reached the desired value, the catalyst was charged into the reactor. Samples were taken at regular intervals and the conversion of tributyrin was monitored using gas chromatography (Perkin Elmer Clarus 500) with BP1 capillary column and FID detector. N-decane was used as an internal standard. Reaction progress

was followed through the conversion of tributyrin but the formation of fatty acid methyl ester, methyl butyrate, was also followed, as was the formation of dibutyl glycerol, monobutyl glycerol and glycerol, although the GC peak for glycerol was invariably very broad. A sufficiently high stirring speed was applied to avoid diffusion control due to mass transfer limitations.

### **6.3. Results and discussion**

#### **6.3.1. Catalyst characterization**

The characteristics and properties of the synthesised and commercially available lithium zirconate catalysts are presented in Table 6.1. The last of these, “1597/03” was calcined by MEL Chemicals, at 700 °C before being supplied to us. The surface areas of the catalysts were found to decrease with calcination temperature increases, from 22.6 m<sup>2</sup> g<sup>-1</sup> at 500 °C to only 4.5 m<sup>2</sup> g<sup>-1</sup> at 900 °C.

Figure 6.2 shows powder XRD patterns of the lithium zirconate calcined at 500, 700, and 900 °C and the commercial lithium zirconate MEL 1597/03 calcined at 700 °C. It is clear that on calcination at 500 °C (LIZA-500), the lithium zirconate does not fully form reflection from the ZrO<sub>2</sub> and a lithium salt precursor dominates the XRD pattern. It is possible that the lithium hydroxide/carbonate (L) is formed from lithium acetate on calcination at 500 °C, it is supported by the presence of reflection at 2θ= 30.5 ° [19, 22]. In addition, no reflection is observed at 42.6 ° that corresponds to the plane tetragonal of-Li<sub>2</sub>ZrO<sub>3</sub> [19].

Table 6.2. Characteristics and properties of  $\text{Li}_2\text{ZrO}_3$  catalysts.

Catalyst	Calcination Temperature (°C)	BET surface area ( $\text{m}^2 \text{g}^{-1}$ )	Pore volume ( $\text{cm}^3 \text{g}^{-1}$ )
LiZA-500	500	22.6	0.29
LiZA-700	700	16.4	0.19
LiZA-900	900	4.5	0.03
1597/03	700	10.9	0.03

When the calcination temperature is raised to 700 °C, no lithium hydroxide/carbonate reflectance is observed. Lithium zirconate is formed and the tetragonal phase dominates the pattern, this result is in agreement with the result found by Nair and Fernandez [18-19]. The tetragonal phase can be clearly seen at peak 42.6 °. Evidence for the tetragonal phase of lithium zirconate is also presented at  $2\theta = 22.25, 36.02, 39.95, 42.64, 59.79, 61.54$  °, these peaks corresponds to the planes of tetragonal  $\text{Li}_2\text{ZrO}_3$  (JCPDS file No. 20-0647) [18, 24]. These peaks can still be observed on calcination at 800 °C. Further increase to 900 °C yields a mixture of tetragonal and monoclinic lithium zirconate phases. The monoclinic peaks are clearly seen at  $2\theta = 20.27$  ° [18]. This shows that the transformation of lithium zirconate from the tetragonal phase to the monoclinic occurs between 800 and 900 °C. This is in a good agreement with the finding of Fernandez at al. (19) and Wyers at al. (25), who reported that the tetragonal phase of lithium zirconate transformed into the monoclinic phase at 900 °C. The calcination

temperature of 700 °C was selected in the present work because it corresponds to maxima in both catalytic activity and basicity as described later. At this temperature, the tetragonal phase dominates the patterns. This suggests that tetragonal phase is responsible for the catalytic activity.

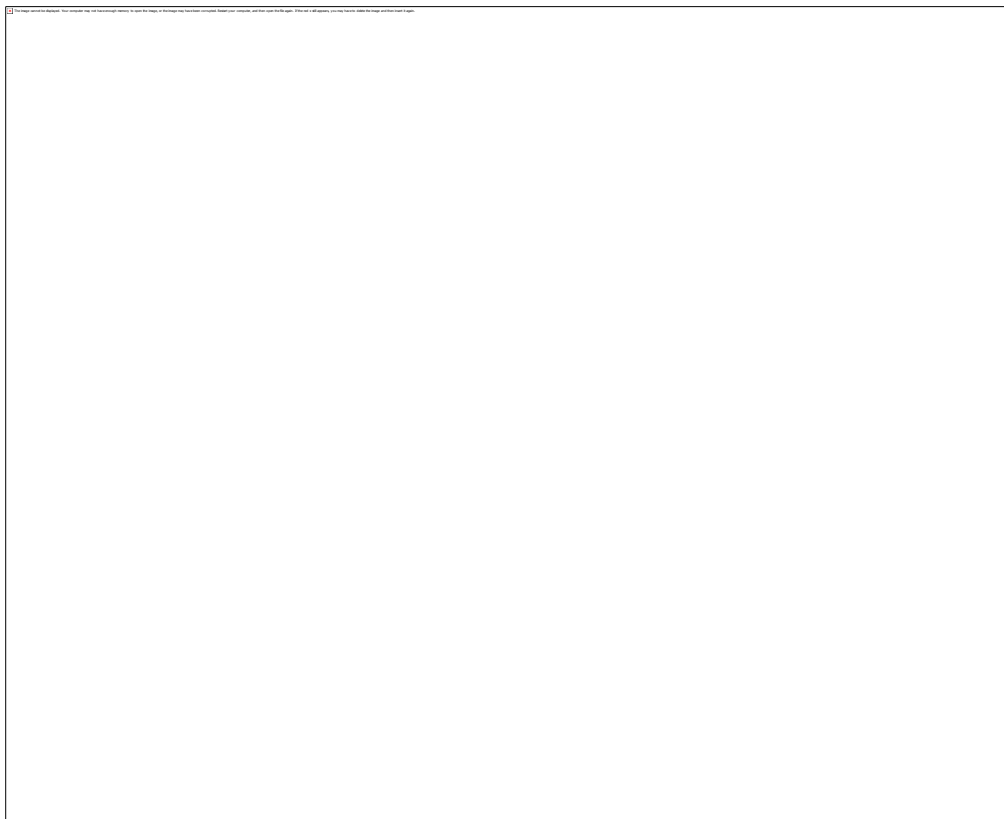


Figure 6.2. Powder XRD patterns of synthesized  $\text{Li}_2\text{ZrO}_3$  after calcination at 500-900 °C and  $\text{ZrO}_2$  calcined at 600 °C. Notations: Z = zirconia, T =  $\text{Li}_2\text{ZrO}_3$  tetragonal, M=  $\text{Li}_2\text{ZrO}_3$  monoclinic, L = calcination product of lithium zirconate.

Scanning electron microscopy (SEM) was used to examine the surface morphology of the catalysts. The images of the synthesised  $\text{Li}_2\text{ZrO}_3$  before (a) and after calcination (b-d) at 500 °C, 700 °C and 900 °C are shown in Figures 6.3 (a), (b) and (c) and (d). The synthesised lithium zirconate before calcination (a) shows agglomerates of bound particles with diameters in the

range 20-100  $\mu\text{m}$ . No pores are observed at this resolution. When the calcination temperature was increased to 500  $^{\circ}\text{C}$  (b), agglomeration was less extensive and aggregates of 20-50  $\mu\text{m}$  are seen. Increasing the calcination temperature to 700  $^{\circ}\text{C}$  (c) reduces particle size to 15-30  $\mu\text{m}$  and small pores are observed. Further increasing to 900  $^{\circ}\text{C}$  (d) reduces particle size further to 1-5  $\mu\text{m}$  and pores can now be clearly seen. This might be expected to translate to an increase in surface area as calcination temperature is increased. In fact the surface area falls as the calcination temperature is increased. The probable explanation for this is that the pores observed in the image represent only the macro pores of the agglomerated crystals. Smaller pores would not be seen at the resolution available, so the full picture is not available through which SEM images could be correlated to surface area data.

$\text{CO}_2$  adsorption microcalorimetry was used to measure the concentration of surface basic sites and the basic strengths of the catalysts. This method gives a profile of molar enthalpy of  $\text{CO}_2$  adsorption against amount of  $\text{CO}_2$  adsorbed (Figure 6.4). In order to convert these plots into simple numbers expressing the concentration and average strength of basic sites, the assumption are made that (i)  $\text{CO}_2$  adsorbs stoichiometrically on basic sites, (ii) only  $\text{CO}_2$  that adsorbs with enthalpy greater than 80  $\text{kJ mol}^{-1}$  represent significantly basic sites. On this basis it is possible to determine a value for the concentration of basic sites and, averaging all the molar enthalpies for  $\text{CO}_2$  pulses that populate basic sites, it is possible to give a value for the average molar enthalpy of  $\text{CO}_2$  adsorption which is an indication of the average strength of the basic sites. Another important feature of this

adsorption profiles is the molar enthalpy of CO<sub>2</sub> adsorption for the first one or two pulses, which are indications of the strength of the strongest basic sites in the catalyst.

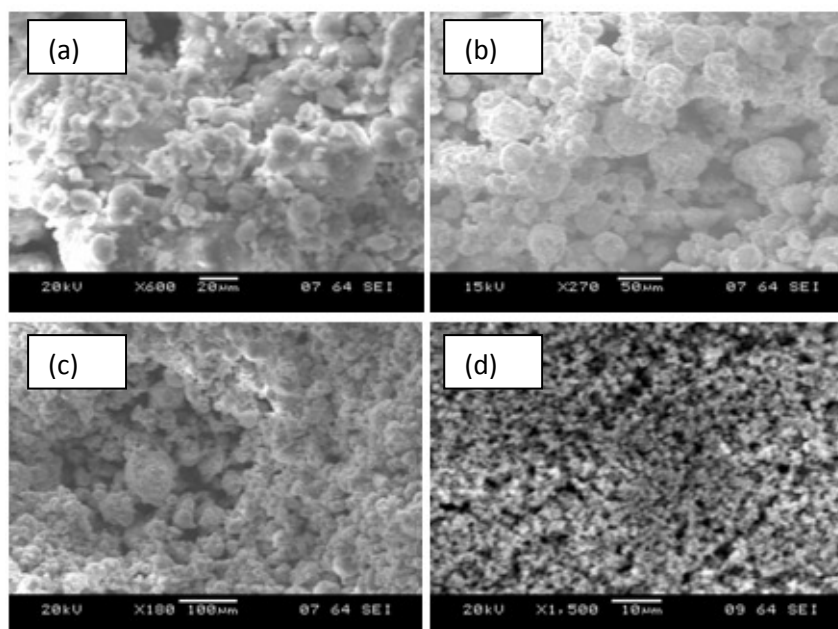


Figure 6.3. Scanning electron micrographs of (a) mixtures zirconium hydroxide and lithium acetate before calcination (b) LIZA- 500 (500 °C), (c) LIZA-700 (700°C) and (d) LIZA-900 (900 °C).

Table 6.2. Characteristics and properties of Li<sub>2</sub>ZrO<sub>3</sub> catalysts.

Catalyst	Calcination Temperature (°C)	BET surface area (m <sup>2</sup> g <sup>-1</sup> )	ΔH <sup>o</sup> <sub>ads</sub> (CO <sub>2</sub> ) kJ mol <sup>-1</sup>	Basic site concentration (μmol g <sup>-1</sup> )
LiZA-500	500	22.6	80	30
LiZA-700	700	16.4	118	170
LiZA-900	900	4.5	100	50
1597/03	700	10.9	123	160

The results of this are tabulated in Table 6.2. The CO<sub>2</sub> adsorption profiles in Figure 6.4 and the data in Table 6.2 show that the concentration of basic sites of the catalyst depends on the calcination temperature, going from 30 μmol g<sup>-1</sup> for LIZA-500 to 170 μmol for LIZA-700 (700 °C) and back down to 50 μmol g<sup>-1</sup> for LIZA-900. MEL 1597/03 (700 °C) shows the concentration of basic sites of 160 μmol g<sup>-1</sup>. LIZA-700 and MEL-1597/03 show the strongest basic sites. These clear maxima in basicity correspond to maxima in catalytic activity, as might be expected. In addition, at calcination temperature of 700 °C the dominant Li<sub>2</sub>ZrO<sub>3</sub> phase is tetragonal phase. This further support the view that the tetragonal form of Li<sub>2</sub>ZrO<sub>3</sub>, is the most basic and the phase that exhibit the highest catalytic activity.

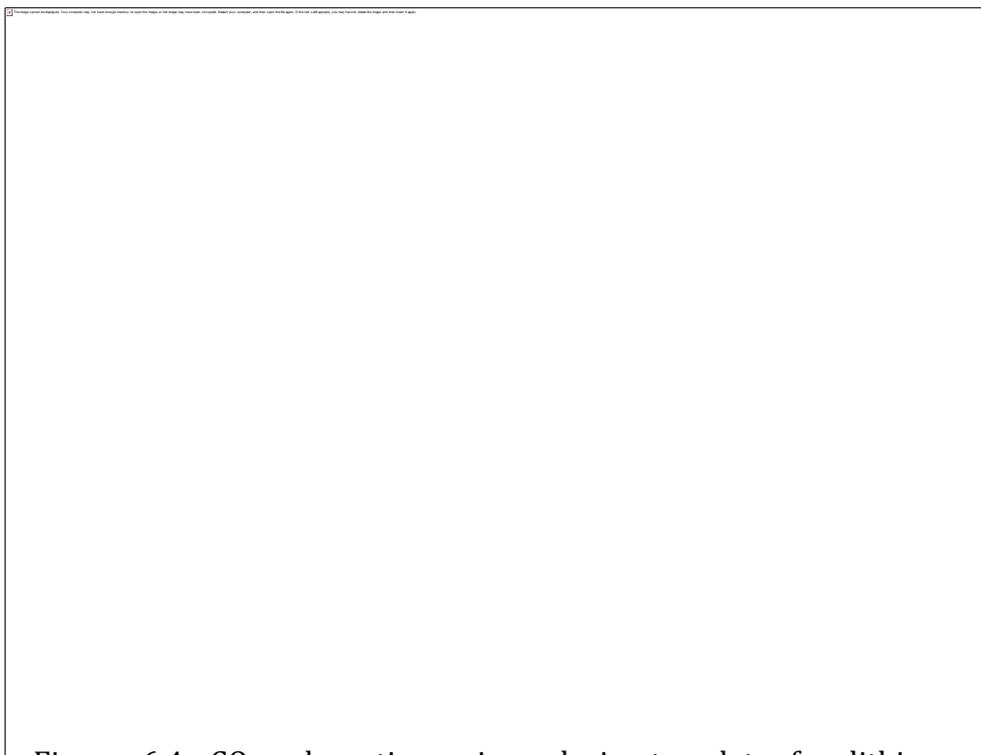


Figure 6.4. CO<sub>2</sub> adsorption microcalorimetry data for lithium zirconate catalyst.

### 6.3.2. Catalytic activity

#### (a) Effect of calcination temperature

Figure 6.5 shows the conversion/time plot for the three synthesised catalysts as a function of calcination temperature for the transesterification of tributyrin with methanol at 63 °C. The optimum calcination temperature appears to be 700 °C (LIZA-700) where full conversion of tributyrin is achieved in ten minutes. This catalyst is very much more active than LIZA-900 and LIZA-500 for which the conversions at ten minutes are only 35 % and 10 % respectively.



Figure 6.5. Conversion vs time for tributyrin transesterification using lithium zirconate calcined at 500, 700 and 900 °C.

By comparing the calorimetric CO<sub>2</sub> adsorption data with the catalytic activity data in Figure 6.5, there is a clear correlation between the concentration of basic sites / strength of basic sites and catalytic activity. The concentrations

of basic sites on the three catalysts vary in the ratios 30:170:50 but the reaction rates vary by much more than this. This strongly suggests that the strength of basic sites also has a controlling influence on catalytic activities.

### **(b) Effect of catalyst synthetic route**

The activity of the synthesised catalyst LIZA-700 is compared with that of the commercial lithium zirconate MEL 1597/03 and with lithium zirconate prepared using lithium carbonate precursor LIZC-700. Figure 6.6 shows conversion with time at 50 °C using 0.5 % catalyst and an alcohol/tributyryn ratio of 10:1. The catalysts were tested at 50 °C to obtain observable reaction rates. The figure shows that the MEL 1597/03 is slightly more active than LIZA-700. In contrast, LIZA-700 and LIZC-700 show almost the same rates. The three materials were made in different ways. MEL 1597/03 was prepared from wet slurry of lithium carbonate and zirconia. LIZA-700 was prepared from dry (in acetone) mixture of the lithium acetate and zirconia and the LIZC was prepared from lithium carbonate and zirconia using the same condition of LIZA. The catalytic activities of the three catalysts are almost within experimental error of each other, although the commercial catalyst MEL 1597/03 maybe slightly more active than the other two. The overall conclusion is that the synthesis method has relatively little effect on catalytic activity.

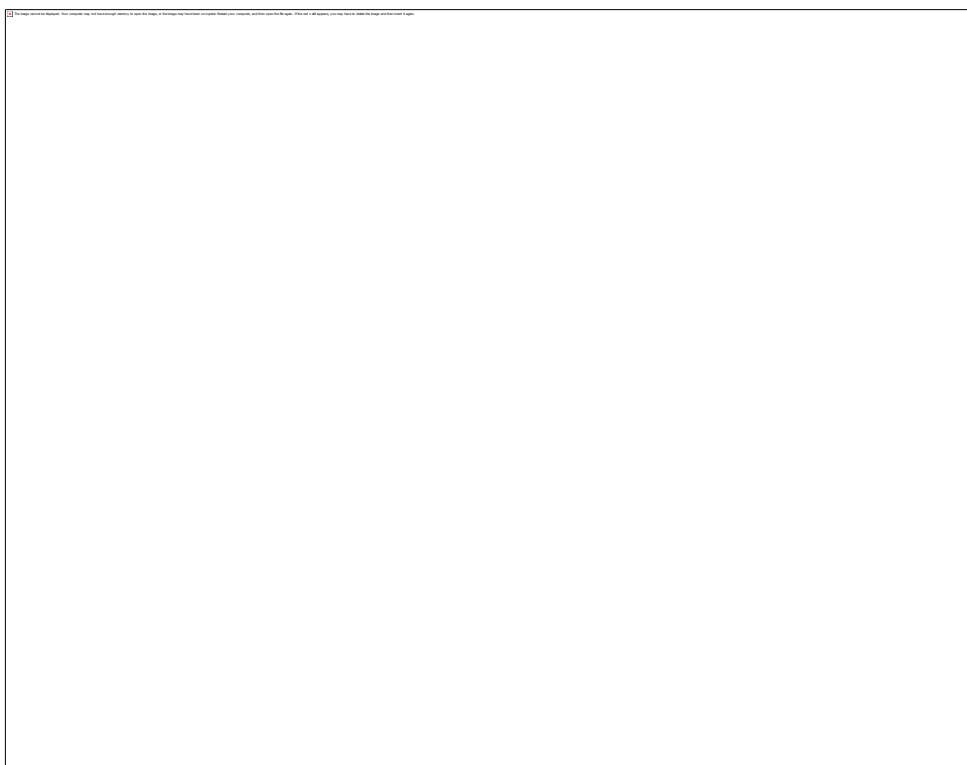


Figure 6.6. Comparison of the catalytic activities of three different catalysts.

### **(c) Effect of reactant molar ratio**

Transesterification usually requires a large excess of methanol to shift the equilibrium favourably. This experiment is to find the optimum tributyrin/methanol molar ratio used in the transesterification of tributyrin and methanol using LIZA-700 catalyst. Three different molar ratios of tributyrin to methanol were studied: 1:10, 1:5 and 1:2.5.

The experimental results are presented in Figure 6.7. The conversion based on tributyrin was essentially 100 % when using a 1:10 and 1:5 of tributyrin to methanol ratio, but at 1:2.5 the conversion was restricted to about 20 %. The reaction rate increased with increasing alcohol content of the reaction mixture.

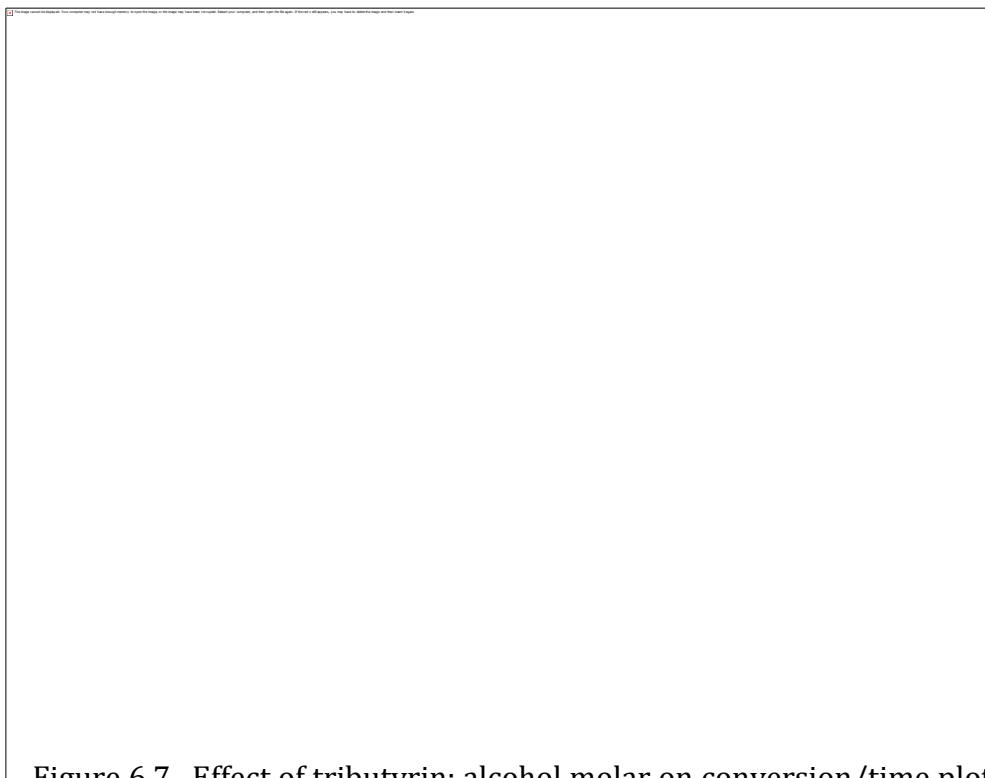


Figure 6.7. Effect of tributyrin: alcohol molar on conversion/time plot for the transesterification of tributyrin with methanol at 63 °C (molar ratio 1 : 10).

#### **(d) Effect of catalyst quantity**

Figure 6.8 shows the effect of the catalyst amount by % weight to the tributyrin towards the tributyrin conversion using LIZA-700. Three different catalyst concentrations were used 1 %, 0.5 % and 0.25 %. It would be reasonable to assume the rate would be proportional to the amount of catalyst up to a certain level. The results here show a clear dependence but the relationship is not linear. Increasing catalyst amount from 0.25 % to 0.5 % increases the initial rate (based on conversion at 5 minutes) by almost ten times, the explanation of the this behaviour remains uncertain. Doubling catalyst amount from 0.5 % to 1.0 % show more expected behaviour, approximately doubling the rate.

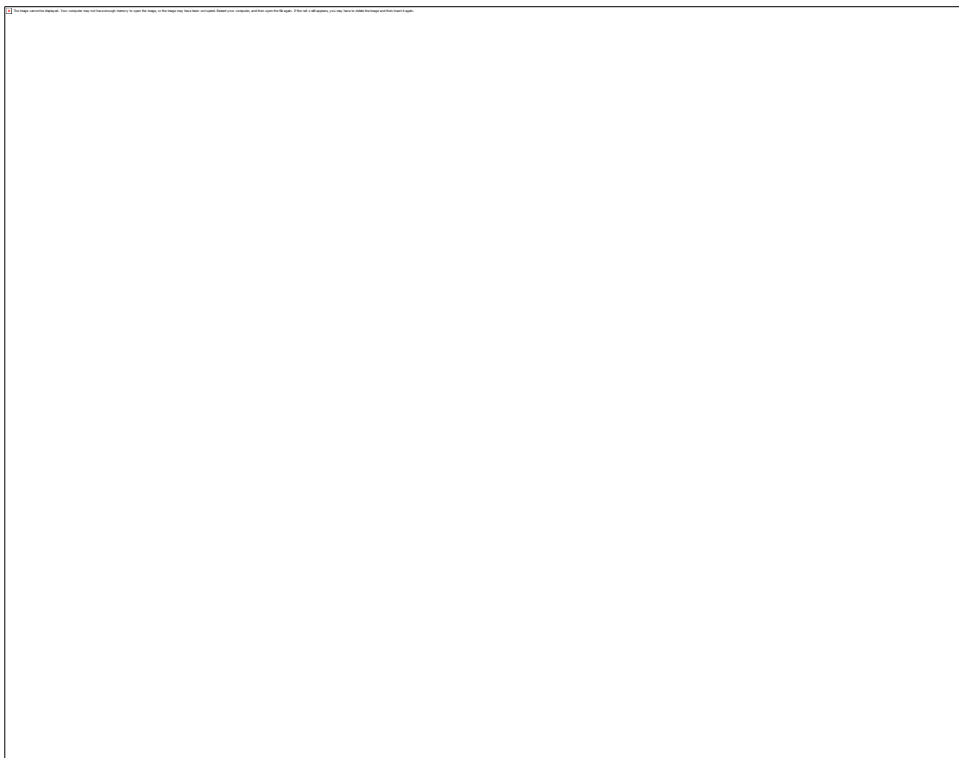


Figure 6.8. The effect of the catalyst amount on the conversion of tributyrin at 63 °C.

### 6.3.3. Reusability and leaching test

It was reported by Ding et al., that the immobilised lithium on zirconia catalyst prepared using a sol-gel method suffered from leaching of lithium to the reactant solution [20], resulting in catalyst activity (triglyceride conversion) decreasing from 97.9 % to 10.5 % after three consecutive runs. In this experiment, reusability tests were conducted in essentially the same way. The test was conducted at 63 °C using the same molar ratio of tributyrin to methanol of 1:10, with 1% catalyst. The catalyst was removed after 30 minutes reaction time. The catalyst was filtered, washed, dried and re-calcined at 700 °C before being reused each time.



Figure 6.9. Reusability test of LIZA-700 on transesterification of tributyrin with methanol at 63 °C (30 minutes).

Figure 6.9 shows the catalytic performance in multiple cycles. After four cycles, the catalyst exhibited high catalytic activity with only a small loss being observed. The conversion after 30 minutes is in the range of 92-98 %. This shows the stability and robustness of lithium zirconate as a solid base catalyst for the transesterification reaction.

Figure 6.10 shows conversion/time plots in the transesterification of tributyrin with methanol test for catalyst leaching to the reaction mixture. After fifteen minutes, the catalyst was removed from the reaction mixture by filtering. After that the reaction mixture was poured back into the reactor and samples were taken every fifteen minutes up to one hundred minutes and analysed using gas chromatography. The figure shows the comparison between with and without catalyst removal. With catalyst removal, the

reaction stopped and no further conversion is observed. Without catalyst removal, it is clear that the reaction continued and almost achieved equilibrium after one hour. This is evidence that the activity of the catalyst is not due to a homogeneous system arising from leached lithium salts.



Figure 6.10. Leaching test of LIZA-700 in the transesterification of tributyrin with methanol.

#### **6.4. Conclusions**

Lithium zirconate is a promising solid base catalyst for transesterification reactions. The calcination temperature affects the catalytic activity and the optimum calcination temperature is 700 °C. At this temperature, the catalyst shows the highest basic site concentration at 170  $\mu\text{mol/g}$  and these sites are stronger than those detected after calcination at

lower and higher temperature. The tetragonal phase is dominant on calcination at this temperature and it is concluded that this phase is almost certainly responsible for the catalytic activity of the catalyst.

In general, the conclusions from this study are as follows:

- (i)  $\text{Li}_2\text{ZrO}_3$  is a very active heterogeneous catalyst for the transesterification of triglycerides with methanol.
- (ii)  $\text{Li}_2\text{ZrO}_3$  exhibits a tetragonal structure on calcination up to about 800 °C and a monoclinic structure at higher temperature.
- (iii) Maximum catalytic activity is associated with the tetragonal phase (calcinations at 700 °C) as is the maximum concentration of basic sites and the highest strength of basic sites.
- (iv) The specific surface area of the lithium zirconate is relatively low and catalyst activity is not dependent on surface area.
- (v) Catalytic activity does not appear to be dependent on the method of synthesis of lithium zirconate.
- (vi) The catalyst can be successfully re-used with only minimal loss in activity. Evidence suggests that the catalyst does not leach to the reaction mixture appreciably.

## References

1. Ma, F.; Hanna, M. A., Biodiesel production: a review. *Bioresource Technology* 1999, 70, (1), 1-15.
2. Felizardo, P.; Neiva Correia, M. J.; Raposo, I.; Mendes, J. o. F.; Berkemeier, R.; Bordado, J. o. M., Production of biodiesel from waste frying oils. *Waste Management* 2006, 26, (5), 487-494.
3. Kulkarni, M. G.; Gopinath, R.; Meher, L. C.; Dalai, A. K., Solid acid catalyzed biodiesel production by simultaneous esterification and transesterification. *Green Chemistry* 2006, 8, (12), 1056-1062.
4. Wang, Y.; Ou, S.; Liu, P.; Xue, F.; Tang, S., Comparison of two different processes to synthesize biodiesel by waste cooking oil. *Journal of Molecular Catalysis A: Chemical* 2006, 252, (1-2), 107-112.
5. Kouzu, M.; Hidaka, J.-s.; Komichi, Y.; Nakano, H.; Yamamoto, M., A process to transesterify vegetable oil with methanol in the presence of quick lime bit functioning as solid base catalyst. *Fuel* 2009, 88, (10), 1983-1990.
6. Hattori, H., Heterogeneous Basic Catalysis. *Chemical Reviews* 1995, 95, (3), 537-558.
7. Ebiura, T.; Echizen, T.; Ishikawa, A.; Murai, K.; Baba, T., Selective transesterification of triolein with methanol to methyl oleate and glycerol using alumina loaded with alkali metal salt as a solid-base catalyst. *Applied Catalysis A: General* 2005, 283, (1-2), 111-116.
8. Demirbas, A., Biodiesel from sunflower oil in supercritical methanol with calcium oxide. *Energy Conversion and Management* 2007, 48, (3), 937-941.
9. Liu, X.; He, H.; Wang, Y.; Zhu, S.; Piao, X., Transesterification of soybean oil to biodiesel using CaO as a solid base catalyst. *Fuel* 2008, 87, (2), 216-221.

10. Watkins, R. S.; Lee, A. F.; Wilson, K., Li-CaO catalysed tri-glyceride transesterification for biodiesel applications. *Green Chemistry* 2004, 6, (7), 335-340.
11. Zhu, H.; Wu, Z.; Chen, Y.; Zhang, P.; Duan, S.; Liu, X.; Mao, Z., Preparation of Biodiesel Catalyzed by Solid Super Base of Calcium Oxide and Its Refining Process. *Chinese Journal of Catalysis* 2006, 27, (5), 391-396.
12. Granados, M. L. p.; Poves, M. D. Z.; Alonso, D. M. N.; Mariscal, R.; Galisteo, F. C.; Moreno-Tost, R.; Santamara, J.; Fierro, J. L. G., Biodiesel from sunflower oil by using activated calcium oxide. *Applied Catalysis B: Environmental* 2007, 73, (3-4), 317-326.
13. Macedo, C. C. S.; Abreu, F. R.; Tavares, A. P.; Alves, M. B.; Zara, L. F.; Rubim, J. C.; Suarez, P. A. Z., New heterogeneous metal-oxides based catalyst for vegetable oil trans-esterification. *Journal of the Brazilian Chemical Society* 2006, 17, 1291-1296.
14. Babu, N. S.; Sree, R.; Prasad, P. S. S.; Lingaiah, N., Room-Temperature Transesterification of Edible and Nonedible Oils Using a Heterogeneous Strong Basic Mg/La Catalyst. *Energy & Fuels* 2008, 22, (3), 1965-1971.
15. Georgogianni, K. G.; Katsoulidis, A. P.; Pomonis, P. J.; Kontominas, M. G., Transesterification of soybean frying oil to biodiesel using heterogeneous catalysts. *Fuel Processing Technology* 2009, 90, (5), 671-676.
16. Sree, R.; Seshu Babu, N.; Sai Prasad, P. S.; Lingaiah, N., Transesterification of edible and non-edible oils over basic solid Mg/Zr catalysts. *Fuel Processing Technology* 2009, 90, (1), 152-157.
17. Ida, J.-i.; Lin, Y. S., Mechanism of High-Temperature CO<sub>2</sub> Sorption on Lithium Zirconate. *Environmental Science & Technology* 2003, 37, (9), 1999-2004.
18. Nair, B. N.; Yamaguchi, T.; Kawamura, H.; Nakao, S.-I.; Nakagawa, K., Processing of Lithium Zirconate for Applications in Carbon Dioxide

- Separation: Structure and Properties of the Powders. *Journal of the American Ceramic Society* 2004, 87, (1), 68-74.
19. Ochoa-Fernández, E.; Ranning, M.; Grande, T.; Chen, D., Synthesis and CO<sub>2</sub> Capture Properties of Nanocrystalline Lithium Zirconate. *Chemistry of Materials* 2006, 18, (25), 6037-6046.
  20. Ding, Y.; Sun, H.; Duan, J.; Chen, P.; Lou, H.; Zheng, X., Mesoporous Li/ZrO<sub>2</sub> as a solid base catalyst for biodiesel production from transesterification of soybean oil with methanol. *Catalysis Communications* 2011, 12, (7), 606-610.
  21. Hamad, B.; Perard, A.; Figueras, F. o.; Rataboul, F.; Prakash, S.; Essayem, N., Zirconia modified by Cs cationic exchange: Physico-chemical and catalytic evidences of basicity enhancement. *Journal of Catalysis* 2010, 269, (1), 1-4.
  22. Iwan, A.; Stephenson, H.; Ketchie, W. C.; Lapkin, A. A., High temperature sequestration of CO<sub>2</sub> using lithium zirconates. *Chemical Engineering Journal* 2009, 146, (2), 249-258.
  23. Koujout, S.; Brown, D. R., Calorimetric base adsorption and neutralisation studies of supported sulfonic acids. *Thermochimica Acta* 2005, 434, (1-2), 158-164.
  24. Kang, S.-Z.; Wu, T.; Li, X.; Mu, J., Low temperature biomimetic synthesis of the Li<sub>2</sub>ZrO<sub>3</sub> nanoparticles containing Li<sub>6</sub>Zr<sub>2</sub>O<sub>7</sub> and high temperature CO<sub>2</sub> capture. *Materials Letters* 2010, 64, (12), 1404-1406.
  25. Wyers, G. P.; Cordfunke, E. H. P.; Ouweltjes, W., The standard molar enthalpies of formation of the lithium zirconates. *The Journal of Chemical Thermodynamics* 1989, 21, (10), 1095-1100.

# **CHAPTER 7**

## **CALCIUM OXIDE - MAGNETITE AS SOLID BASE CATALYST**

---

“This chapter describes the use of calcium oxide-magnetite composite as a solid base catalyst in transesterification reactions. This catalyst has magnetic properties which allow easy separation from the reaction mixture. The effect of calcination temperature on catalytic activity and magnetic properties is also reported”.

## 7.1. Overview

Magnetite-CaO composites have been studied as solid base catalysts in biodiesel synthesis. The magnetite-CaO was synthesized using an impregnation method between CaO and magnetite ( $\text{Fe}_3\text{O}_4$ ). The optimum catalytic activity of the catalyst was obtained at the calcination temperature 700 °C. The capacity to separate used catalyst from the reaction mixture using a magnetic field was assessed. The reusability data shows that the CaO-magnetite can be reused with small loss of its activity but it retains its magnetic properties. Therefore, this preliminary work provides a potential approach for design and synthesis of a composite catalyst which can be used for practical use in biodiesel synthesis or other application.

## 7.2. Introduction

Calcium oxide (CaO), an alkaline metal oxide solid, is one of the most studied solid base catalyst for the transesterification reaction in biodiesel synthesis [1-9]. Most of the reports show reasonable activities. The catalytic activity of CaO was described by Lizuka et al. [10]. He argued that the catalytic activity of CaO is due to its surface oxygen anion. Calcium oxide is an ionic crystal with low Lewis acidity. The conjugated oxygen anion shows strong basic properties. The basic sites on the surface of CaO have been characterised using infrared spectroscopy in the presence of acidic molecule probes such as benzaldehyde [10]. The strength and the amount of basic sites on calcium oxide have been measured using  $\text{CO}_2$  adsorption techniques by Zhang et al. [11]. Zhang compared the basicity of CaO with MgO, SrO and BaO.

They found that the concentration of basic sites was in the order  $\text{BaO} < \text{SrO}, \text{MgO} < \text{CaO}$ . However, the basic strengths of the catalysts were in the order  $\text{MgO} < \text{CaO} < \text{SrO} < \text{BaO}$ . Kouzu et al. [12], applied three of these catalysts in the transesterification reaction of soybean oil, and found that activity was in the order  $\text{MgO} < \text{CaO} < \text{SrO}$ . His findings showed that the transesterification reaction needs strong basic sites. The only problems with SrO is that it is quite easily dissolved in the reaction mixture, with associated problem of contamination and poor reusability.

The catalytic mechanism for CaO in transesterification has been reported by Kouzu et al. [12]. The transesterification mechanism of triglycerides using CaO catalyst involves several steps. Figure 7.1 illustrates a mechanism for transesterification using calcium oxide as a solid base catalyst. The first step is the attachment of oxygen from the alcohol to the calcium, forming the methoxide ion. The second step is the attack of the oxygen on the carbonyl carbon of the triglyceride molecule. Rearrangement forms the methyl ester leaving the diglyceroxide ion. Step three is recovering the proton from CaO which reacts with the diglyceroxide to form diglyceride. The cycle continues until all three carbonyl groups in the triglyceride have been consumed to form methyl esters, leaving glycerol as by-product.

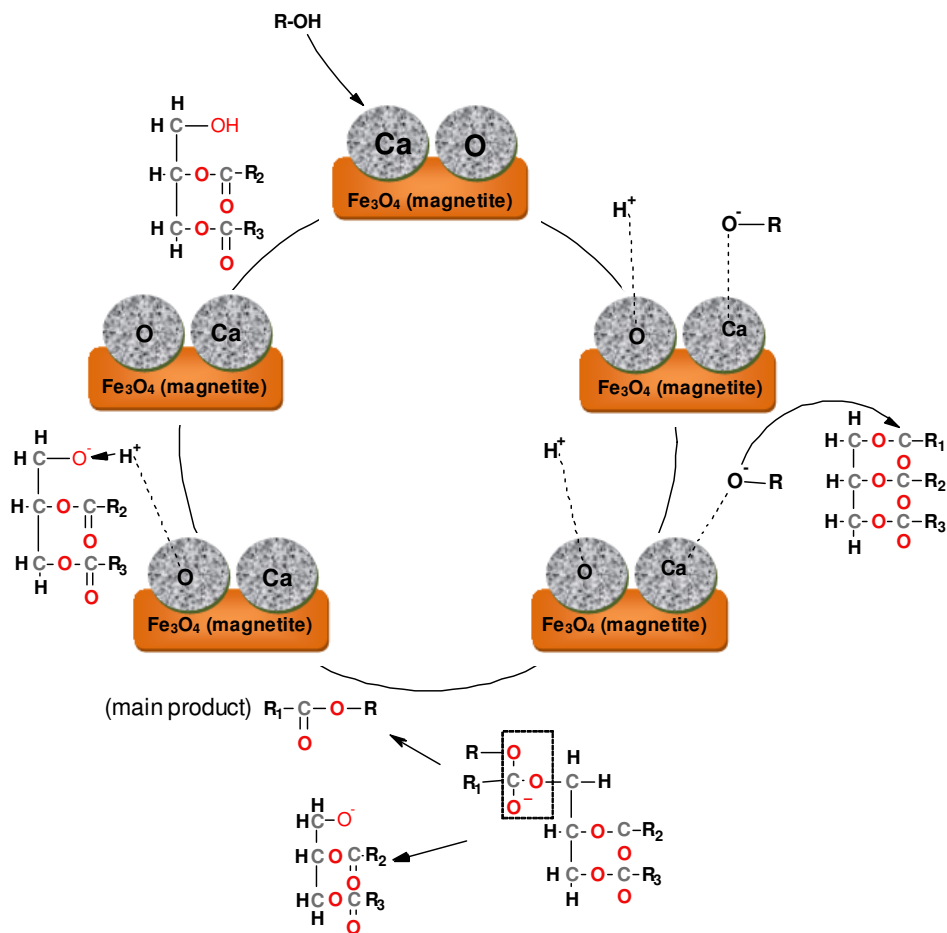


Figure 7.1. Reaction mechanism for transesterification of a triglyceride with methanol over CaO-magnetite catalyst.

Hattori studied the effect of calcination temperature of MgO on its activity in the isomerisation of 1-butene [13]. He found that the optimum temperature was 800 K. The catalytic activity of calcium oxide also depends on the calcination temperature. Granados et al. studied the stability and surface poisoning of calcium oxide catalyst and he found that the active sites of calcium oxide were very easily poisoned by carbon dioxide and water in the atmosphere and transformed into CaCO<sub>3</sub> and Ca(OH)<sub>2</sub> [14].

Concerning the practical use of CaO catalyst in biodiesel production, ideas have been discussed using fixed bed reactors with continuous flow of reactant rather than batch type processes [15]. In the case of batch processes, powdered CaO may be used to give maximum activity. There is however a problem with separation and recovery. Designing recoverable solid catalysts has been a challenge in recent years. Magnetically recoverable catalysts have been developed for several years for reactions such as hydrogenations, oxidations, C-C bond formation, hydrations, photo-catalytic processes, condensations and many more [16-18].

In this chapter a study of magnetically recoverable CaO is reported. These materials have been prepared as composites of CaO with magnetite  $\text{Fe}_3\text{O}_4$ , using an impregnation technique. The effect of calcination temperature on the catalytic activity of the catalyst and on its capacity for easy separation and magnetic stability are studied. The reusability of the catalyst is reported and discussed. These experiments demonstrate the CaO/ $\text{Fe}_3\text{O}_4$  system as a model of recoverable solid base catalysts for biodiesel synthesis.

### **7.3. Experimental and methods**

#### **7.3.1. Materials**

The materials used for making the catalysts were  $\text{Ca}(\text{NO}_3)_2 \cdot 4\text{H}_2\text{O}$ ,  $\text{FeSO}_4 \cdot 7\text{H}_2\text{O}$  (MW=278),  $\text{Fe}_2(\text{SO}_4)_3 \cdot 5\text{H}_2\text{O}$  (MW=489), ammonia solution (20%) and CaO.  $\text{Ca}(\text{NO}_3)_2 \cdot 4\text{H}_2\text{O}$  was supplied by Sigma Aldrich. CaO was obtained from Wilkinson-Vickers, UK.  $\text{FeSO}_4 \cdot 7\text{H}_2\text{O}$  and  $\text{Fe}_2(\text{SO}_4)_3 \cdot 5\text{H}_2\text{O}$  were

purchased from Fluka, UK. Ammonia solution was supplied by Fluka Analytical, UK. Tributyrin was purchased from Acros Organic, UK. Methanol was obtained from Fischer Scientific, UK.

### **7.3.2. Magnetite (Fe<sub>3</sub>O<sub>4</sub>) preparation**

Magnetite particles were synthesised using procedure described by Liu et al. [19]. A solution of 0.5 M iron(III) sulfate pentahydrate Fe<sub>2</sub>(SO<sub>4</sub>)<sub>3</sub>·5H<sub>2</sub>O (MW=489) and 1 M iron (II) sulfate heptahydrate FeSO<sub>4</sub>·7H<sub>2</sub>O (MW=278) were prepared by dissolving Fe<sub>2</sub>(SO<sub>4</sub>)<sub>3</sub>·5H<sub>2</sub>O (19.56 g, 0.04 mol) in 80 ml H<sub>2</sub>O and FeSO<sub>4</sub>·7H<sub>2</sub>O (5.58 g, 0.02 mol) in 20 ml 2 M HCl respectively (molar ratio of Fe<sup>3+</sup> /Fe<sup>2+</sup> is 2:1 ). The two solutions were then mixed together under N<sub>2</sub> condition. Then ammonia aqueous solution (1.5 M) was dropped into it with vigorous stirring until pH of the solution raised to 9. The obtained magnetite precipitate was collected using permanent magnet NeFeB. The magnetic material was washed with DI water until the pH of the material was 7. A black colored powder (Fe<sub>3</sub>O<sub>4</sub> particles) was obtained upon drying at 40°C for 18 h.

### **7.3.3. CaO-magnetite (CaFe) catalyst preparation**

The CaO-magnetite (CaFe) catalyst was prepared by dissolving 23.6 g (0.1 mol, MW= 236) of calcium nitrate tetrahydrate [Ca(NO<sub>3</sub>)<sub>2</sub>·4H<sub>2</sub>O] in 200 ml distilled water. The black colored powder magnetite (2.32 g, 0.01 mol) prepared in the previous section was added to the calcium nitrate solution, then followed by addition dropwise of ammonia solution (20 %) under vigorous stirring until pH 9 was achieved. The mixture was aged for 24 h at

room temperature and the magnetic catalyst was recovered with a permanent magnet. The recovered catalyst was washed with distilled water to pH 7 and then the material was dried at 60 °C for 5 h in oven. The catalyst was then calcined to the desired temperature. The catalysts were calcined at 500, 700 and 900 °C denoted as CaFe-500, CaFe-700 and CaFe-900. The catalyst was then applied in the transesterification reaction and compared with commercial CaO calcined at 700 °C.

#### **7.3.4. Catalytic testing**

The catalytic activities of the catalysts were tested in the transesterification reaction of tributyrin with methanol at 63 °C with molar ratio of 1:20 tributyrin to methanol. The CaFe catalyst amount used was 5 % w/w on the tributyrin. The reaction was performed in a 50 ml round bottom reactor equipped with a reflux condenser, magnetic stirrer, oil heater and temperature controller. Samples were taken at regular intervals and the conversion of tributyrin was monitored using gas chromatography (Perkin Elmer Clarus 500) with 50 m BP1 capillary column and FID detector. N-decane was used as an internal standard

#### **7.3.5. Catalyst characterization**

Powder XRD patterns were recorded on a Bruker D-8 diffractometer using Cu K $\alpha$  radiation (1.5418 Å) at 40 kV and 20 mA. The patterns were collected over the range 15-70 ° for 2 $\theta$  with a step size of 0.02 ° at a scanning speed of 2 °/min. N<sub>2</sub> adsorption and desorption isotherms were measured at 77 K using Micrometrics ASAP 2020 equipment. Before the adsorption, the

sample was outgassed for 6 h at 300 °C. FTIR spectra were performed using a Nicolet 380 spectrometer working in the range 4000-600 cm<sup>-1</sup>. The basicity and basic strength of the catalysts was measured using CO<sub>2</sub> adsorption as described in chapter 6.

## 7.4. Results and discussion

### 7.4.1. Catalyst characterization

Table 7.1. Surface area and porosity data for CaO and CaO/Fe<sub>3</sub>O<sub>4</sub> composites.

Catalyst	BET surface area (m <sup>2</sup> g <sup>-1</sup> )	Pore Volume (cm <sup>3</sup> g <sup>-1</sup> )	Pore Diameter (nm)
CaFe-500	41.0	0.26	22.3
CaFe-700	37.1	0.20	30.9
CaFe-900	4.1	0.009	85.0
CaO-700	46.9	0.12	8.72

The BET surface areas, pore volumes and pore diameters are presented in Table 7.1. The surface area of CaFe is decreased with increasing the calcination temperature. The surface area of the composite calcined at 700 °C is only slightly lower than that of pure CaO calcined at the same temperature. Pore volume of the composites calcined at 700 °C is slightly higher than the pure CaO calcined at the same temperature. In general, increasing the calcination temperature results in a decrease in the pore volume of the composite. Calcining at 900 °C decreases the pore volume dramatically. Pores of the composites are evidently wider than for CaO calcination temperature. Pores become wider with the increasing calcination temperature.

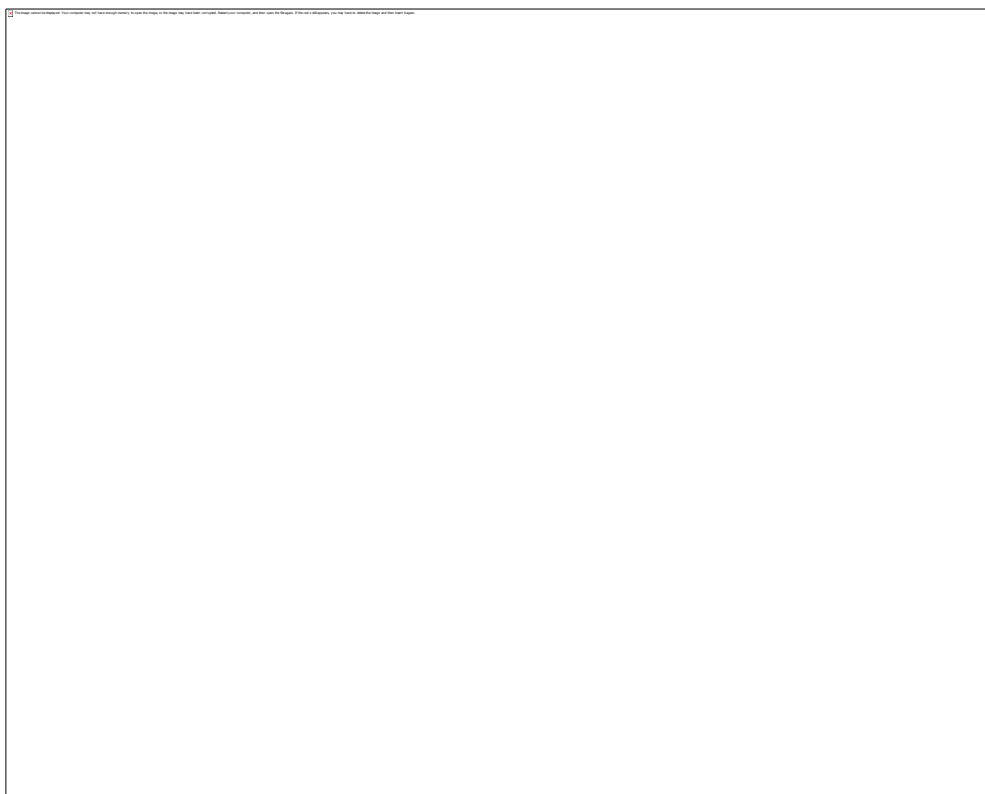


Figure 7.2. XRD patterns of CaO and CaO-Magnetite (CaFe) calcined at difference temperatures.

Figure 7.2 shows the XRD patterns of pure CaO calcined at 700 °C and the CaO (CaFe) composite (CaFe) calcined 500 °C, 700 °C and 900 °C. The calcination of pure CaO at 700 °C was done to establish the XRD pattern for this compound in which, before calcination, might be in the form of the hydroxide. The CaO calcined at 700 °C shows reflections at 29.4 °, 32.3 °, 37.5 °, 54.0 °, 62.5 °, 65.2 ° and 67.5 ° which is consistent with those previously reported [12, 14]. Zaki reported the strongest reflectance of cubic CaO at  $2\theta = 37.50^\circ$  consistent with JCPDS 82-1691 [20]. The mixture of CaO-Fe<sub>3</sub>O<sub>4</sub> (CaFe) XRD patterns give completely different peaks from CaO precursor. Calcining at 500 °C, no peaks are observed, suggesting that the material was in the amorphous phase. However, increasing the calcination

temperature to 700 °C and 900 °C, sharp peaks are formed. In CaFe-700 and CaFe-900 there is no strong peak due to CaO at 37.5 °. Instead a strong peak at 36 ° is seen which is typical of Fe<sub>3</sub>O<sub>4</sub> (JCPDS card 19-629) [21]. A strong peak at 29.4 ° is seen for CaFe-700 which may be due to a CaO phase, but this is absent for CaFe-900.



Figure 7.3. CO<sub>2</sub> adsorption calorimetric data for CaFe-500, CaFe-700 and CaFe-900.

CO<sub>2</sub> adsorption calorimetric data taken at 100 °C is shown in Figure 7.2. This figure shows the molar enthalpy of carbon dioxide adsorption plotted against the amount of adsorbed carbon dioxide for the three composite catalysts studied. The assumption is that the carbon dioxide adsorbed stoichiometrically on the basic sites of the catalyst and that only sites exhibiting enthalpies greater than 80 kJ mol<sup>-1</sup> are significantly basic. From this, the concentration of basic sites can be determined. The basic

strength, taken as the average enthalpy of adsorption on basic site, and the concentration of basic sites are tabulated in Table 7.2.

Table 7.2. Basic strength and basic site concentration data.

Catalyst	BET surface area (m <sup>2</sup> g <sup>-1</sup> )	$\Delta H_{\text{ads CO}_2}$ Basic strength (kJ mol <sup>-1</sup> )	Basic sites concentration (μmol g <sup>-1</sup> )
CaFe-500	41.0	106	150
CaFe-700	37.1	120	225
CaFe-900	4.1	104	75

In term of base strength and basic sites concentrations, CaFe-700 exhibits both the strongest and the most abundant sites. Calcining at 900 °C result in a in a dramatic decrease in basic site concentration. This is probably linked to the very low surface area of the catalyst calcined at this temperature which is 4.1 m<sup>2</sup> g<sup>-1</sup> compared to 37.1 m<sup>2</sup> g<sup>-1</sup> for the CaFe-700. The lower concentration of basic sites on CaFe-500 is possibly an indication that conversion of Ca(OH)<sub>2</sub> or CaCO<sub>3</sub> is not complete at this temperature.

Figure 7.4 shows IR spectra of the catalysts (CaFe) calcined at different temperatures and compares with uncalcined CaO and calcined CaO at 700 °C. The spectrum of CaO displays a sharp band at 3656 cm<sup>-1</sup>, a medium band at 1420 cm<sup>-1</sup> and very weak peak at 878 cm<sup>-1</sup>. This result is in agreement with Zaki at al. [20] who found the absorption bands for pure CaO at 3656 cm<sup>-1</sup>, medium peak at 1444 cm<sup>-1</sup> and very weak band at 878 cm<sup>-1</sup>. So these peaks can be taken as markers for CaO.



Figure 7.4. FTIR analysis of CaO and CaFe catalysts calcined at different temperature.

Figure 7.4 shows that the same peaks are detected for CaO calcined at 700 °C. The CaO/magnetite composite shows the 878  $\text{cm}^{-1}$  and 1420  $\text{cm}^{-1}$  peaks on calcination up to 700 °C, but these are lost as the calcination temperature is taken to 800 °C and 900 °C. In contrast, the 3656  $\text{cm}^{-1}$  peak seen for CaO is completely absent for the CaFe composites. It is not clear why

this peak is not seen but we are assuming that detection of the other two is evidence for the existence of CaO in the three composite materials.

#### 7.4.2. Catalytic activities

The catalytic activities of CaO-Fe<sub>3</sub>O<sub>4</sub> (CaFe) calcined at 400-900 °C were evaluated in the transesterification of tributyrin with methanol as a model reaction for the transesterification of triglycerides in vegetable oils. The reaction was run at 63 °C with 5% w/w catalyst based on tributyl glycerate (tributyrin). The methanol to tributyrin molar ratio was 20:1. The tributyrin conversion profiles for the catalysts varied with calcination temperature as shown in Figure 7.5.

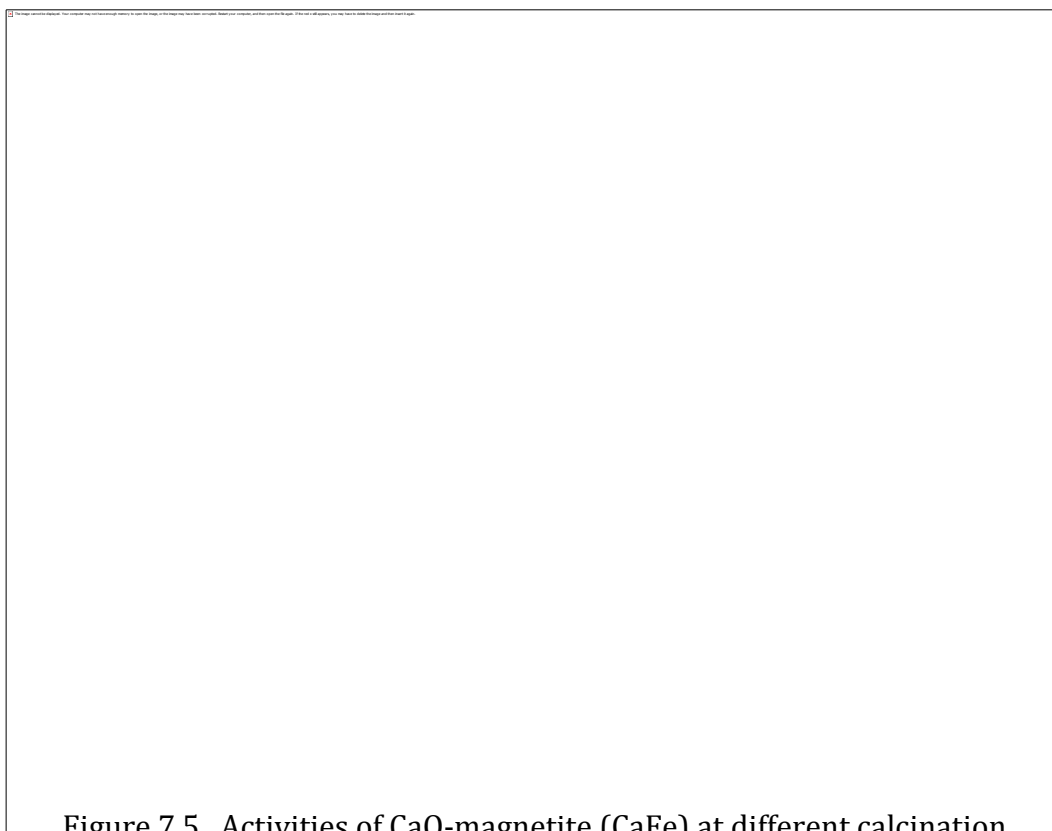


Figure 7.5. Activities of CaO-magnetite (CaFe) at different calcination temperature.

The reaction rate is highly dependent on the catalyst calcination temperature and the highest rate was achieved when the catalyst was calcined at 700 °C. At 400 °C, the catalyst has no catalytic activity. As is well known, CaO at room temperature and without calcination is partially hydrated and carbonated to form Ca(OH)<sub>2</sub> and/or CaCO<sub>3</sub> which are inactive as base catalysts.

The catalyst was prepared initially as Ca(OH)<sub>2</sub> from aqueous Ca(NO<sub>3</sub>)<sub>2</sub> solution, so there is no doubt that at low calcination temperature it remains in the hydrated and carbonated forms. The XRD pattern also shows that at this temperature it is an amorphous form, no crystalline peaks are observed. The crystallinity of the material increases with increased calcination temperature. The activity of the catalysts also increases with calcination temperature to 700 °C and then decreases above this value. No activity was observed on calcination at 900 °C. Catalytic activity correlates well with surface basicity, both of which are maximised on 700 °C calcination. The IR data suggest that the form of the CaO changes on calcination at above 700 °C. It seems likely that calcination below 700 °C does not adequately convert calcium hydroxide or carbonate to the oxide and calcination above 700 °C appears to change the form of the CaO in some undetermined way.

#### **7.4.3. Magnetic susceptibility**

Magnetic susceptibility of the catalyst was tested using an external magnetic field and it was measured qualitatively by taking photographs of the reaction mixtures after magnetic separation so that the extent to which

the powdered catalyst has been removed from the bulk of the liquid can be assessed. This method is comparing visually the turbidity of the reaction mixture in the presence of magnetic field (using strong bar magnet-NdFeB). By observing the turbidity of the reaction mixtures after 30 seconds, we are able to compare the magnetic susceptibilities of the catalysts when calcined at different temperatures. Figure 7.6 shows the photograph of the reaction mixtures before and after application of the magnetic field. The effectiveness of magnetic separation depends, surprisingly, on the calcination temperature of the catalyst, with the catalyst calcined at 700 °C being the most easily separated. This calcination temperature also corresponds to the maximum catalytic activity.

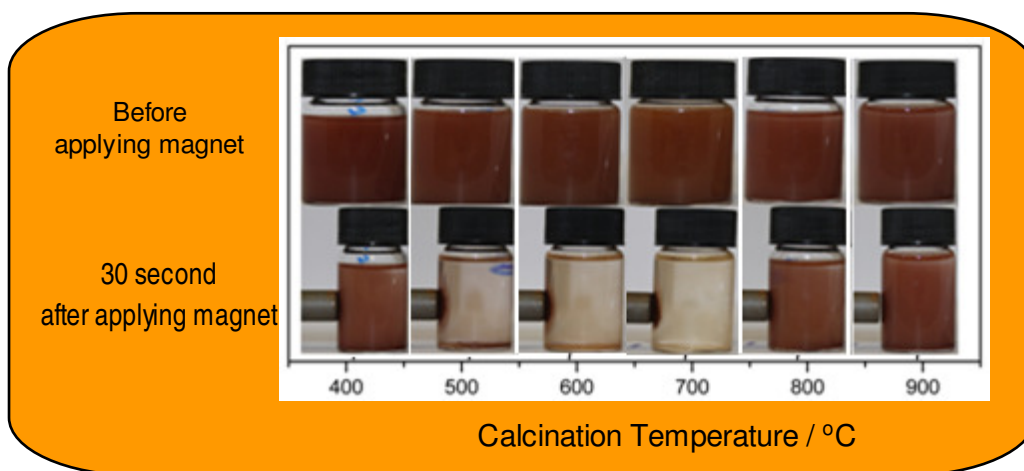


Figure 7.6. Tributyrin methanol reaction mixtures containing 5 % w/w CaFe catalyst.

#### 7.4.4. Catalyst Reusability

Figure 7.7 shows the result of the study on the reusability of the CaFe-700 catalyst in the transesterification of tributyrin. The catalyst was

recovered by filtration and reused for the next reaction. The collected catalyst was washed with methanol three times and dried, and re-calcined at 300 °C to remove any possible organic molecules on the catalyst surface before it was reused. The reuse of the catalyst was repeated two times. Tributyrin conversion decreased gradually with each run. This is a disappointing and surprising result in view of the lack of solubility of both CaO and Fe<sub>2</sub>O<sub>3</sub> in the reaction mixtures. It is possible that the re-calcination temperature was simply not high enough to remove organic contaminants and to convert any hydrated and solvated Ca(OH)<sub>2</sub> back to CaO. It would have been useful to have carried out this experiment with a higher re-calcination temperature.

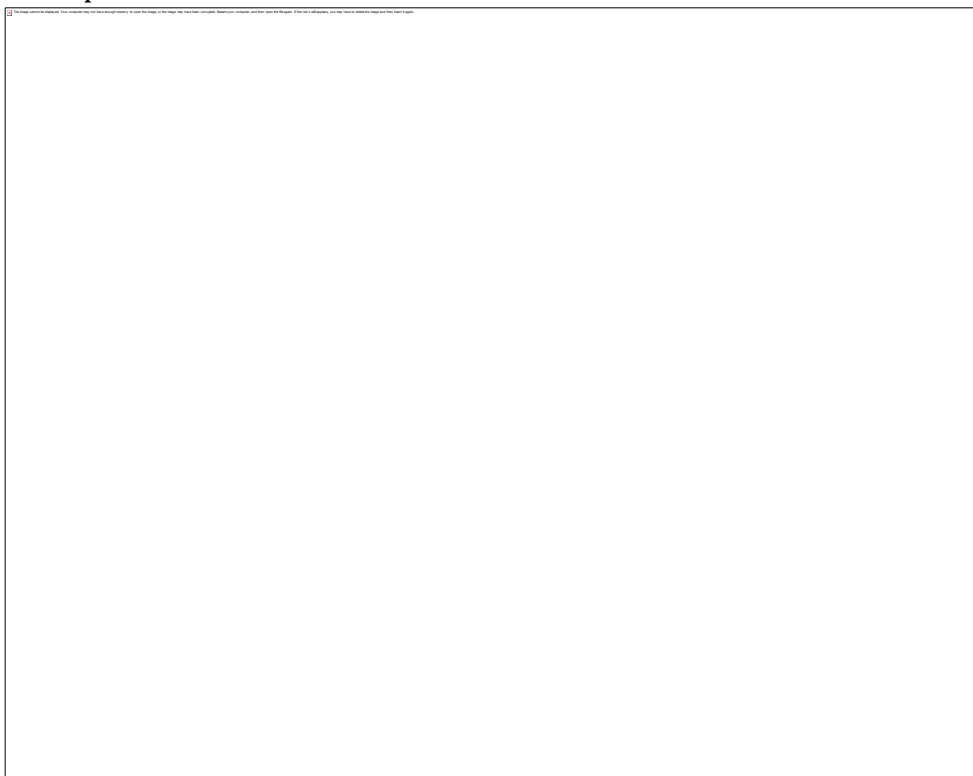


Figure 7.7. Catalyst reusability of CaFe-700 in the transesterification reaction of tributyrin at 63 °C (conversion after 30 minutes).

## 7.5. Conclusions

The difficulties associated with a separation of a solid catalyst from a liquid reaction medium when the solid requires use as fine particles or powder can be overcome by preparing catalyst composites with magnetite which can then be separated magnetically. This study represents only preliminary work and the CaO/Fe<sub>3</sub>O<sub>4</sub> composite will require refinement. It is clear however that effective binding between CaO and Fe<sub>3</sub>O<sub>4</sub> can quite easily be achieved and CaO formed from precipitated Ca(OH)<sub>2</sub> can be combined with magnetite. Catalytic activity is highly dependent on the calcination temperature of the composite and it is essential to avoid formation of undesired “compound” through the calcination process. In this work no effort was made to optimise the composition of the composite. Another essential aspect still to be studied is the reusability of the catalyst. Figure 7.7 shows that the improvement is needed if then the catalyst are to be of practical use.

## References

1. Veljkovic, V. B.; Stamenkovic, O. S.; Todorovic, Z. B.; Lazic, M. L.; Skala, D. U., Kinetics of sunflower oil methanolysis catalyzed by calcium oxide. *Fuel* 2009, 88, (9), 1554-1562.
2. Kouzu, M.; Tsunomori, M.; Yamanaka, S.; Hidaka, J., Solid base catalysis of calcium oxide for a reaction to convert vegetable oil into biodiesel. *Advanced Powder Technology* 2010, 21, (4), 488-494.
3. Gryglewicz, S., Rapeseed oil methyl esters preparation using heterogeneous catalysts. *Bioresource Technology* 1999, 70, (3), 249-253.
4. Kouzu, M.; Kasuno, T.; Tajika, M.; Sugimoto, Y.; Yamanaka, S.; Hidaka, J., Calcium oxide as a solid base catalyst for transesterification of

- soybean oil and its application to biodiesel production. *Fuel* 2008, 87, (12), 2798-2806.
5. Kawashima, A.; Matsubara, K.; Honda, K., Acceleration of catalytic activity of calcium oxide for biodiesel production. *Bioresource Technology* 2009, 100, (2), 696-700.
  6. Liu, X.; He, H.; Wang, Y.; Zhu, S.; Piao, X., Transesterification of soybean oil to biodiesel using CaO as a solid base catalyst. *Fuel* 2008, 87, (2), 216-221.
  7. Zhu, H.; Wu, Z.; Chen, Y.; Zhang, P.; Duan, S.; Liu, X.; Mao, Z., Preparation of Biodiesel Catalyzed by Solid Super Base of Calcium Oxide and Its Refining Process. *Chinese Journal of Catalysis* 2006, 27, (5), 391-396.
  8. Wen, L.; Wang, Y.; Lu, D.; Hu, S.; Han, H., Preparation of KF/CaO nanocatalyst and its application in biodiesel production from Chinese tallow seed oil. *Fuel* 2010, 89, (9), 2267-2271.
  9. Taufiq-Yap, Y. H.; Lee, H. V.; Hussein, M. Z.; Yunus, R., Calcium-based mixed oxide catalysts for methanolysis of *Jatropha curcas* oil to biodiesel. *Biomass and Bioenergy* 2011, 35, (2), 827-834.
  10. Iizuka, T.; Hattori, H.; Ohno, Y.; Sohma, J.; Tanabe, K., Basic sites and reducing sites of calcium oxide and their catalytic activities. *Journal of Catalysis* 1971, 22, (1), 130-139.
  11. Zhang, G.; Hattori, H.; Tanabe, K., Aldol condensation of acetone/acetone d6 over magnesium oxide and lanthanum oxide. *Applied Catalysis* 1988, 40, (0), 183-190.
  12. Kouzu, M.; Kasuno, T.; Tajika, M.; Sugimoto, Y.; Yamanaka, S.; Hidaka, J., Calcium oxide as a solid base catalyst for transesterification of soybean oil and its application to biodiesel production. *Fuel* 2008, 87, (12), 2798-2806.
  13. Hattori, H., Solid base catalysts: generation of basic sites and application to organic synthesis. *Applied Catalysis A: General* 2001, 222, (1-2), 247-259.

14. Granados, M. L. p.; Poves, M. D. Z.; Alonso, D. M. n.; Mariscal, R.; Galisteo, F. C.; Moreno-Tost, R.; Santamaría, J.; Fierro, J. L. G., Biodiesel from sunflower oil by using activated calcium oxide. *Applied Catalysis B: Environmental* 2007, 73, (3-4), 317-326.
15. Yan, S.; Lu, H.; Liang, B., Supported CaO Catalysts Used in the Transesterification of Rapeseed Oil for the Purpose of Biodiesel Production. *Energy & Fuels* 2007, 22, (1), 646-651.
16. Polshettiwar, V.; Varma, R. S., Green chemistry by nano-catalysis. *Green Chemistry* 2010, 12, (5), 743-754.
17. Shylesh, S.; Schünemann, V.; Thiel, W. R., Magnetically Separable Nanocatalysts: Bridges between Homogeneous and Heterogeneous Catalysis. *Angewandte Chemie International Edition* 2010, 49, (20), 3428-3459.
18. Lu, A.-H.; Salabas, E. L.; Schüth, F., Magnetic Nanoparticles: Synthesis, Protection, Functionalization, and Application. *Angewandte Chemie International Edition* 2007, 46, (8), 1222-1244.
19. Liu, C.; Lv, P.; Yuan, Z.; Yan, F.; Luo, W., The nanometer magnetic solid base catalyst for production of biodiesel. *Renewable Energy* 2010, 35, (7), 1531-1536.
20. Zaki, M. I.; Kalzinger, H.; Tesche, B.; Mekhemer, G. A. H., Influence of phosphonation and phosphation on surface acid base and morphological properties of CaO as investigated by in situ FTIR spectroscopy and electron microscopy. *Journal of Colloid and Interface Science* 2006, 303, (1), 9-17.
21. Shao, M.; Ning, F.; Zhao, J.; Wei, M.; Evans, D. G.; Duan, X., Preparation of Fe<sub>3</sub>O<sub>4</sub>-SiO<sub>2</sub> Layered Double Hydroxide Core Shell Microspheres for Magnetic Separation of Proteins. *Journal of the American Chemical Society* 2011, 134, (2), 1071-1077.

# **CHAPTER 8**

## **CONCLUSIONS AND RECOMMENDATIONS**

---

“This chapter gives overall conclusions and the recommendations for future work to improve the quality of this research”.

## **8.1. Conclusions**

The overall conclusions of this research relative to the objectives stated in chapter 1 are as follows.

### **8.1.1. Use of sulfonated hypercrosslinked polystyrene resin as a solid acid catalyst**

The use of sulfonated hypercrosslinked polystyrene resins as solid acid catalysts for the pre-esterification reactions of free fatty acids (FFA) and methanol has been demonstrated in this work. The sulfonated hypercrosslinked resins used in this work were Purolite D5081 and D5082 which have high BET surface areas of 701 and 381 m<sup>2</sup> g<sup>-1</sup> respectively. The catalytic activities of both resins were compared with conventional macroreticular resins Amberlyst-15, Amberlyst-35, and Nafion SAC-13. The catalytic activities of the catalysts were compared in the esterification of oleic acid and rearrangement of  $\alpha$ -pinene to camphene and limonenes.

The results show that the sulfonated hypercrosslinked resins are more active than the Amberlyst resin catalysts in the relatively facile esterification reaction, despite exhibiting low concentrations of acid sites and low acids strengths. The behaviour is thought to be due to the high surface area and highly accessible acid sites throughout the catalyst particles. The activity of sulfonated hypercrosslinked polystyrene resins in the esterification reaction is not influenced by the particle size. This confirms the absence of reaction rate diffusion control.

The reusability of sulfonated hypercrosslinked resin (D5081) catalyst depends on the temperature of reaction. At 65 °C the catalytic activity is substantially lost after one reaction because of reduced surface area and acid site concentration. This could be due to pore blocking. However, in contrast, at the higher temperature of 85 °C, the catalytic activity remains stable on repeated use. At this temperature the pore blockage evidently does not occur, or at least not to the same extent compared to lower temperature, and the activity is retained in multiple cycles without the need for catalyst regeneration.

The high activity exhibited by the sulfonated hypercrosslinked polystyrene resins towards esterification reaction has led to the possible use of this catalyst in commercial biodiesel production as replacements for homogeneous acid catalysts.

### **8.1.2. Sulfonated polyvinyl alcohol as a solid acid catalyst**

The use of sulfonated polyvinyl alcohol (S-PVA) catalyst as a solid catalyst has been studied in the same way as the sulfonated hypercrosslinked polystyrene resins for esterification of oleic acid and, as an addition test, in the rearrangement of  $\alpha$ -pinene. The activity of the catalyst was compared with sulfonated “macroreticular” polystyrene resin Amberlyst-35 and Nafion SAC-13. In the esterification reaction, sulfonated polyvinyl alcohol shows better activity than Amberlyst-35 resin catalyst even though the surface area is much lower. The results show that in the esterification reaction where high acid strength is not required and therefore highly accessible acid sites

throughout the catalyst material via diffusion is more important than through the surface particle.

The catalytic activity in the esterification of oleic acid of sulfonated polyvinyl alcohol (s-PVA) is also higher than SAC-13 for the same reason; the s-PVA is almost tenfold higher in concentration of active sites although its surface area is much lower than SAC-13. In fact, the activity of s-PVA towards oleic acid esterification appears to be under diffusion control in the early stages of reaction. This is shown by the presence of an induction period, but after this, the reaction is under kinetic control. In contrast, in the isomerisation/rearrangement of  $\alpha$ -pinene, the non-polar reactant is not able to swell the polar sulfonated PVA catalyst, and accessibility of the active sites depends on the surface area which is very low. The result is the s-PVA shows lower activity than Amberlyst-35 and SAC-13. The highest activity is shown by Amberlyst-35 which has a relatively high surface area and high acid concentration than s-PVA and perhaps more importantly, exhibit relatively strong acid sites and shows activity to non-polar reactants like  $\alpha$ -pinene.

The reusability in the esterification reaction for the sulfonated PVA crosslinked using glutaraldehyde is better than for catalyst prepared without this extra crosslinking. However, both of them suffer from catalytic activity loss after four consecutive runs. Infrared measurement suggests that sulfonic acid group leaching is not significant so it seems most likely that access to acid sites is being poisoned by adsorbed reactant.

### 8.1.3. Sulfated zirconia as a solid acid catalyst

Strongly acidic sulfated zirconia is intended to work as catalyst for simultaneous esterification of free fatty acid and the transesterification of triglycerides. This was tested using model compounds, a mixture of oleic acid and tributyl glycerate as a triglyceride. The catalyst was synthesised by an impregnation method of zirconia with sulphuric acid solution. The effect of calcination temperature on the catalyst activity was investigated. For comparison purposes, a commercial sulfated zirconia catalyst XZO-1720 was also used. This catalyst was obtained from MEL Chemicals. The optimum calcination temperature of sulfated zirconia to yield the highest conversion for both reactions was 600 °C. The study revealed that at this temperature, the acidity of the catalyst was the highest and the XRD patterns show that at 600 °C, the crystal structure is tetragonal.

The catalytic activity test in the transesterification of tributyl glycerate with methanol at 120 °C showed sulfated zirconia exhibits reasonable activity but is probably not active enough to be considered an alternative to homogeneous basic catalysts. Evaluation in the simultaneous transesterification and esterification reactions show that the sulfated zirconia catalysts are more active in transesterification than resin catalysts. In the esterification reaction, sulfonic acid resins catalyst show higher activity than sulfated zirconia.

The reusability of sulfated zirconia was found to be poor, again suggesting that this type of catalyst may not be a practical alternative to

homogeneous caustic catalysts. The deactivation is quite likely due to leaching of  $\text{SO}_4^{2-}$ , since recalcination does not help to recover the activity.

#### **8.1.4. Lithium zirconate as a solid base catalyst**

In this study, the synthesis, characterization and catalytic activity of lithium zirconate as a solid base catalyst for a transesterification reaction was studied. The work covers the study of the effect of calcination temperature, reactant molar ratio and the amount of catalyst used, on the conversion of tributyl glycerate.

The optimum calcination temperature was obtained at 700 °C. At this temperature, the catalyst shows the highest basic site concentration and these sites are stronger than those detected after calcination at lower or higher temperatures. At this point the tetragonal phase is dominant and this phase is thought to be responsible for the high surface basicity and the catalytic activity.

In general, lithium zirconate is a very active heterogeneous catalyst for transesterification reactions of triglycerides with methanol. This catalyst exhibits a tetragonal structure on calcination up to 800 °C and a monoclinic structure at higher temperature. The catalytic activity of lithium zirconate catalyst is independent of surface area, and the specific surface area of this catalyst is relatively very low, and falls progressively as the calcination temperature is increased above 500 °C. The catalytic activity of this catalyst appears to be independent of the method of synthesis for lithium zirconate.

Importantly this catalyst was successfully re-used with only minimal loss in activity.

### **8.1.5. Calcium oxide-magnetite composite as a recoverable solid base catalyst**

Calcium-magnetite composites have been studied as solid base catalysts for biodiesel synthesis. This catalyst was synthesised using an impregnation method between CaO and magnetite ( $\text{Fe}_3\text{O}_4$ ). The effect of calcination temperature on catalytic activity was studied. The optimum activity value was obtained at 700 °C. The capacity to separate used catalyst from the reaction mixture using a magnetic field was assessed. The study shows that the catalytic activity of the catalyst is highly dependent on the calcination temperature of the composite and it is important to avoid the formation of undesired compounds through the calcination process. In this study, no effort was made to optimise the composite composition. The reusability data shows that the catalyst suffers from catalytic lost and improvement is needed if the catalyst is to be of practical use.

## **8.2. Recommendations for future work**

### **8.2.1. Sulfonated hypercrosslinked polystyrene resin catalyst**

Further work is needed to explore the possibility the use of the sulfonated hypercrosslinked polystyrene resins in a fixed bed column using vegetable oil with high free fatty acid content, since the catalyst suffers from

loss in its activity when it is run in a batch process. The fixed bed column provides the chance to work in a continuous flow process.

It would be useful to examine scaling up the system to reduce free fatty acid content in vegetable oils, especially using high temperature 85 °C operation. The reusability test shows that the activity is retained at this temperature for multiple cycles without the need catalyst regeneration.

### **8.2.2. Sulfonation polyvinyl alcohol catalyst**

Further work is needed due to the poor reusability. It is necessary to explore the possible reason why this catalyst lost its activity, even though FTIR spectra show that the sulphonate group is retained in the polymer matrix. Applying high temperature operation 70 °C or 80 °C could possibly reduce catalyst deactivation as in the case of in sulfonated hypercrosslinked resin.

### **8.2.3. Sulfated zirconia catalyst**

Catalyst deactivation for the sulfated zirconia shows that further work is required despite having high catalytic activity for simultaneous esterification and transesterification reactions. A number of reports show that water produced during the esterification reaction had a negative effect on this solid acid catalyst. Therefore, study into more detail of the effect of water to the catalyst activity should be carried out in the future.

This study was using a relatively low temperature reaction of 120 °C. Hence, it is imperative for future work to investigate the possible enhancement of reusability of the catalysts at higher temperatures.

#### **8.2.4. Lithium zirconate catalyst**

This catalyst has very good performance in transesterification reactions. This catalyst also has excellent reusability for several uses. Further work is needed to evaluate the performance of this catalyst using real vegetable oils.

Semi batch system should be developed using a fixed bed reactor to see the parameters required in larger processes, since the study was done only using batch reactors.

#### **8.2.5. Calcium oxide – magnetite composite catalysts**

Further work is required, due to poor reusability of the catalyst, to investigate the potential leaching of calcium in the reaction mixture. In this study, catalyst was used in the form of powder. It would be worth investigating whether different forms of the catalyst such as pellets could resolve the reusability problem.

Improvement of the stability of the catalyst is necessary to optimise the potential use of this catalyst in biodiesel production and other reactions. Extensive studies of the effect of composition (CaO content) would be useful in the opetimisation of these catalysts.

# APPENDIXES

## APPENDIX - A

Biodiesel feedstock, targets and production in selected countries [107].

Adapted from Kline et al. (2007).

Country	Primary Deedstock	Forecast Production in 2007 (million gallons)	Blending target for biodiesel
Argentina	soybeans	53	5 % blends, 2010
Brazil	soybeans, palm oil, castor oil	64	5 % blend, 2013
Canada	animal fat, vegetable oils	25	2% blends, 2012
China	vegetable oils, Jathropa	30	10% blends
Colombia	palm oil	13	5 % by 2008
EU	rapeseed, sun flower, soybeans	1,732	10% by 2020
India	Jathropa, imported palm oil	12	5% in diesel by 2012
Indonesia	palm oil, Jathropa	108	10% by 2010
Malaysia	palm oil	87	5% in diesel
Mexico	animal fat, recycle oils	1	no targets
Thailand	palm oil	69	10% by 2012
United States	soybean, other	445	15 billion gallons by 2012

## APPENDIX -B

### Nitrogen Adsorption : Micrometrics ASAP 2020

This method was used to measure BET surface area, pore volume and pore diameter of the catalyst. The analysis was run at 77 K or -196°C. Surface area measurement on catalyst D5081 is shown below.

#### b) Equipment Micrometrics ASAP 2020



Sample: P5081  
Operator: EAD  
Submitter: Eko  
File: G:\ASAP\001-008.SMP

Started: 15/03/2011 9:53:09PM	Analysis Adsorptive: N2
Completed: 15/03/2011 18:13:11PM	Analysis Bath Temp.: -195.766 °C
Report Time: 17/03/2011 10:23:46PM	Thermal Correction: No
Sample Mass: 0.1278 g	Warm Free Space: 28.6565 cm <sup>3</sup> Measured
Cold Free Space: 88.7342 cm <sup>3</sup>	Equilibration Interval: 10 s
Low Pressure Dose: None	Automatic Degas: Yes

Comments: Ion exchange resin beads, ground

### Summary Report

#### Surface Area

Single point surface area at P/Po = 0.202058978: 714.8441 m<sup>2</sup>/g

BET Surface Area: 701.7905 m<sup>2</sup>/g

#### Pore Volume

Single point adsorption total pore volume of pores  
less than 82.1488 nm width at P/Po = 0.975855487: 0.501871 cm<sup>3</sup>/g

BJH Adsorption cumulative volume of pores  
between 1.7000 nm and 300.0000 nm width: 0.405304 cm<sup>3</sup>/g

BJH Desorption cumulative volume of pores  
between 1.7000 nm and 300.0000 nm width: 0.392345 cm<sup>3</sup>/g

#### Pore Size

Adsorption average pore width (4V/A by BET): 2.86052 nm

BJH Adsorption average pore width (4V/A): 19.9286 nm

BJH Desorption average pore width (4V/A): 19.4321 nm

## APPENDIX - C

### Microcalorimetry Measurement

Microcalorimetry was used to measure the basic concentration and basic sites of catalyst.

#### a) Operating Conditions

Degassing (activation) :

- Sample (20-50 mg)
- Temperature : 100°C
- Time : 1 h

Analysis :

- Gas probe : 1% Ammonia in nitrogen for acid catalyst and CO<sub>2</sub> for base catalyst
- System : Flow through Setaram 111 differential scanning calorimeter
- Carrier gas : Nitrogen
- Detector : Mass spectrometer at 175°C

#### b) Apparatus



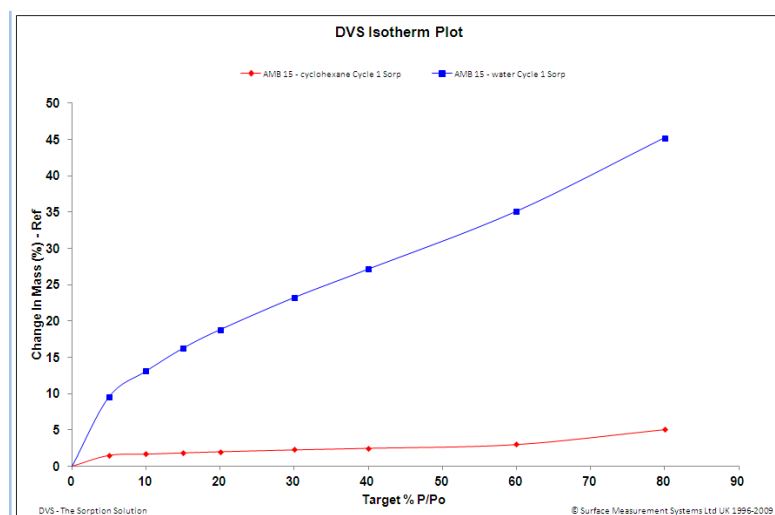
## APPENDIX -D

### Dynamic Vapour Sorption (Advantage™)

a) The use of this apparatus was to measure water/cyclohexane adsorption isotherm of resin catalysts used in chapter 3. The sample used for the analysis was 20 mg. Isotherm was recorded at 25°C both for water and cyclohexane. The activation of the catalyst was done at 100°C. Fully description of the method was described by Hill (Reference 28, Chapter 3).

### b) Results

DVS adsorption result on Amberlyst-15 in water and cyclohexane are shown in Figure below.



### b) Equipment



## APPENDIX - E

### Glass reactor (50 ml)

#### a) Methods

Reaction mostly was run in batch wise using 50 ml round bottom glass reactor equipped with glass condenser, magnetic stirrer and thermo controller. The heating is provided by oil bath put on hot plate. The heating and stirring is automatically controlled by digital control attached in the hot plate. The system is shown in the picture below.

#### b) Apparatus



## APPENDIX - F

### Gas Chromatography Clarus 500 Perkin Elmer

This work utilised gas chromatography technique to monitor sample (reactant and product) for transesterification and isomerisation/rearrangement reactions. The GC used for this purpose was Perkin Elmer Clarus 500 with 50 m capillary column (BP1 column), equipped with FID detector.

#### a) GC operation conditions

Unit	Operating Conditions
Column	BP1 50 m
Detector	Flame Ionisation Detector (FID) at 250°C
Oven Temperature	Initial Temp. : 60°C, hold 0 min Ramp 1 : 10° / min to 160°, hold for 0 min Ramp 2 : 20° / min to 290°, hold for 2 min
Carrier Gas	Helium at 2 ml min <sup>-1</sup> Air at 450 ml min <sup>-1</sup> H <sub>2</sub> at 45 ml min <sup>-1</sup>
Injector	On Column injector Injection temperature: 250 °C Injection volume : 0.5 µml
Channel	Run Time : 18.5 min Sampling rate : 12.5 pts/s

b) GC Perkin Elmer Clarus 500



c) Chromatogram sample: transesterification of tributyrin with methanol using lithium zirconate catalyst calcined at 700°C (LIZA-700) catalyst and it was monitored and taken the samples every 5 minutes from 0-15 min.



## APPENDIX -G

### Pressurised Reactor (Autoclave Engineer™)

#### a) Method

Pressurised reactor was used to perform high temperature and pressure experiment (Chapter 5), where transesterification and esterification was conducted in the same vessel using sulfated zirconia SZ-01 and commercial sulfated zirconia XZO-1720.

The experiment conditions :

1. Reactor temperature : 120°C
2. Heater temperature : 140°C
2. Process pressure : 4.6 bar (auto-pressure)
3. Stirring : 900 rpm

#### b) Apparatus (Autoclave Engineer™)



## APPENDIX - H

### CALCULATION OF TOF for CATALYSTS

Catalyst	acid site concentration (by titration) (mmol g <sup>-1</sup> )	TOF (h <sup>-1</sup> )	
		Isomerisation	Esterification
Purolite D5081	1.0	37	65
Purolite D5082	2.0	52	26
Amberlyst-15	4.7	113	4.8
Amberlyst-35	5.4	118	2.4
Nafion SAC-13	0.15	740	80

#### **Example TOF calculation for D5081 in esterification of oleic acid**

$$\text{TOF} = \text{TON}/\text{time (h)}$$

$$\text{TON} = \frac{(\text{Initial conversion} \times \text{initial mol of reactant})}{(\text{concentration of active sites} \times \text{amount of catalyst used})}$$

At 30 minutes (0.5 h) give 46 % conversion

- Conversion (%) of oleic acid using D5081 catalyst = 46 % (0.46) after 0.5 h (30 mins)
- Initial reactant (tributyrin) used was 4 g (MW=282) = 4/282 = 0.0142 mol = 14.2 mmol
- Concentration of active sites for D5081 = 1.0 mmol g<sup>-1</sup>
- Amount of catalyst used = 0.2 g

Hence,

$$\text{TON} = (0.46 \times 14.2) : (1 \times 0.2 \text{ g}) = 32.6$$

$$\text{TOF for D5081 in esterification} = \text{TON}/\text{time} = (32.6)/(0.5) = 65.2 \text{ (65)}$$

## APPENDIX -I

### FTIR -Nicolet 380

a) Analysis of functional groups, especially for Chapter 4 and 5 has been conducted using FTIR Nicolet 380.

b) Apparatus



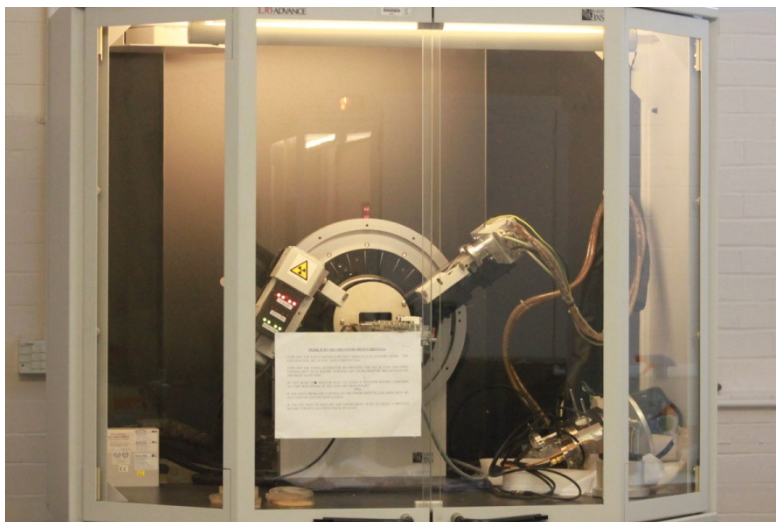
## APPENDIX -J

### Powder X-ray Diffraction Bruker D8

#### a) Operating conditions

- Operating conditions : 40 kV, 20 mA using nickel-filtered Cu K $\alpha$  radiation (1.5406 Å)
- Scan Axis 2 theta
- Start 5 and stop 70°
- Step size : 0.02
- No. of steps : 3250
- Time/step : 1
- Total scan : 0:54:11

#### b) XRD –Equipment Bruker D8



## APPENDIX - K

### Programmable furnace : VULCAN 3-120™

Temperature controlled furnace was used for calcination of catalysts (Chapter 5, 6 and 7). The parameters of the furnace such as ramp rates, temperatures, and hold times can be pre-programmed.

a) Calcination temperature for LIZA-700 (i.e. example 1)

#### Heating

Programme-1:  $R1 = 1^\circ \text{C} / \text{min}$ ,  $T1 = 120^\circ\text{C}$ ,  $H1 = 3 \text{ h}$  (from  $25^\circ\text{C}$  to  $120^\circ\text{C}$ )

Programme-2:  $R2 = 1^\circ \text{C} / \text{min}$ ,  $T2 = 700^\circ\text{C}$ ,  $H2 = 5 \text{ h}$  (from  $120^\circ\text{C}$  to  $700^\circ\text{C}$ )

#### Cooling

Programme-3:  $R3 = 10^\circ\text{C} / \text{min}$ ,  $T3 = 150^\circ\text{C}$ ,  $H3 = 10 \text{ h}$  (from  $700^\circ\text{C}$  to  $150^\circ\text{C}$ )

b) Apparatus



## APPENDIX- L

### PUBLICATIONS AND PRESENTATIONS

1. **Andrijanto, E.;** Dawson, E. A.; Brown, D. R., *Hypercrosslinked polystyrene sulphonic acid catalysts for the esterification of free fatty acids in biodiesel synthesis*. *Applied Catalysis B: Environmental* 2012, 115-116, (0), 261-268. (Paper).
2. Nair, G. S., Andrijanto, E., Alsahme, A., Kozhevnikov, I. V., Cooke, D. J., Brown, D.R. and Shiju, N. R. (2012) *Glycerol utilization: solvent-free acetalisation over niobia catalysts*. *Catalysis Science & Technology*. ISSN 2044-4753. In press. (Paper).
3. **Andrijanto, E.;** Atwood, J.; Dvininov, E.; Stepenson, H.;Brown, D.R., *Lithium zirconate solid base catalyst for transesterification of triglycerides in biodiesel synthesis*, 2012, (prepared for submission) (Paper).
4. **Andrijanto, E.;** Atwood, J.; Dvininov, E.; Stepenson, H.;Brown, *The use of sulphated zirconia for simultaneous esterification of oleic acid and transesterification of triglycerides in biodiesel synthesis*, 2012, (prepared for submission) (Paper).
5. **Andrijanto, E.;** Brown, D.R. *A New Microporous Polystyrene Sulfonic Acid Catalyst with High Activity Towards Free Fatty Acid Esterification in Biodiesel Production*. In: 10<sup>th</sup> International Conference on Material Chemistry (MC 10), 4th-7th July 2011, Manchester, UK. (Paper presentation).
6. Brown, D.R.; **Andrijanto, E.;** *A New Microporous Polystyrene Sulfonic Acid Catalyst for Free Fatty Acid Esterification*. IEX 2012: The International Ion Exchange Conference, 19<sup>th</sup>-21<sup>st</sup> September, Cambridge, UK. (Paper presentation).
7. **Andrijanto, E.;** *Acid-Base functionalized mesoporous silica for biodiesel production*, MC9 at 42<sup>nd</sup> IUPAC, Congress, 2-7 August, 2009, Glasgow. (Poster)